REFERENCE NO. 64 377

COPIES

BELLCOMM, INC
1100 17th ST., N. W.
WASHINGTON 6, D. C.

TECHNICAL OPERATING REPORT [redacted]

C72 12569

CLASSIFICATION CHANGE
TO - UNCLASSIFIED
By authority of [redacted], GDS [redacted] GP-4
Changed by D. L. Merritt Date 11/17/75

[redacted]

APOLLO HEAT SHIELD

MONTHLY PROGRESS REPORT

Prepared by

RESEARCH AND ADVANCED DEVELOPMENT DIVISION
AVCO CORPORATION
Wilmington, Massachusetts

RAD-SR-64-98
Contract M3J3XA-406012
Avco Report Series 201

THIS REPORT WAS PREPARED IN ACCORDANCE WITH NAA S&ID CONTRACT M3J3XA-406012. IT IS SUBMITTED IN PARTIAL FULFILLMENT OF THE CONTRACT AND IN ACCORDANCE WITH NAA S&ID PROCUREMENT SPECIFICATION MC999-0025

(NASA-CR-127996) APOLLO HEAT SHIELD Monthly Progress Report (Avco Corp., Wilmington, Mass.) 118 p

N79-76519

Unclas
00/18 11702

April 1964

CLASSIFICATION CHANGE
To UNCLASSIFIED
By authority of GDS [redacted] GP-4 Date 12/31/72
Changed by D. L. Merritt
Classified Document Master Control Station, NASA
Scientific and Technical Information Facility

Prepared for

NORTH AMERICAN AVIATION, INC.
SPACE AND INFORMATION SYSTEMS DIVISION
Downey, California

This document contains information affecting the National Defense of the United States [redacted] 18, U.S.C., Section [redacted] the transmission or revelation [redacted] in any manner to an unauthorized person is prohibited by la[redacted]

[redacted]

TECHNICAL OPERATING REPORT [redacted]

This document consists of 118 pages,
92 copies, Series A

[redacted]

APOLLO HEAT SHIELD
MONTHLY PROGRESS REPORT

Prepared by

RESEARCH AND ADVANCED DEVELOPMENT DIVISION
AVCO CORPORATION
Wilmington, Massachusetts

RAD-SR-64-98
Contract M3J3XA-406012
Avco Report Series 201

THIS REPORT WAS PREPARED IN ACCORDANCE WITH NAA S&ID CONTRACT M3J3XA 406012. IT IS SUBMITTED IN PART AL FULFILLMENT OF THE CONTRACT AND IN ACCORDANCE WITH NAA/S&ID PROCUREMENT SPECIFICATION MC999 0025

9 April 1964

APPROVED

W. Leh
Project Manager
Apollo Vehicle Design

C. L. Hoffine
Project Manager
Materials Development and Fabrication

E. Offenhartz
Project Director
Manned Space Systems

Prepared for

NORTH AMERICAN AVIATION, INC.
SPACE AND INFORMATION SYSTEMS DIVISION
Downey, California

[redacted]

[redacted]

(NOT USED)

[redacted]

[redacted]

CONTENTS

[redacted]

[redacted]

ILLUSTRATIONS

[redacted]

[redacted]

ILLUSTRATIONS (Cont'd)

[redacted]

[redacted]

ILLUSTRATIONS (Concl'd)

[redacted]

[redacted]

TABLES

[redacted]

[redacted]

(NOT USED)

[redacted]

[redacted]

I. CURRENT STATUS

Avco's program accomplishments during the month of March continue to reflect the integration of NAA revised heating and drawing changes through Revision N. The implementation of these changes is very closely related to the receipt of data from NAA and resultant schedule changes.

A. VEHICLE DESIGN

1.0 Aerothermodynamics

1.1 Thermal Design

1.1.1 Main Ablator

Analysis of the radiation view factors was initiated for the windward and leeward abort tower wells. This study considers the actual well geometries and the heating definition contained in the "P" revision.

New rendezvous window well ablator thicknesses are being calculated for the revised heating received at the 5-6 March T.I.M.

A study was begun to determine the effects of the abort tower attach rods on main ablator thicknesses in the vicinity of the rods. Calculations are based on local undisturbed heating.

Reentry temperature histories one inch up-stream from NAA/RAD interface areas are being obtained for trajectories HSE-1, HSE-2, HSE-4A, HSE-6, and HSA-3. Until heating at additional points is available for these trajectories, the calculations will be performed only for those interfaces which are relatively close to a defined heating point.

Mass loss and shape change histories are being calculated for trajectory HSE-1. Histories were completed at 62 body locations for HSE-3A.

A reanalysis of the "E" maintenance panel edge member was undertaken. This analysis will reflect the "P" revision panel location.

Using programs 1600 and 1327, an effort is in progress to compare predictions of mass loss and shape change. Initial results will be available during the next report period.

The analysis of voids in the ablator was continued. The Thermal Analyzer Program 1459 is being used to analyze simultaneous radiation and conduction across the void. Work was started to determine effects of voids in the RTV-560 gasket material.

[redacted]

[redacted]

Work has started on the development of a $q^* - \Delta H$ curve for OVERS test data.

Using the upper and lower bounds on the $T_{WALL} - q_c$ correlation, comparisons will be made between temperatures predicted by the present design technique and OVERS test results.

Work is continuing on the effort to use the ψ technique for the analysis of combined convective and radiant heating.

Additional data were received from specimens of Avcoat 5026-39/HC-G subjected to pure radiant heating in the Solar Furnace. The heat fluxes varied from 280 to 1400 Btu/ft^2-sec. All tests were run in air at 1 atmosphere.

1.3 Test Planning and Analysis

Experimental data, obtained in the Avco 10-Megawatt Arc Facility, has shown that local accelerated erosion of Avcoat 5026-39HC-G occurs due to heating perturbation. These perturbations are produced by the differential ablation between Avcoat and certain materials adjacent to Avcoat.

OVERS splash data showing the thermal response of Avcoat 5026-39/M to heat fluxes up to 290 Btu/ft^2-sec have been compiled.

Analysis of eleven uninstrumented splash specimens of the plug-shroud configuration has been started. The objective is to establish the portion of energy blocked due to char removal and consequently a value for the transpiration factor (η_1). Data have been reduced to q^* values and these results are now being analyzed. The material being studied is Avcoat 5026-39/HC-T.

2.0 Structural Studies

2.1 Thermostructural Analyses of Aft Compartment with Moment Tie

Thermostructural analyses are being redone for temperature soak environments of +600°F, -60°F, -260°F (-85°F inside S/M), -260°F (+130°F inside S/M) and the heat shield fabrication cure environment to evaluate the aft compartment heat shield inclusive of the new moment tie design. All of these studies utilize Avco's 1322 orthotropic shell of revolution computer program.

2.2 Unsymmetrical Load Analysis of Aft Compartment

An analytical model of the aft compartment heat shield has been devised which uses Avco's 1095X general frame program to describe the structural

[redacted]

[redacted]

behavior of the aft compartment under unsymmetrical loading. The model is presently being evaluated in order to establish a practical working model.

2.3 Intercompartmental Gap at $X_c = 81$

The study of the effects of HSE-3A reentry on the variation of the meridional gap with time is continuing. Reentry was assumed to be initiated from a spaceflight condition in which the sunlight shines on the $-Z_c$ axis with an incidence angle of 57.5 degrees. The meridional gap has been determined for reentry times of 0, 200, 500 and 700 seconds, assuming the forward compartment is free to rotate. For the times investigated the maximum meridional gap is 0.20 inch occurrring at 700 seconds. The details of the analysis and complete results are given in section IV.

2.4 Forward Compartment Fabrication Deformations

A study has been initiated to determine the deformations due to curing and machining of the ablator. The 1322 orthotropic shell program will be utilized to determine the deformations of a rotationally symmetric cone and will be superimposed on the circumferential bending deformations found by the 1095X ring program.

2.5 Crew Hatch Analysis

The analysis for the crew hatch-heat shield interactions is being revised to include the latest ablator properties and to remedy several inadequacies of the original analysis. The beam network used to described the hatch has been revised to include nodal points at each latch location. The nodal points in the original network do not coincide with the latch locations, making it extremely difficult to extract the actual latch loads, Also, a flexibility matrix rather than a stiffness matrix is being used in the revised analysis. In addition to free deflections and latch loads, the flexibility matrix will make it possible to calculate internal loads and stresses at the nodal points. The analysis is for a -260° soak temperature.

2.6 Scalloping Analysis at $X_c = 23.2$

The analysis to determine the amount of scalloping at $X_c = 23.2$ due to a -260°F vehicle soak temperature has been stopped temporarily, pending an investigation of the behavior of the skirt region between $X_c = 23.2$ and $X_c = 43.4$ under the action of a concentrated load.

2.7 Fabrication Deformation-Crew Compartment

An analysis to determine the fabrication deformation of the crew compartment from $X_c = 23.2$ to $X_c = 81.1$ has been started. The following cases are being considered. First, the holding fixtures are assumed to provide

[redacted]

[redacted]

simple supports at X_c = 23.2 and 81.1 and the deformation of the structure before machining the ablator and after machining the ablator are calculated. Secondly, the free deflection of the structure after machining the ablator will be calculated. For the analysis, the deformation of a rotationally symmetric cone with a meridional ablator thickness variation, as found by program 1322, will be superimposed on the bending deformation due to circumferential ablator thickness variation as found by the 1095X ring program.

2.8 Ablator Reentry Analysis

The ablator reentry analysis study outlined in the 9 March 1964 monthly progress report is continuing. The initial effort is being concentrated towards determining maximum ablator stresses and strains as a function of temperature in both the parallel and perpendicular directions. These results will then be evaluated to determine which conditions and vehicle stations warrant detailed analyses. This portion of the effort is approximately 50 percent complete.

2.9 Failure Criteria Analysis Effort

A simplified model of the crew compartment has been set up for analysis to study the effects of a cracked heat shield. The aim of the study is to determine a realistic prediction of the temperature of cracking, the number and location of cracks, and the loads that must be transferred across a cracked heat shield section. The loads that must be transferred will then be compared with the failure criteria test results to determine margins of safety. The study effort is described in further detail in section IV.

3.0 Design

Manufacturing drawings are being revised to incorporate outstanding EC's and to reflect effectivity for vehicle 006. New top assemblies for each compartment are being created specifically for 006. Incorporation of the mandatory P change to the structures diagram into Avco's drawings for vehicle 006 and 009 is in process.

Work is continuing on Engineering mockups. A full scale mockup of a yaw rocket panel with a cast in place RTV-560 gasket was completed. Mockups of the rendezvous window frame and the forward compartment pitch engine panel are progressing satisfactorily. The pitch mockup will be used for casting RTV-560 gaskets.

Design of the closeouts and ablator around the crew compartment C-band antenna for vehicles 006, 008 and 011 is complete. The drawings for this revision, which are part of the P change, are presently being checked. Due to the lack of complete definition by NAA of the aft compartment C-band antenna installations,

[redacted]

[redacted]

Avco has made sufficient assumptions to permit completion of the design defined by LA 5514.

Because the new heating perturbations for the ablator tower wells were not received from NAA in sufficient time to permit generation of new ablator thicknesses, the tower well ablator design is based on the thicknesses presented in the 9 March 1964 Monthly Progress Report.

Work continues on the creation of interface control drawings.

LA-5518, Air Vent - Scimitar Antenna and Steam Vent, LA-5521, Closeout Blocks - Tension Tie (LES Tower), and LA-5520, Gap Problem Test Specimen 9, were completed. LA-5520 defines a test specimen for a type of intercompartment gap seal (X_c = 81.130) which may be capable of surviving the complete environmental spectrum.

The three shear compression pads are identical, with the resulting effect being that the 3 pad extends approximately 7/8 inch above the ablator OML and the 1 pads falls approximately 3/8 inch below the theoretical ablator OML requiring a local flat to be machined into the ablator at pad 1. Substructure temperature in this area will exceed 600°F.

In spite of the fact that umbilical definition was received from NAA late in this reporting period, studies and layouts are in process which will allow incorporation of this change onto the affected vehicles. Design of the Avco/NAA umbilical interface is based on NAA drawings V16-321003 sheet 2, V16-321036 and V16-932041 and Avco LA-5522. To meet existing schedules, Avco has assumed that the interface exists along X_c = 43.585 and towards the aft end of the vehicle along both elemental sides of the umbilical to, but not including, the intercompartment interface at X_c = 23.2. LA-5522 defines the size and material of the gaskets along the three interface surfaces which Avco recommends NAA use.

The current weight summary shows a decrease of 34.7 pounds from the last report. The new weight is 1477 pounds ±2 percent heatshield thickness changes from X_c = 30.0 to X_c = 133.50 as presented in the February 10, 1964 Progress Report has resulted in a drop in weight of 5026-39 HC-G ablator, RTV-560 gaskets and fiberglass closeout members of the forward nose cone and forward and crew compartments. However, the total change in weight was lessened by a consideration of moisture absorption by the ablator. An increase of 3 percent in weight is consistent with the results of tests made for this purpose.

Work continues on an asymmetric computer program and while substantial progress has been made, results are preliminary and the program is being rigorously checked for validity.

[redacted]

APOLLO WEIGHT SUMMARY

Compartment	Weight (pounds)							CG (of Total) (inches)			MI (of Total) (slug ft^2)		
	Ablator	Adhesive	Sealer	F'Glas	Gasket	S/C Pads	Total	X_c	Y_c	Z_c	I_{xx}	I_{yy}	I_{zz}
Nose Cone	44.4	1.8	0.7	0.5	0.4	----	47.8	118.7	0	0.9	2.1	1.3	1.2
Forward	130.8	6.2	2.5	2.1	0.9	----	142.5	94.0	0	2.2	34.0	19.9	19.3
Crew	455.9	22.6	9.0	22.3	4.6	----	514.4	48.0	0	9.1	464.3	276.2	256.4
Aft	708.7	20.5	8.2	4.5	10.2	20.5	772.6	8.7	0	5.4	585.2	309.0	290.0
Totals	1339.8	51.1	20.4	29.4	16.1	20.5	1477.3	34.2	0	6.2	1087.5	920.9	879.5

1. $\rho = 31$ lb/ft^3
2. Perturbations are included for shear pads, windows, tower wells and scimitar antennae
3. An estimate of 3 percent for moisture absorbtion is included.

[redacted]

APOLLO ABLATOR WEIGHT

Item	Weight		
Forward Compartment	142.5		
5026-39/HC-G	130.8		
Fwd Compartment		117.0	
Tower Wells		10.8	
Leeward (2)			4.8
Windward (2)			6.0
Fwd Comp. Door		1.8	
Pitch Eng. Panel		1.2	
Closeout-Fiberglass	2.1		
Station 112.25		0.5	
Station 81.13		1.0	
Fwd Comp. Door		0.2	
Pitch Eng. Panel		0.1	
Fwd Compartment		0.3	
Adhesive - Ht-424	6.2		
Surface Sealer (Barrier Coat BR-C-8)	2.5		
Gasket - RTV 560 (Station 81.13)	0.9		

[redacted]

[redacted]

APOLLO ABLATOR WEIGHT

ITEM	WEIGHT		
Crew Compartment	514.4		
5026-39/HC-G		455.9	
Crew Comp.		352.8	
Crew Hatch		17.4	
Crew Hatch Win.		4.6	
Side Window (2)		10.3	
Docking Window (2)		18.3	
Sex., Teles. Door		8.5	
Maintenance Doors		33.3	
Type A 0°			4.0
Type A 180°			4.0
Type A 239°			2.4
Type A 301°			2.4
Type B 207° 30'			2.7
Type B 332° 30'			2.7
Type C 270°			2.7
Type E 45°			6.2
Type E 135°			6.2
A. C. Motors		10.7	
Pitch			2.1
Yaw (2)			4.4
Roll (2)			4.2
Closeout Members & Bolt Plug Sleeves (F'glas)		22.3	
Crew Compartment		8.1	
Crew Hatch		1.0	
Crew Hatch Win.		0.6	
Side Window (2)		1.3	
Docking Window (2)		1.8	
Sex., Telesc. Door		0.6	
Maintenance Doors (Fiberglass)		5.3	

[redacted]

[redacted]

APOLLO ABLATOR WEIGHT

ITEM	WEIGHT		
Type A 0°			0.7
Type A 180°			0.7
Type A 239°			0.5
Type A 301°			0.4
Type B 207° 30'			0.4
Type B 332° 30'			0.4
Type C 270°			0.4
Type E 45°			0.9
Type E 135°			0.9
A. C. Motors		3.6	
Pitch			0.7
Yaw			1.6
Roll (2)			1.3
Gaskets - RTV 560	4.6		
Crew Compt.		3.0	
Crew Hatch		0.4	
A. C. Motors		1.2	
Pitch			0.3
Yaw (2)			0.6
Roll (2)			0.3
Adhesive - HT 424	22.6		
Surface Sealer (Barrier Coat BR-C-8)	9.0		

[redacted]

[redacted]

APOLLO ABLATOR WEIGHT

ITEM	WEIGHT	
Aft Compartment	772.6	
5026-39/HC (Aft Compartment)	708.7	
Shear Pad (3)	20.5	
Closeout - Fiberglass	4.5	
Shear Pad (3)		0.6
C-Band (3)		1.0
Station 23.2		2.9
Gasket - RTV 560	10.2	
Station 23.2		9.3
C-Band		0.9
Adhesive - HT 424	20.5	
Surface Sealer (Barrier Coat BR-C-8)	8.2	

[redacted]

[redacted]

APOLLO ABLATOR WEIGHT

DETAIL BREAKDOWN

Item	Weight
Forward Nose Cone	47.8
5026-39/HC-G (Fwd Nose Cone)	44.4
Closeout-Fiberglass Station X_c = 112.25	0.5
Gasket - RTV 560 Station X_c = 112.25	0.4
Adhesive - HT 424	1.8
Surface Sealer Barrier Coat BR-C-8	0.7

4.0 Ground Test

The status of the thermal, structural and mechanical properties development testing is given in tables I, II, and III.

4.1 Structural Tests

During this reporting period, the significant tests conducted included: back-to-back cold soak panel tests, bolt plug tests, beam bending tests, zero stress beam tests, beam humidity tests. Details of these tests are reported in section IV.

4.2 Thermal Tests

Twenty-two turbulent pipe tests were conducted in the 10-Megawatt Air Arc Facility during this reporting period. The purposes of these experiments were as follows:

a. Parametric evaluation of filling the intercompartmental gap (seventeen samples). (5026-39/HC-G)

b. Reference Joint Evaluation (two samples) (5026-39/HC-G)

[redacted]

[redacted]

TABLE I

STATUS OF THERMAL OPTICAL
& ABLATION DEVELOPMENT TESTS

Type of Tests	Planned	Tested	Percent Completion
Thermal Conductivity	367	368	100
Specific Heat	137	136	99
Heat of Degradation	35	45	129
Optical Properties	279	446	160
Solar Simulation	100	116	116
Model 500 Arc (Q* and Ascent)	700	641	92
OVERS Stagnation Heating	894	722	81
OVERS Two-Dimensional	371	106	29
10-mw Arc Turbulent Pipes	337	170	50
Sequential Ablation	81	0	0
Total	3301	2750	83

[redacted]

[redacted]

TABLE II

STATUS OF STRUCTURAL DEVELOPMENT TESTS

Type of Tests	Planned	Tested	Percent Completion
Cold Soak Evaluation	37	93	250
Flat Panel Reentry	16	14	88
Temperature Gradient	21	26	124
Beams	8	22	275
Stress Concentration	32	21	66
Curved Panel Reentry	16	4	25
Panel Sequential & Cyclic	68	54	79
Special Design Problem	9	50	556
Dynamic Test	4	5	125
Repair Evaluation Tests	9	5	56
Total	220	294	134

[redacted]

[redacted]

TABLE III

STATUS OF MECHANICAL PROPERTIES DEVELOPMENT TESTS

Type of Tests	Planned	Tested	Percent Completion
Tension	2660	2664	100
Compression	1176	892	76
Shear	332	274	82.5
Thermal & Moisture Expansion	1024	504	49.2
Bond	1570	1674	106.7
Total	6762	6003	89

[redacted]

[redacted]

c. Evaluation of compatibility of main ablator (5026-39/HC-G) and gasket material (one sample)

d. Evaluation of interface between main ablator (5026-3/8HC-G) and C-band antenna window (one sample)

e. Differential ablator problem (one sample) (5026-39/HC-G)

Only the stream conditions at which the samples were exposed are reported. Sample temperature data recorded during the tests are currently being reduced.

The current series of OVERS stagnation tests (AP1308) 5026-39/HC-T, concerning the effects of oxidation on the thermal performance of the Apollo heat shield material, was completed. The four remaining specimens were tested in the OVERS facility during the March reporting period, and the performance data is included herein. In addition, surface temperature and radiation measurements are presented for tests in this series which were conducted and partially reported in the February 1964 Apollo Monthly Progress Report.

Eight instrumented, 5026-39/HC-G samples (AP-1551), and four instrumented 5026-39/M samples (AP1552), were also tested in the OVERS. The purpose of these tests is to provide internal temperature data for use in corroborating design analysis. Ablation data (length loss, weight loss, and char depth) and thermocouple measurements were obtained for each sample and are presented. Spectral radiant intensity measurements were also performed during the course of each test. Reduction of the data, however, is incomplete and, consequently, surface temperature, total radiation and emittance values are unavailable.

The model 500 ablation data for the silicone rubber RTV-560 and the phenolic fiberglass specimens are presented.

B. MATERIALS DEVELOPMENT AND MANUFACTURING

1.0 Materials Development

1.1 5026-39 Ablator Preparation

a. During this reporting period approximately 56 batches of ablator were prepared.

b. The use of a recorder to monitor batch temperatures has been stopped. Its use requires almost continuous correlation with the actual material temperature in the Hobart bowls. Each bowl recording has a slightly different correlation. The potted thermocouple wires are

[redacted]

[redacted]

often pulled out when the bowls are moved requiring recorrelation. Metal thermometers will be used to monitor future batches.

c. Mixing process charts have been posted above each Hobart mixer. These charts serve as an on spot guide and are especially valuable in training new operators.

1.2 Fabrication of Test Structures

a. Gunned 5026-39 H/C - Various cold soak, beam, toroidal and flat panels with and without splices have been fabricated during this reporting period.

1. Toroidal sections are being filled by the gun-push-gun method resulting in the best filling of toroidal honeycomb to date. This work, done on two inch thick honeycomb will be continued. Also work will commence on gunning 3 inch thick toroidal honeycomb.

2. Five special panels have been fabricated for NDT. These contain simulated defects of various kinds

b. Fiberglass Layups

1. Two 0.080-inch thick fiberglass retainers for the rendezvous window, crew compartment wooden mockup were fabricated and trimmed to size. These retainers were fabricated with 181 fiberglass fabric using a room temperature cure resin.

2. Approximately 6 feet of bolt plug sleeve material was fabricated using epoxy resin and fiber glass 181 cloth laid up around a metal mandrel. The layup was silica-tape wound, vacuum bagged and cured in accordance to RAD Spec. P-70057A. The sleeves were then machined and threaded to proper dimension.

c. Gaskets

Two RTV 560 silicone gaskets were fabricated with very good results. Before injecting RTV 560 material the top surrounding area was masked off and the gap area sealed with plexiglass and zinc chromate putty. The RTV 560 was injected through holes drilled in the plexiglass using a Semco Sealant Gun at approximately 30-35 psi. It was not necessary to use any vacuum. X-rays of the gaskets revealed one small void in each gasket plus 2 tiny metallic inclusions.

Repairs will be made to one gasket which will then be bonded into the forward compartment mockup door.

[redacted]

[redacted]

d. Moisture Barrier Coatings

Approximately 20 experimental panels have been coated in accordance with RAD P-70063. This is a 3 coat operation, 1 epoxy sealer coat and two vinyl top coats.

e. Repairs

Approximately 10 gunned panels were repaired during this report period in accordance with RAD G-70002. Repairs include a) Side wall voids b) Low density surface voids c) Missed cells and d) Small pin hole voids.

Tests are underway to determine the tensile strength of gunned honeycomb which has been held 21 days before curing. This will be compared with results of a 1 day lag between gunning and curing. It has previously been determined that there is little variation in tensiles with up to 16 days gun/cure lag.

1.3 Facilities and Mechanization

a. Some difficulties have developed in the electro-mechanical temperature selectors of the Apollo Blue "M" ovens. Signs of wear in these devices have prompted the purchase of a stand-by replacement component.

b. The large Young and Bertke Apollo ovens have been contaminated from material (paper, dust, etc.) believed to be lodged in the duct work. These ovens are being purged and if this does not completely relieve this situation the sealed ducts will be opened for cleaning.

c. The 250 ton Apollo press although operable for pressing has required repair of the electric platen heating elements. Repair and reinstallation of these elements should be completed by April, 1964.

d. Work on an automatic stuffer (ablator into cartridges) has been resumed. The screw extruder method will be delayed in favor of the more promising pressure cutting method. Equipment is being fabricated for this latter method.

e. The revised Apollo overhead gunning spider fixture has been completed. This new design gives maximum width for gunning. The control panel mounted on the column, instead of on the frame, incorporates both a voltmeter and an ammeter to control the gun heat. Filtered air in the new manifold affords air nozzles for cleaning parts without interfering with the gun's air pressures. The shallow design of the new structure permits a much higher elevation and should result in much less confusion to the gunners because of dangling wires and hoses.

[redacted]

[redacted]

A panel composed of stainless steel substructure, fiberglass honeycomb and fiberglass honeycomb closeout members has been fabricated by the Pilot Plant for the purpose of evaluating known procedures for inspection of the bonds involved. It was noted that the ultrasonic through transmission technique that will be used to inspect the fiberglass honeycomb to substructure bond is applicable in all instances except where spot welding in used to attach the stainless steel closeout member. Visual inspection of the closeout member to substructure bond can be performed at the outer exposed edges.

Manufactureres of NDT equipment are being surveyed for a small diameter pencil transducer suitable for inserting down into the fiberglass honeycomb to inspect the fiberglass closeout member to substructure bond.

The abort tower well ablator, 5026-39M, can be adequately inspected with current radiographic techniques for voids, inclusions, and fiber clumps. Radiography can also be used for the detection of voids in the bonding material (Silgard) used to bond the abort tower well ablator to its substructure. Voids as small as 0.050 inch diameter by 0.050 inch in thickness can be detected.

The ultrasonic methods normally employed for bond inspection were found to be unsatisfactory for the 5026-39M material to substructure bond. The high acoustic attenuation of the heat shield material prevents techniques which require that an ultrasonic wave propagate through the heat shield from being used.

The choice of ultrasonic techniques are limited to those dealing with inspection from the substructure side. The wide difference in acoustical impedance that the ultrasound encounters in going from the substructure to the layer of Silgard eliminates the longitudinal pulse echo and ringing technique.

Collimators have been designed and fabricated for use on the PG 200 X-ray unit (for process control radiography of green ablator) and for use on the 150 Norelco X-ray unit (for final inspection). Approximately 100 radiographs have been made in the interest of establishing reference standards of interpretation.

[redacted]

[redacted]

2.0 Manufacturing

2.1 Manufacturing Engineering

Approximately 90 percent of the Apollo tooling is now complete and manufacturing effort is being applied to tooling requirements resulting from "N" and "P" changes.

Manufacturing engineering inputs for coordinating numerical control for the Betts V. T. L. continue on schedule.

Bills of material and process sheets for detail parts and vehicle assembly are being updated to reflect latest revisions and E. C. actions.

Training of manufacturing personnel is continuing on prefit, layup, bonding and gunning using the steel crew compartment mockup.

2.2 Tool Fabrication

A second gunning fixture is in fabrication. Fixture bases are being modified to reflect better manufacturing techniques found during mockup fabrication.

Rework of sealing rings is progressing on schedule.

Miscellaneous tools such as special drills, counter bores, hole saw adapters, and honeycomb cutters are being fabricated.

2.3 Raw Materials and Material Preparation

Purchase orders have been placed for approximately 95 percent of the raw material requirements.

Approximately 75 percent of raw material requirements for vehicles 006 & 009 with back up are in-house.

First shipment of production honeycomb core has been received, with balance for first two vehicles scheduled for delivery during next reporting period.

Detail parts fabrication will continue per production schedule, and as molds are modified per EC's and mandatory change requirements.

[redacted]

C. RELIABILITY AND QUALITY

1.0 Reliability

The reliability assessment model is being revised and updated so as to develop an estimate of the maximum back face temperature, in each region considered, for several trajectories. Those regions will be subdivided into 35 nodes, 21 of which represent the ablative material.

Test cases are being run on the IBM 1401 computer to check the accuracy and running time of a revised computer program written to process statistical and reliability analyses on back face temperature control.

Statistical Support service has included these more important activities:

a. An error analysis of the heat of ablation (q*) versus air enthalpy (H/RTO) test data derived from the model 500 ablator apparatus was initiated during the reporting period.

b. Preliminary tasks were completed in the analysis of tensile, compression, shear, and thermal strain properties of laminated phenolic fiberglass material. Definitive analyses will be performed upon receipt of all applicable test data of the test program.

c. Preliminary regression analyses are in process in the evaluation of mechanical versus chemistry data of the 5026-39 honeycomb (gunned) material.

2.0 Quality

The fluoroscopic unit for the detection of metallic inclusions in Avcoat 5026-39 material before gunning has been installed at the Lowell facility.

The preliminary Index B for Apollo Spacecraft 009 has been completed and released. The index will be amended and updated as EC or specification changes are made. Thirteen Quality Assurance Test Procedures have been released to date.

The four additional stainless steel substructure flat panels have been received from Avco-Nashville and are at incoming inspection.

Weekly meetings with Quality Control were initiated this month to review released specifications and to revise them as necessary to comply with current requirements and practices.

Qualification Test Procedures detailing the tests to be performed are flat panels, Abort Power wells and special samples have been reviewed and are being published. Submission to NAA is scheduled for 27 March.

Many molds have been received from the Nashville Division and discharged after inspection for manufacturing use. In-house tool manufacturing is being performed under the surveillance of Quality Control. Several Engineering changes have been incorporated into many edgemember molds and inspected in accordance with the requirements. As the Engineering Changes are being incorporated and inspected, records are also being maintained to indicate the latest configuration of each tool. The inspection of tools and fixtures will continue during the incorporation of ACP's - 008, 015, and 017. It is expected that the CG fixture will be positioned permanently in this coming period and followed with the calibration of scales and try-out on the crew compartment.

The full size crew compartment mockup is now being inspected for the fitting of the edgemembers and the fiber glass honeycomb core to the substructure prior to cleaning and bonding. All deviations have been recorded and reported for Engineering action. Considerable rework is being made to replace the detail parts that do not properly fit the substructure.

The forward compartment is currently being machined to proof the machining technique and tools.

Over 200 edgemembers intended for the first deliverable vehicle have been submitted for inspection. These edgemembers are being inspected for conformance to outside mold line and the integrity of the material only. Excess stock is being left until the prefit takes place and at which time the trimming will be done. Process controls are being maintained during fabrication to assure that controlled materials are being used and that proper curing cycle is accomplished.

D. DOCUMENTATION

During the month of March, the following reports were submitted to NAA/S&ID:

Monthly Progress Report (March 9, 1964)
(RAD-SR-64-73)
PERT Reports
Monthly Financial Management Report
Monthly Financial Management TWX Report
Monthly Subcontracts Report
Weekly Status Reports
Monthly Milestone Status Report
Aerodynamics Final Report, RAD-SR-64-55
(18 March 1964)

[redacted]

II. PROBLEMS AND ACTIONS

The problems presented in this section are those which threaten to impair program implementation in accordance with schedule requirements. The decisions, inputs, or other actions required to solve each problem area are presented. This section does not attempt to identify all areas that require further definition and coordination, but rather those areas requiring action within the immediate future.

A. VEHICLE DESIGN

1.0 Aerothermodynamics

a. Problem

Before adequate calculations can be performed to obtain temperature histories at interface areas for trajectories other than HSE-3A, heating at the 196 additional points is required for trajectories HSE-1, HSE-2, HSE-4A, HSE-6, and HSA-3.

Action

These data were requested through an action item at the March T. I. M.

b. Problem

Two-dimensional analyses, in the following areas, are being delayed pending receipt of interface temperature histories:

1. Crew compartment C-Band antenna
2. S/M-C/M umbilical
3. Air vent
4. Oxidizer dump
5. Windward scimitar antenna
6. Leeward scimitar antenna

Action

Interface temperature data have been requested from NAA/S&ID (Apollo MPR, 9 March 1964) for all NAA/Avco interface areas. Definition of 1. D

[redacted]

[redacted]

temperatures 1.0 inch away from each interface was provided in R&D/DMM/30.

c. Problem

Reentry heating discrepancies exist on the forward compartment nose cone.

Action

Clarification of these discrepancies was requested in R&D/DMM/26 dated 7 January 1964.

d. Problem

Overheating has been found to exist at several RCS engine interfaces.

Action

Avco has informed (January T.I.M.) NAA that NAA two-dimensional temperature histories at the following interface areas exceed 600° F:

1. RCS Positive Pitch Engine Aperture
2. RCS Negative Pitch Engine Aperture
3. RCS Yaw Engine
4. RCS Roll Engine

NAA stated that a change can be expected correcting this overheating.

2.0 Structural Studies

a. Problems

The forward-to-crew compartment interference and associated gaps at $X_c = 81$ are dependent upon the preload and spring constant of the springs at the thrusters. NAA presented preliminary values for the preload and spring constant at the 26 to 27 September 1963 technical interchange meeting, but Avco pointed out that such springs do not satisfy the vibration environment in the Procurement Specification. At the 5 to 6 March 1964 technical interchange meeting NAA stated that the springs are adequate for the vibration environment and requested that Avco present its analysis showing the problem area.

Action:

A letter is in preparation presenting Avco's analyses.

[redacted]

[redacted]

b. Problem

As indicated in sections I and IV of the 9 November monthly progress report, the deformations of the crew compartment edge closure ring at X_c = 81 above the astro-sextant panel are of such a magnitude that it will not be possible to close the doors when the command module is at a temperature of -260° F.

Action

A letter was sent informing NAA of this situation. The problem has also been listed in section II of the 9 March 1964 monthly progress report.

c. Problem

Current structural design data required by Avco and not yet supplied by NAA are listed below:

1. Current loads on the compression pads and shear-compression pads reflecting the flexibility of the C/M and S/M structures.

2. Interaction loads applied to the ablator at discontinuities such as C-band antennas, nozzle extensions, steam vent, air vent, umbilical, etc.

3. The following thermomechanical properties of Marinite 65 over the temperature range -65° F to +600° F:

a) Tension modulus

b) Compression modulus

c) Tensile Strength

d) Compressive strength

e) Tensile strain to failure

f) Coefficient of thermal expansion

g) Poisson's ratio

h) Shear strength

[redacted]

[redacted]

Action

These items were reviewed with NAA at the 22 to 23 August 1963 technical interchange meeting, and Avco's need for the data was reiterated at the 26 to 27 September 1963 and 5 to 6 March 1964 technical interchange meetings. The problem has been carried in section II of all monthly progress reports since November 1963.

d. Problem

The results of Avco's analyses of the gap at X_c = 81 for a space flight environment of -260° F which were presented at the September and November 1963 technical interchange meetings show that it is not possible to effect a solution of the gap problem for this environment by means of a simple gasket. The gap filler required for a -260° F environment cannot be designed according to schedules for the first four airframes.

Action

NAA was informed of this problem at the November 1963 meeting and by letter. The problem has been carried in section II of all monthly progress reports since January 1964.

e. Problem

Avco has updated analyses on the shear-compression pads for the present loads. Results indicate that, with the present design, an increase of attachment bolt size to 3/8 inch diameter is required and that an increase in the minimum preload from 14, 500 to 21, 500 pounds limit is required.

Action

NAA was informed of this at the January 1964 technical interchange meeting. A letter was also prepared informing NAA of this situation, and a copy of Avco's analyses was transmitted to NAA. The problem was listed in the February and March 1964 monthly progress reports.

f. Problem

As shown on drawing V16-932003 "Structures Diagram Heat Shield, " it is not clear as to whether the crushable cores 1, 2, 3 and 4 located between X_c = 23. 2 and X_c = 43. 4 are attached to the heat shield or not. If there is an attachment to the heat shield, detailed information of the core material and method and location of attachment will be necessary for crew compartment analysis.

[redacted]

[redacted]

Action

A letter is being sent to NAA regarding this situation.

g. Problem

Frames 4 and 7 in the area X_c = 23.2 to 43.4, as shown on drawing V16-932003, revision P, "Structures Diagram Heat Shield," are not clearly defined. Detail drawings of these frames will be necessary for analyses in this area.

Action

A letter is being sent to NAA regarding this situation.

h. Problem

Analyses of the aft compartment heat shield to include the new moment tie design as given in the "P" revision of the Structures Diagram are being delayed because of lack of detailed drawings of the moment tie.

Action

A letter is being prepared requesting these drawings from NAA.

i. Problem

Definition of the space flight temperature distributions of the moment tie in the aft compartment is required to perform aft compartment thermostructural analyses.

Action

Avco requested NAA to provide this information at the 5 to 6 March 1964 technical interchange meeting. In addition, a letter is being prepared detailing the conditions needed.

j. Problem

Definition of the space flight temperature distributions of the aft compartment inside and neighboring the service module is required to perform thermostructural analyses of the aft compartment.

Action

A letter is being prepared requesting this information from NAA.

[redacted]

[redacted]

k. Problem

Face skin buckling has been defined as a failure for the Failure Criteria Test Program. To insure the validity of the test results Avco needs the ultimate compressive stress values based on intercell buckling for the substructure face skins as a function of temperature to -260° F.

Action

A letter is being prepared requesting this information from NAA.

3.0 Design

a. Problem

An overhang of approximately 1.0 inch of Avcoat 5026-39M ablator exists on one of the rendezvous window frames.

Action

Avco is still studying this situation. A NAA design change may be requested.

b. Problem

Short edge distances existing on the NAA rendezvous window frame make it impossible to use standard bolt plugs in some locations.

Action

New, smaller diameter bolt plugs will be used in this area.

c. Problem

Avco has not received verification from NAA that a substructure access port to the crew hatch mechanism exists and that Avco is required to provide access to this port.

Action

NAA to provide verification and drawings of structural details in this area.

d. Problem

Avco lacks definition of forward pitch engine rocket nozzle orifice extension through the loose panel.

[redacted]

[redacted]

Action

Avco forwarded to NAA under cover letter LA-5465, Study Forward Compartment pitch engine, definition of the problem in this area. No response has been received.

e. Problem

NAA does not define dimensionally the location or size of the five fasteners shown pictorially for the loose panel.

Action

Avco continues to show four fasteners on production drawings. NAA to define fastener sizes and locations.

f. Problem

The forward pitch engine nozzle extensions (Rocketdyne 207601 and 206919) are not long enough for the revised ablator thicknesses.

Action

NAA must revise Rocketdyne drawings to reflect new ablator thicknesses.

g. Problem

Due to the change of tolerances on the machined surfaces of the tower well castings, a sharp corner can exist at the intersection of the tower well floor and the OML.

Action

Avco requests that a corner radius of 0.32 be used.

h. Problem

V16-326265 Rev. B, Intercompartment Ring (X_c = 112.25) produces a possible mismatch of 0.043 inch with the forward compartment ring.

Action

Avco requests clarification of this area.

i. Problem

An updated drawing list including effectivities is needed.

[redacted]

[redacted]

Action

NAA to supply updated drawing list.

j. Problem

The shear pad thickness of 2.625 inches is 0.375 inch less than the thickness of the surrounding ablator at pad 1.

Action

The ablator will be machined flat in the shear pad area with the result that the substructure temperature will exceed 600° F.

k. Problem

The NAA aft compartment attachment bolt receptacle flange which extends beyond the ablator OML interferes with the Avco closeouts around the compression pads. Drawing Sk - 9791A was transmitted to NAA at the March T. I. M. which clearly defined this problem.

Action

1. Avco will consider compression pads of different diameters in an effort to meet present schedules with a workable solution. It appears that a pad diameter of 5-1/2 inches is most satisfactory.

2. NAA should consider substructure redesign in this area and in particular relocation of those aft compartment attach bolts adjacent to the compression pads.

4.0 Manufacturing

Problem:

Inability of vendor to supply good fiberglass billets for shear pads could cause schedule problems. Vendor expects, however, to correct problem as soon as new compression mold is complete.

[redacted]

[redacted]

III. FORECAST

A. VEHICLE DESIGN

1.0 Aerothermodynamics

1.1 Thermal Design

Mass loss and shape change history calculations will be continued for all trajectories.

Temperature histories at interface areas for the remaining trajectories will be continued.

The revised edge member analysis will be completed.

Analyses of voids will continue. Analyses will be conducted at several stations, utilizing various void sizes and locations in depth. Two-dimensional analyses will be included at one or more of these stations utilizing the Thermal Analyzer Program. Work will continue in investigating voids in the RTV-560 gasket material using one and two-dimensional analyses.

The determination of the radiation view factors for the escape tower wells will be completed.

Ablator thickness increases associated with the abort tower attach rods will be established to ensure that the surrounding substructure does not overheat.

Thermal analysis of the aft compartment attach bolt plugs will be completed.

1.1.1 Two-dimensional areas

Analysis of the edges of the abort tower wells will continue. Side and forward edge analyses are in progress.

The two-dimensional matrix for the analysis of the NAA/Avco interface in the base of the windward abort tower well will be completed.

The two-dimensional thermal analysis of the intercompartmental gap at $X_c = 23.2$ will be completed.

Check-out cases will be run for all completed interface matrices.

Work will be continued on the analysis of the rendezvous window and window frame.

[redacted]

[redacted]

1.2 Analytical Methods

Calculation of pressure histories for every body station during reentry on HSE-3A will be completed during the next month.

Additional data on combined heating tests will be analyzed and compared with convective heating data correlations.

A q*- H curve based on OVERS test data will be completed.

Temperature histories will be obtained for a number of OVERS tests using the present design technique with upper and lower bounds on the T_{WALL}-q_c correlation.

Work will continue in evaluating the ψ technique for combined convective and radiant heating.

Initial efforts will be made to introduce charring effects into digital computer program 1600.

Additional analysis will be performed for radiant heating of Avcoat 5026-39/HC-G in the Solar Furnace. Future data will include the measurements of the heat flux reradiated by the specimen surface. This will allow calculation of q* based on net heating of the specimen, and also surface temperature.

A study of the effects of shear and oxygen content upon surface recession will begin. Data from OVERS and Model 500 tests on the gunned material will be analyzed as they become available.

1.3 Test Planning and Analysis

The analysis of experimental data showing the effects of differential ablation on local heating increases for Avcoat 5026-39/HC-G will continue.

OVERS splash data showing the thermal response of Avcoat 5026-39/HC-G will be compiled.

The evaluation of high enthalpy OVERS splash data for Avcoat 5026-39/HC-T will be completed.

2.0 Structural Studies

2.1 Unsymmetrical Load Analysis of Aft Compartment

The present model will be checked out and compared to results of known classical solutions.

[redacted]

[redacted]

2.2 Updating Aft Compartment Analyses

Aft compartment thermostructural analyses are being updated to include the latest Avcoat 5026-39/HC-G properties, ablator thicknesses and the moment tie design revision.

2.3 Intercompartmental Gap at $X_c = 81$

The reentry study will continue in order to define the maximum meridional gap during the reentry trajectory.

2.4 Forward Compartment Fabrication Deformation

The fabrication deformations analysis for the forward compartment and forward nose cone will be complete.

2.5 Fabrication Deformation-Crew Compartment

The analysis for the fabrication deformation of the crew compartment will be complete.

2.6 Crew Hatch Analysis

The analysis for the crew hatch-heat shield interactions will be 75 percent complete.

2.7 Scalloping Analysis at $X_c = 23.2$

The analysis to determine the amount of scalloping at $X_c = 23.2$ will be complete.

2.8 Ablator Reentry Analysis

Work will continue on the reentry analyses described in the 9 March 1964 monthly progress report.

2.9 Failure Criteria Analysis Effort

Preliminary results of the cracked heat shield analyses will be available for comparison with beam bending test data.

3.0 Design

3.1 Forecast

Use of engineering mockups to aid in the solution of design problems will continue with concentration on the rendezvous window and the forward pitch

[redacted]

[redacted]

engine panel. Revisions of the Avco design made necessary by the implementation of the 'P' change will also continue. Total release of all drawings except window retrofit panels for vehicle 006 reflecting the 'P' change is scheduled for mid-April.

Preparation of the interface control drawings and design support of the instrumentation installation program will continue. Creation of detail drawings for vehicles 008 and 011 will begin.

4.0 Ground Test

4.1 Structural Tests:

4.1.1 Twelve ablator failure criteria beam tests. Test period, 1 April to 20 April 1964.

4.1.2 Flat cold reentry test. Test period, 1 April to 15 April 1964.

4.1.3 Six vibration beam tests. Test period, 1 April to 20 April 1964.

4.1.4 Ten ablator failure criteria tensile tests. Test period, 10 April to 30 April 1964.

4.1.5 Toroidal pipe test. Test period, 16 April to 30 April 1964.

4.2 Thermal Tests

Testing will continue on a series of eighty-five 5026-39/HC-G OVERS splash specimens (AP1683). Thirty of these are in the process of being instrumented with thermocouples. The AP1683 specimens will be employed in tests designed to provide experimental data for the following purposes:

a) Laminar-q* correlations

b) Verification of the analytical model

c) Oxidation studies

d) Radiation studies.

Analysis of the OVERS splash experimental data, obtained from the AP1308 test series (effects of oxidation), will be continued.

Several more RTV-560 and phenolic fiberglass specimens will be tested in the model 500 facility. These data will extend the test enthalpy range covered and a statistical analysis will be performed on all the data.

[redacted]

[redacted]

B. MATERIALS DEVELOPMENT AND MANUFACTURING

1.0 Materials Development

The inspection of the crew compartment will continue throughout the manufacturing process. After the bonding of the edgemembers and honeycomb core to the structure is complete, an ultrasonic inspection will be performed as required to the applicable specification and QATP. During this period it is also expected that the thickness measurement technique will be employed on the forward compartment and prove the eddy current technique.

C. DOCUMENTATION AND PROGRAM MANAGEMENT

During the month of January it is anticipated that the following documents will be submitted to NAA/S&ID:

Monthly Progress Report
PERT Reports
Monthly Financial Management Report
Monthly Financial Management TWX Report
Monthly Subcontracts Report
Monthly Milestone Status Report
Weekly Status Reports.

[redacted]

[redacted]

IV. ANALYSIS

A. VEHICLE DESIGN

1.0 Aerothermodynamics

1.1 Thermal Design

1.1.1 Main Ablator

1.1.1.1 Thickness definition

There is no change of main ablator thicknesses to report at this time. The reference design ablator thicknesses are specified in the Monthly Progress Report dated 9 February 1964.

1.1.1.2 Mass loss histories

Definitions of mass loss and shape change were completed at 62 vehicle locations for trajectory HSE-3A. Surface mass loss includes recession due to both convective and radiant heating (where applicable). The internal decomposition is approximated by tracing the penetration of the 1000°F isotherm. Figures 1 through 5 show mass loss and shape change histories at 5 representative vehicle locations. Table V summarizes the total mass loss and shape change for all 62 points. When available, the histories at all 62 locations will be forwarded to NAA/S&ID.

1.1.1.3 Analysis of voids

During this report period, a Thermal Analyzer Program 1459, was made available for simultaneous analysis of conduction, radiation, and convection between internal nodes. Earlier void analyses employed a conduction analysis and a hand calculation to account for radiation across the void. Program 1459 was studied to determine its adaptability to the void analysis, and it was concluded that future analyses will make use of this aid. A one-dimensional analysis was begun at Station 222 with this new program. Results will be available within the next report period and will be compared to previous calculations. Steps are being taken to determine best node sizes to ensure accuracy with a minimum computer run time. A two-dimensional matrix is also being set up which will utilize this program.

A void analysis was also begun for the RTV-560 gasket material. A one-dimensional analysis is in the process of being set up. A

[redacted]

[redacted]

shear compression pad has been designated as a typical high heating location to analyze the RTV-560 gasket.

1.1.2 Two-Dimensional Areas

1.1.2.1 Side window analysis

A two-dimensional thermal analysis has been completed for the side window and window frame. The matrix for this analysis is shown in figure 6.

The analysis considered the effect of variable thermal properties of the gunned ablator material. Heating per SEM 137 was applied to the glass surface, and unperturbed HSE-3A heating applied to the ablator and Min-k-2000 surface. Ablator reentry thickness protection was provided to the outer frame in all directions where there was a heated surface. Ablator thicknesses were those given in the Apollo MPR dated 9 March, 1964.

The results in the form of temperature histories at three locations are shown in figure 7. There is no substructure overheating at any time during reentry. This is due to:

(a) Low quartz temperatures which result in added heat sink beneath the outer frame,

(b) Use of outer frame only in 1-D design, thus no utilization of added thermal capacity of inner frame.

(c) Use of actual substructure face sheets (0.04 and 0.06 inch thick) in the 2-D analysis, where the 1-D design for area assumes nominal substructure face sheets (0.008 and 0.008 inch).

1.2 Analytical Method

Additional preliminary test results were obtained for Avcoat 5026-39/HC-G subjected to radiant heating in the Solar Furnace. All these tests were run in air at one atmosphere. Table IV presents the test conditions. Figures 8 through 12 present plots of length loss versus test time for each heat flux level. The same technique outlined last month was used to reduce the data. Namely, a least squares straight line was fitted through the length loss versus test time data at each heat flux level. The slope of this line is then the ablation rate (s) at that heat flux level. From this (s) the cold wall thermochemical heat of ablation (q^*_{cw}) can be calculated from:

$$q^*_{cw} = \frac{\alpha \dot{q}_r}{\rho_s \dot{s}} \left(\frac{\text{Btu}}{\text{lb}}\right)$$

[redacted]

[redacted]

TABLE IV

ABLATION DATA FOR THE RADIANT HEATING OF AVCOAT 5026-39/HC-G

Date	Run No.	q_r $\left(\frac{Btu}{ft^2\text{-sec}}\right)$	Exposure Time (seconds)
2/4/64	6	278	15
2/4/64	8	285	15
2/14/64	10	278	15
1/22/64	2	564	15
1/27/64	6	505	15
2/13/64	1	483	15
2/14/64	1	490	15
2/14/64	2	498	15
2/14/64	3	498	15
2/15/64	1	509	7
2/12/64	10	479	15
1/17/64	1	776	10
1/22/64	9	769	15
2/14/64	5	787	15
2/15/64	2	805	15
2/12/64	1	838	15
2/12/64	7	776	15
1/22/64	4	1080	15
2/14/64	6	1127	15
2/15/64	3	1098	15
2/12/64	2	1098	15
2/4/64	1	1387	15
2/4/64	2	1431	15
2/4/64	3	1427	15
2/24/64	8	1402	15
2/12/64	4	1402	15

[redacted]

[redacted]

TABLE V

PRELIMINARY MASS LOSS FOR THE APOLLO COMMAND MODULE
TRAJECTORY HSE-3A

Heating Location No.	Theta (degrees) 0° = Windward	X_c (inches)	Total Mass (lbs/ft^2)
100	Origin of C/M	0	2.04
101	0	4.59	3.20
103	22.5		3.08
105	45		2.44
107	90		1.73
109	135		1.60
111	180.0	4.59	1.92
200	0	15.495	4.30
202	22.5		4.15
204	45		3.65
206	90		2.02
208	135		1.88
210	180	15.495	1.12
222	0	18.0	5.07
224	22.5		3.73
226	45		3.51
228	90		2.00
230	135		1.70
232	180.0	18.0	0.49
244	0	20.0	1.99
246	22.5		1.82
248	45		1.87
250	90		0.71
252	135		0.20
254	180	20.0	0.165
300	0	23.875	1.82
302	22.5		1.38
304	45		1.18
306	90		0.257
308	135		0.118
310	180	23.875	0.084
311	0	30.0	0.87
312	22.5		0.815
313	45		0.415
315	90		0.145

[redacted]

[redacted]

TABLE V (Concl'd)

Heating Location No.	Theta (degrees) 0° = Windward	X_c (inches)	Total Mass (lbs/ft^2)
317	135	30.0	0.025
319	180	30.0	0.008
338	0	48.0	0.696
339	22.5		0.595
340	45		0.36
342	90		0.15
344	135		0.031
346	180	48.0	0.04
356	0	68.0	0.515
357	22.5		0.46
358	45		0.295
360	90		0.165
362	135		0.041
364	180	68.0	0.123
400	0	88	0.385
401	22.5		0.365
402	45		0.25
404	90		0.128
406	135		0.033
408	180	88	0.123
418	0	107	0.25
500	0	115.347	0.25
501	22.5		0.235
502	45		0.195
504	90		0.128
506	135		0.107
508	180.0	115.347	0.15

[redacted]

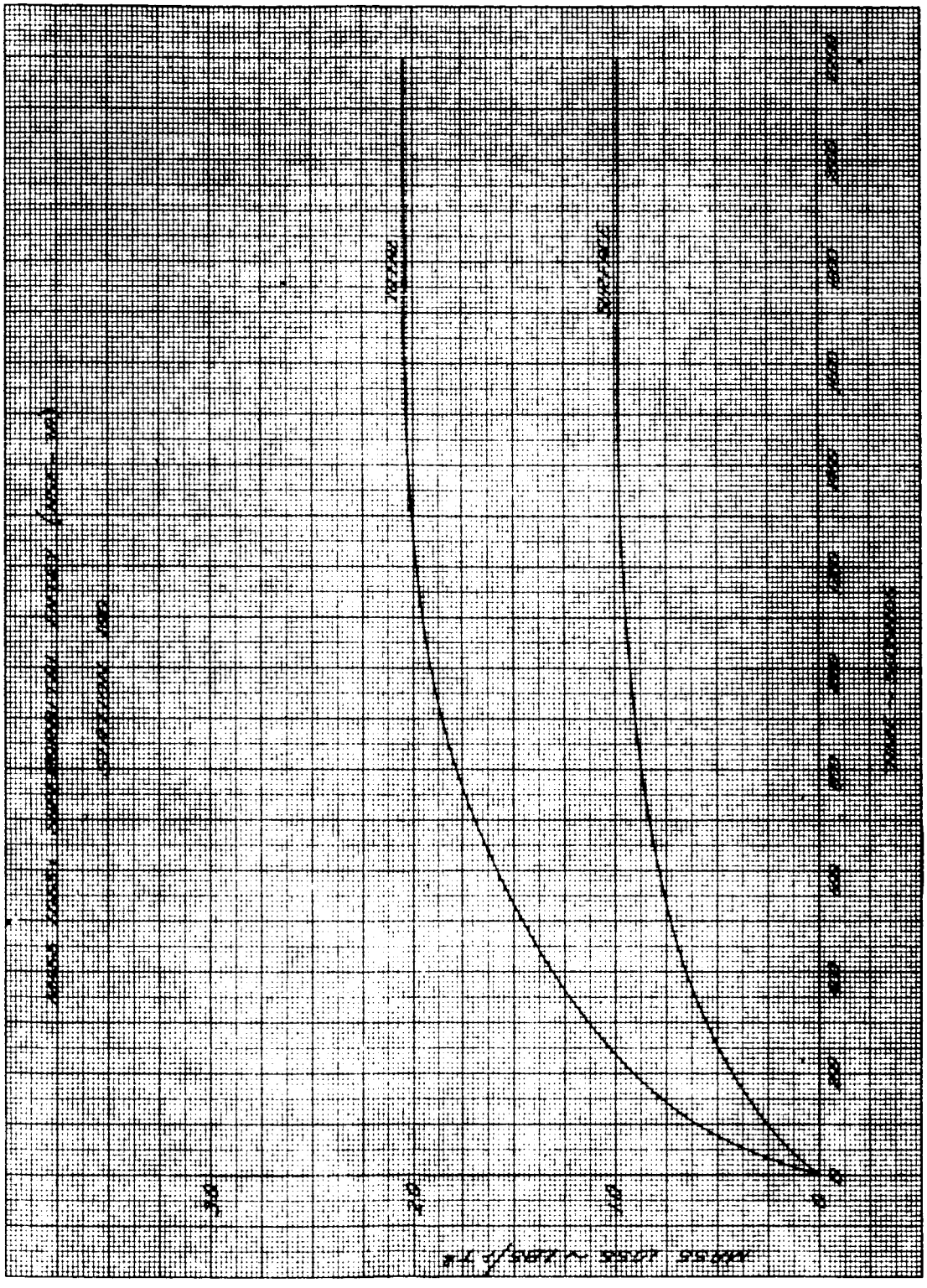

Figure 1 MASS LOSS: SUPERORBITAL ENTRY (HSE-3A) STATION 100

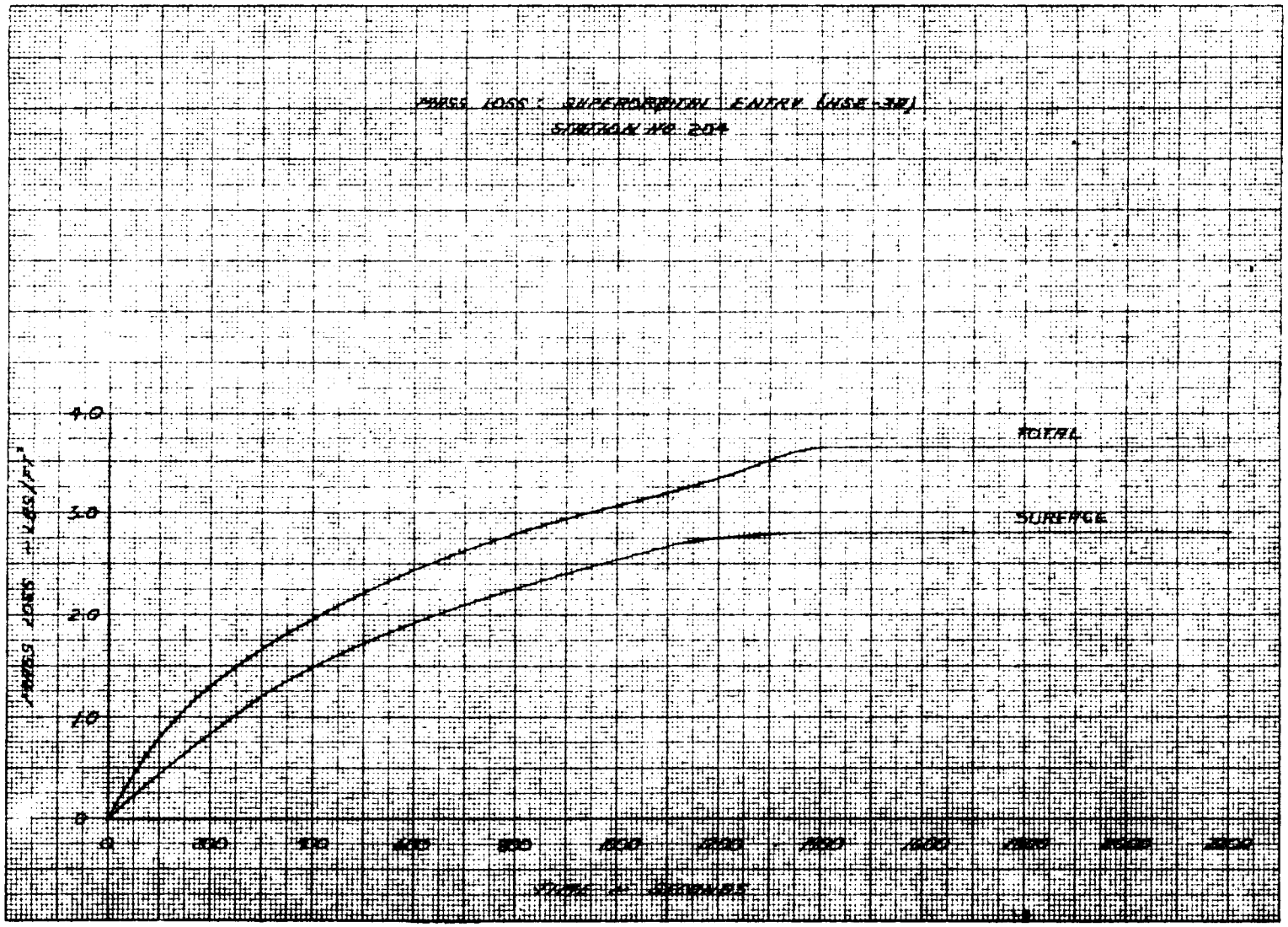

Figure 2 MASS LOSS: SUPERORBITAL ENTRY (HSE-3A) STATION 204

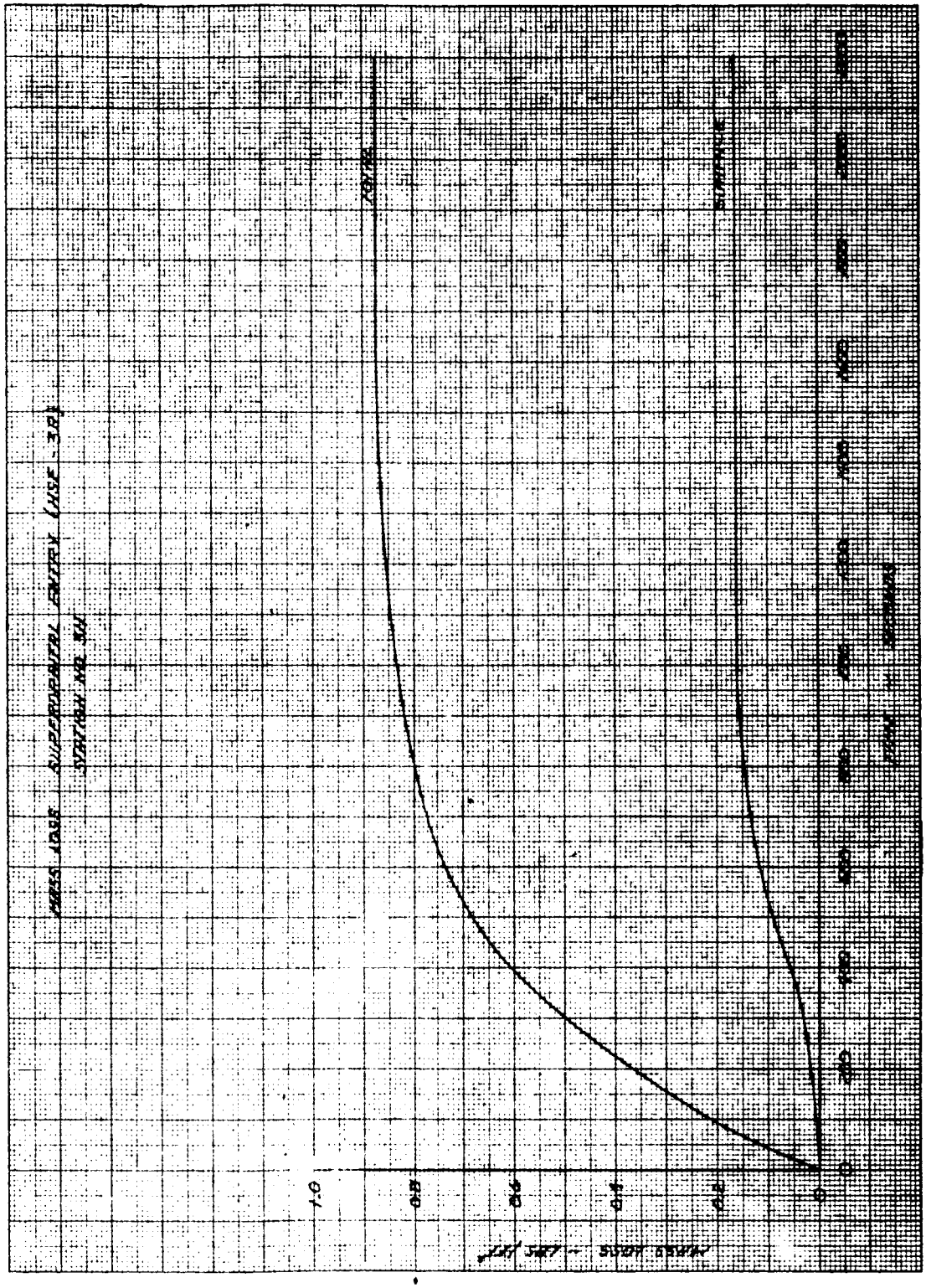

Figure 3 MASS LOSS: SUPERORBITAL ENTRY (HSE-3A) STATION 311

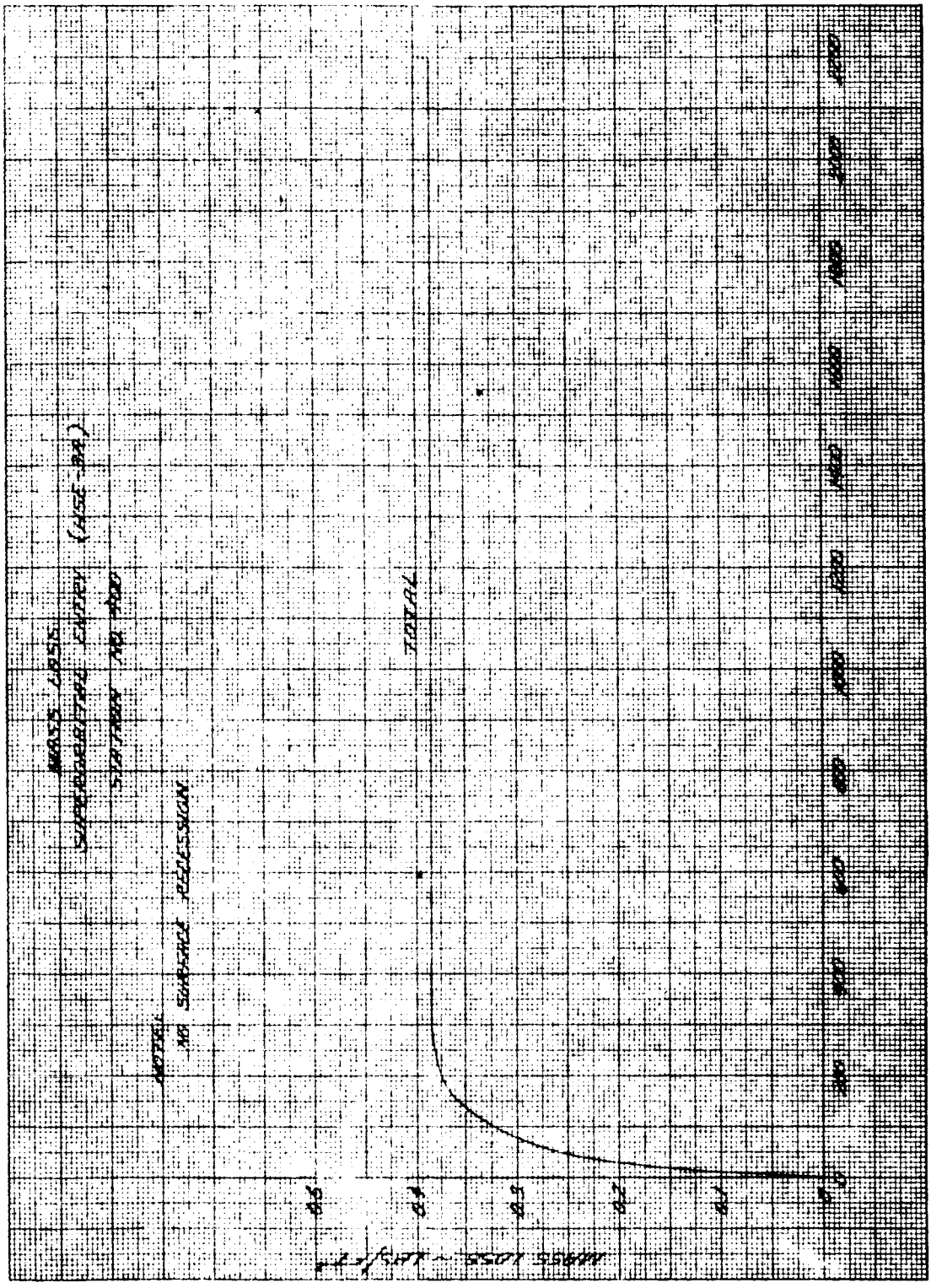

Figure 4 MASS LOSS: SUPERORBITAL ENTRY (HSE-3A) STATION 400

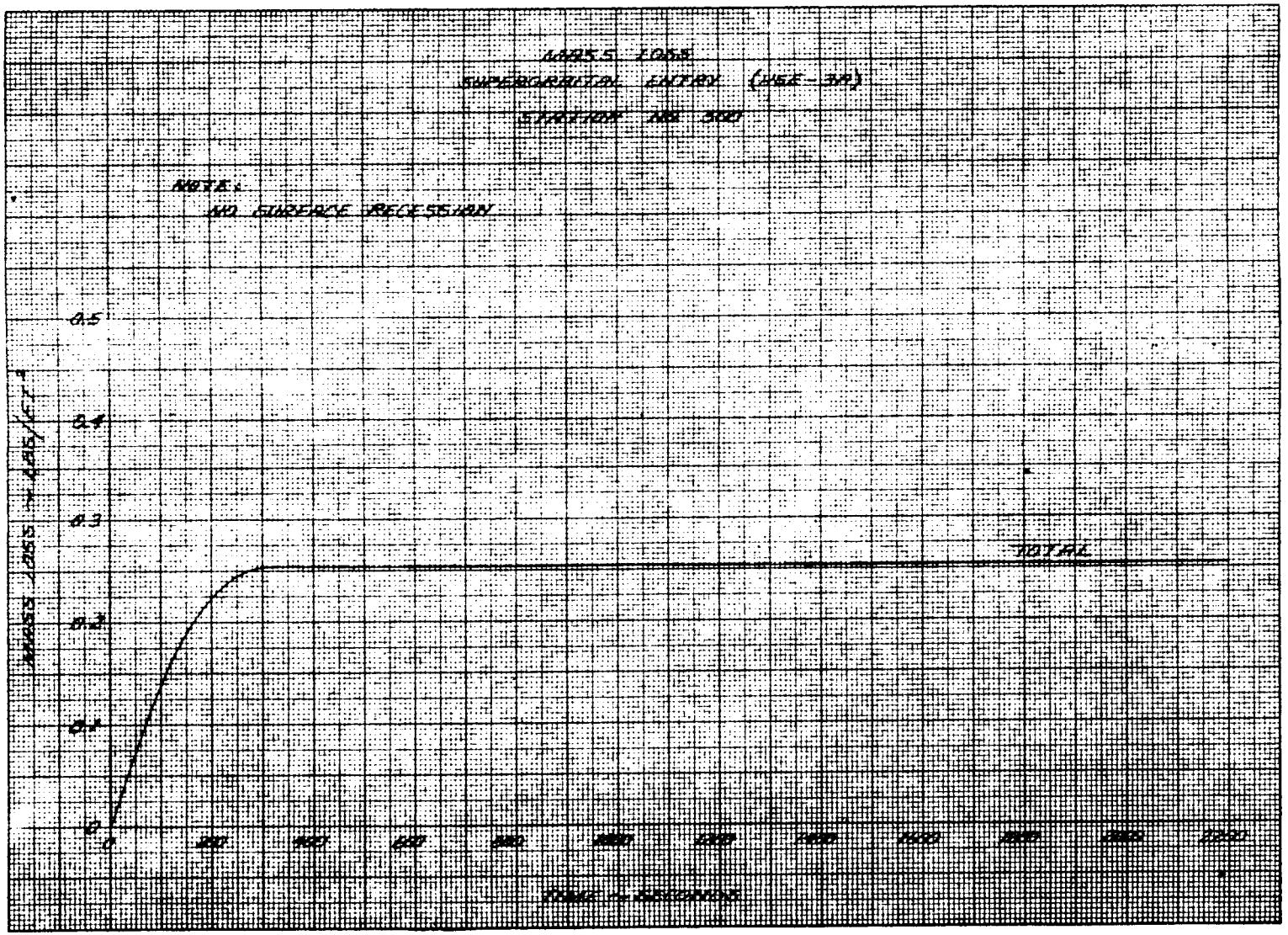

Figure 5 MASS LOSS: SUPERORBITAL ENTRY (HSE-3A) STATION 500

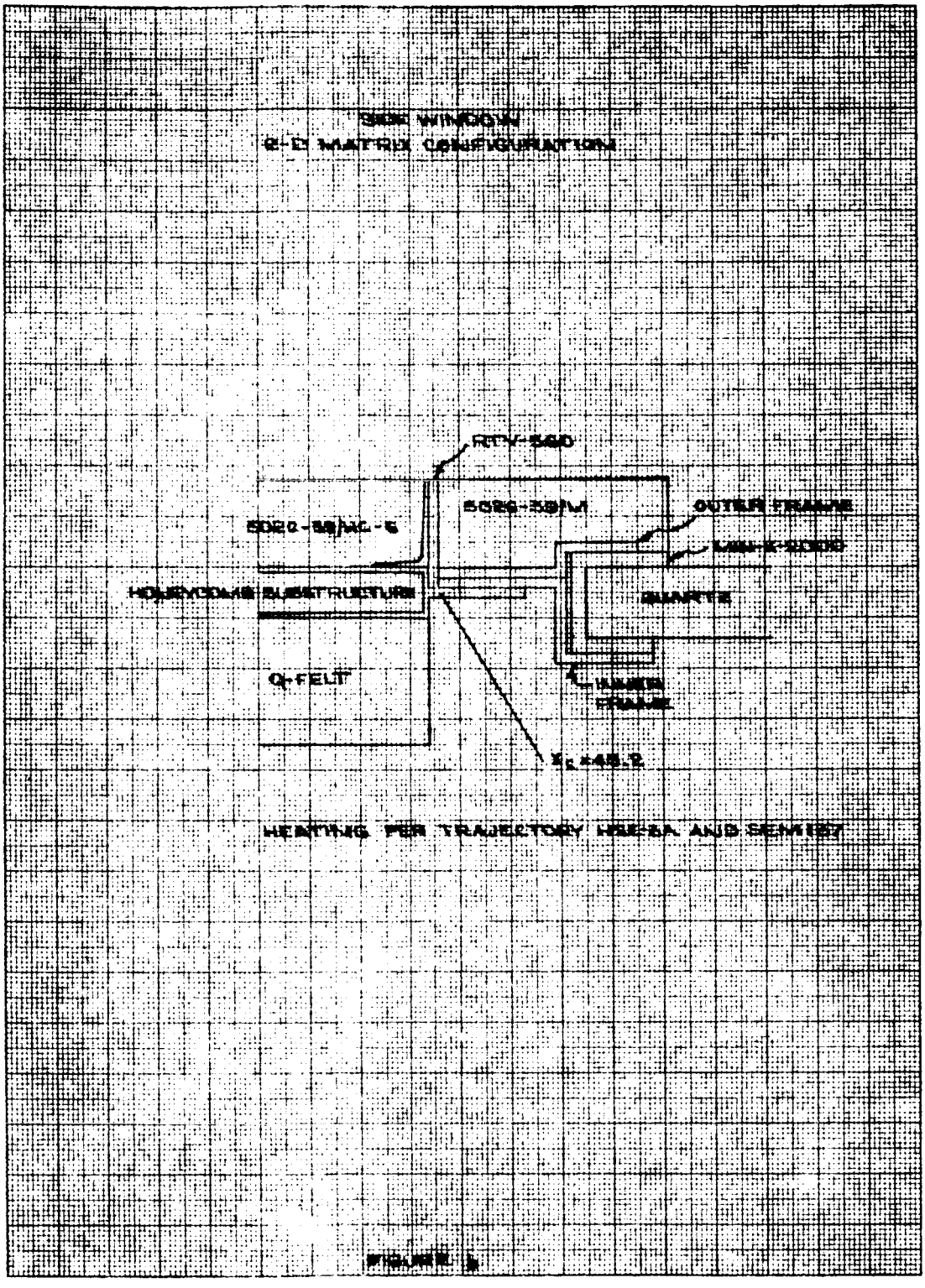

Figure 6 SIDE WINDOW 2-D MATRIX CONFIGURATION

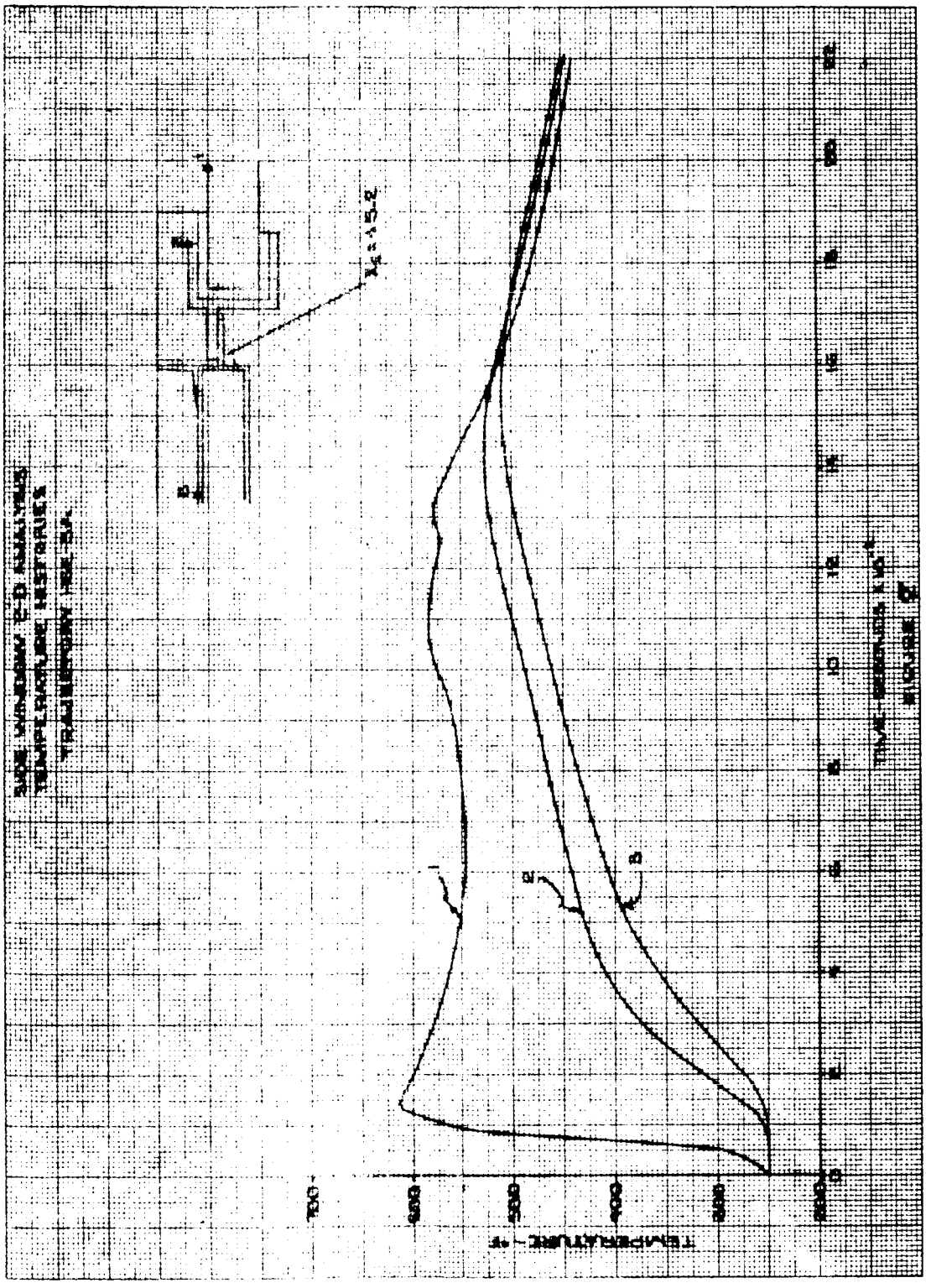

Figure 7 SIDE WINDOW 2-D ANALYSIS, TEMPERATURE HISTORIES
TRAJECTORY HSE-3A

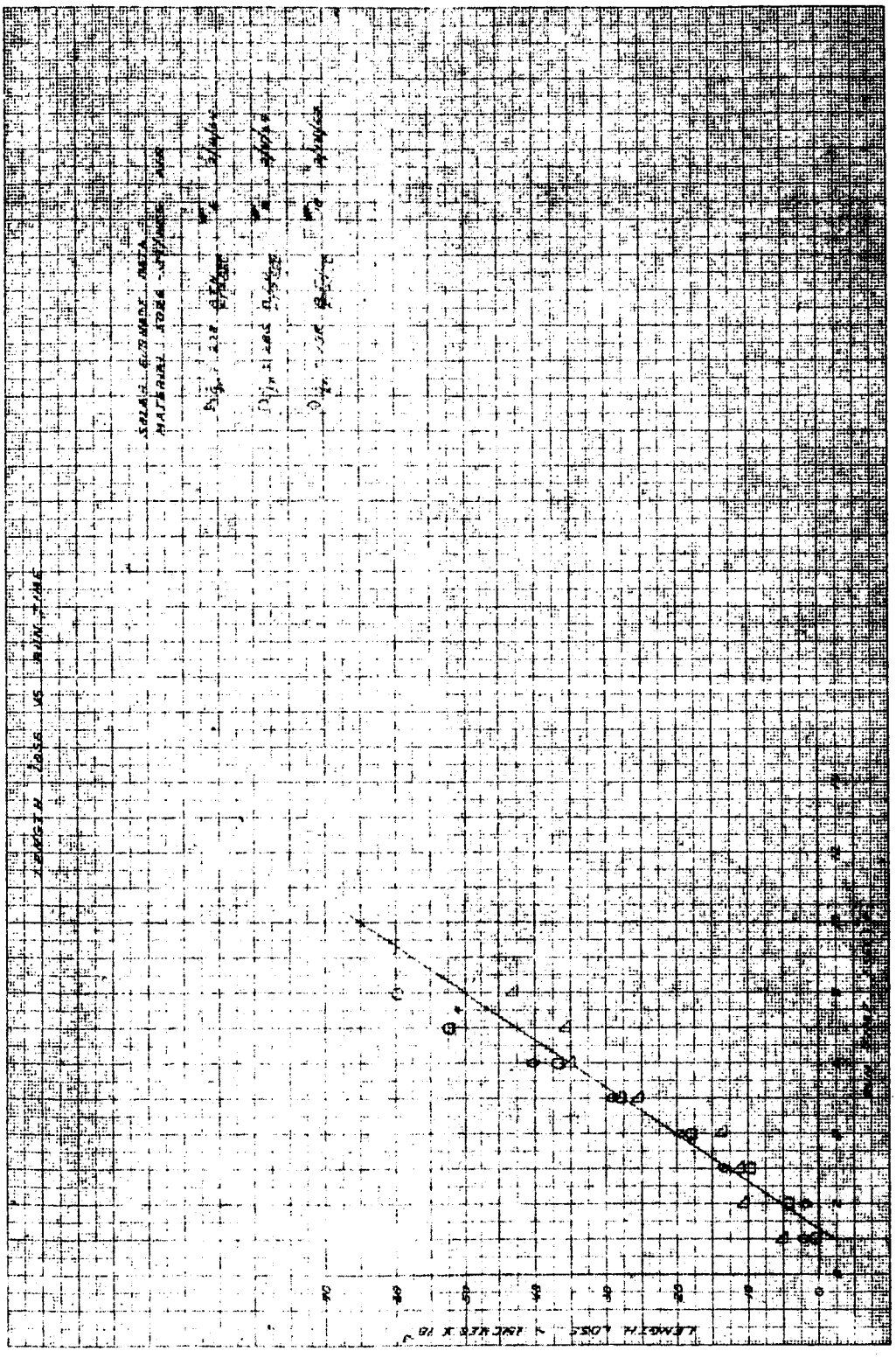

Figure 8 LENGTH LOSS VERSUS RUN TIME

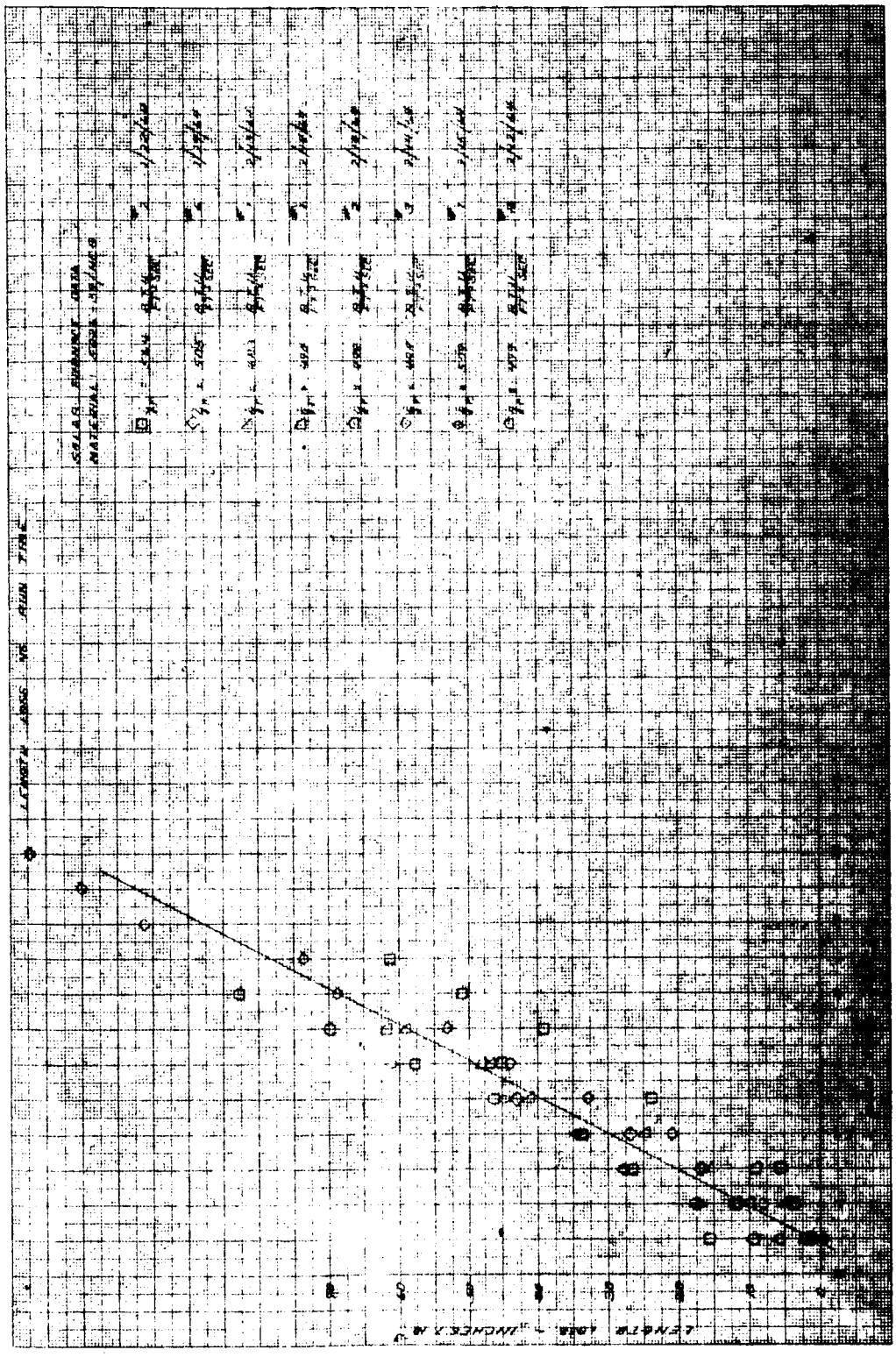

Figure 9 LENGTH LOSS VERSUS RUN TIME

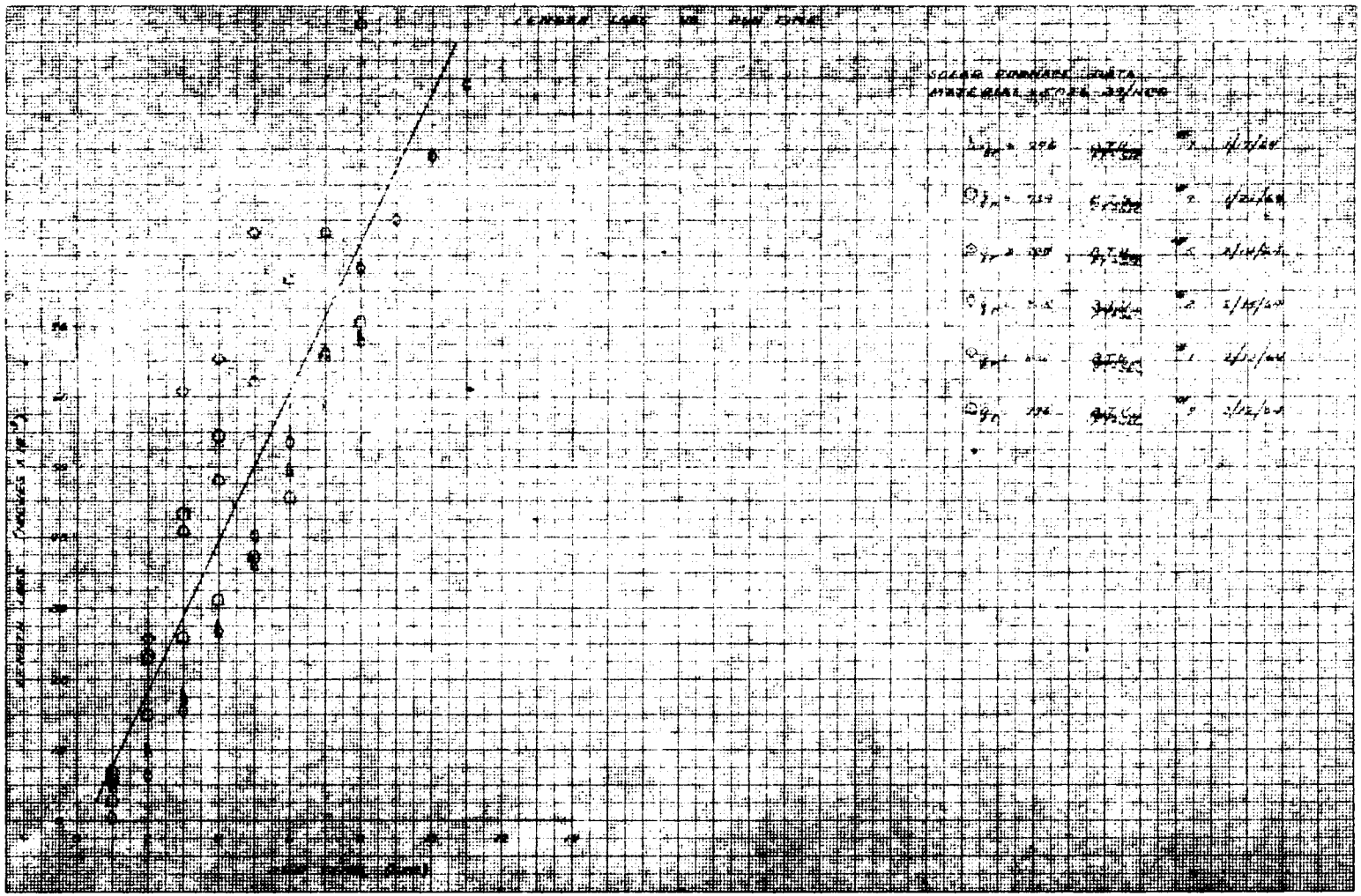

Figure 10 LENGTH LOSS VERSUS RUN TIME

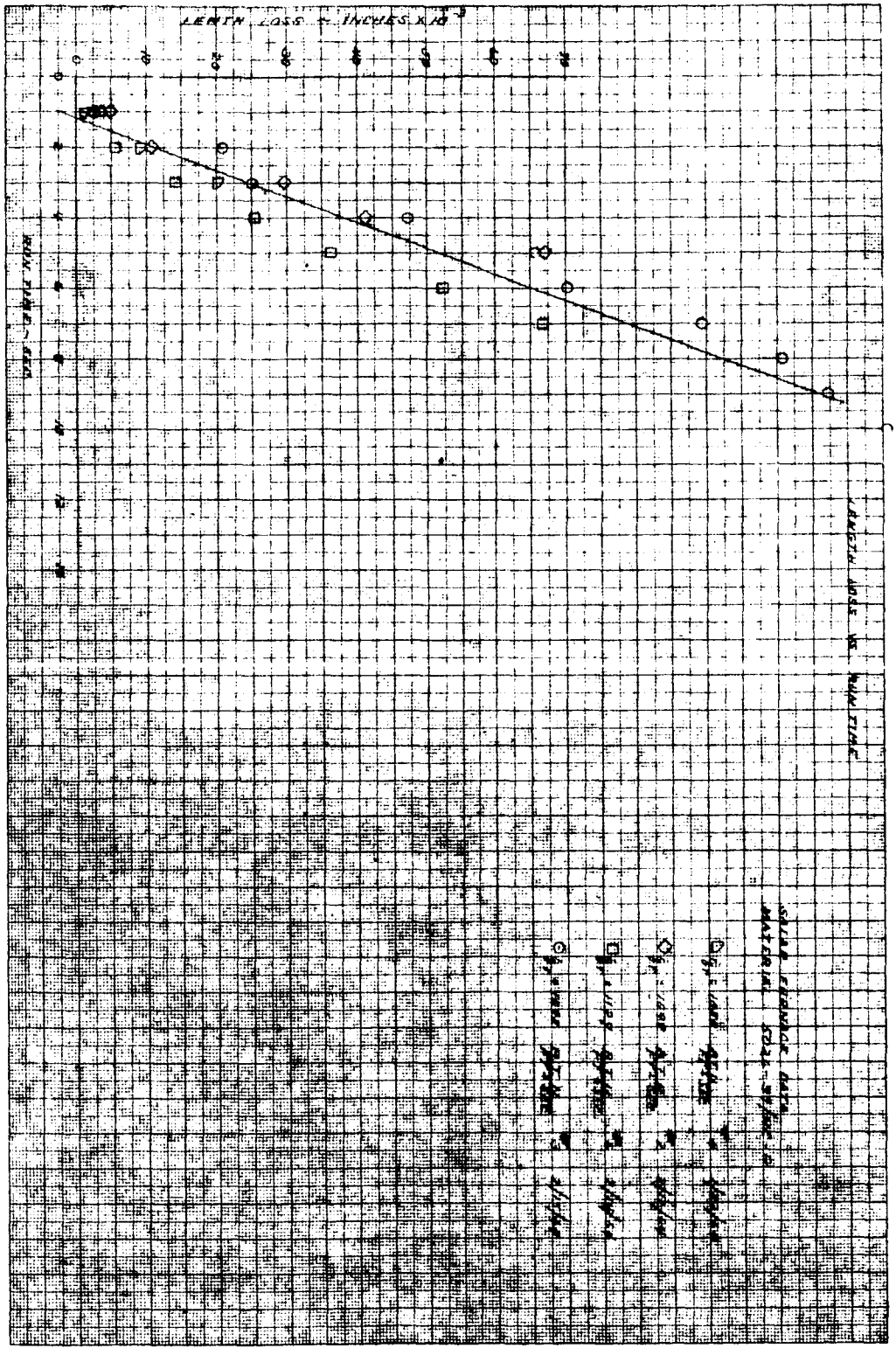

Figure 11 LENGTH LOSS VERSUS RUN TIME

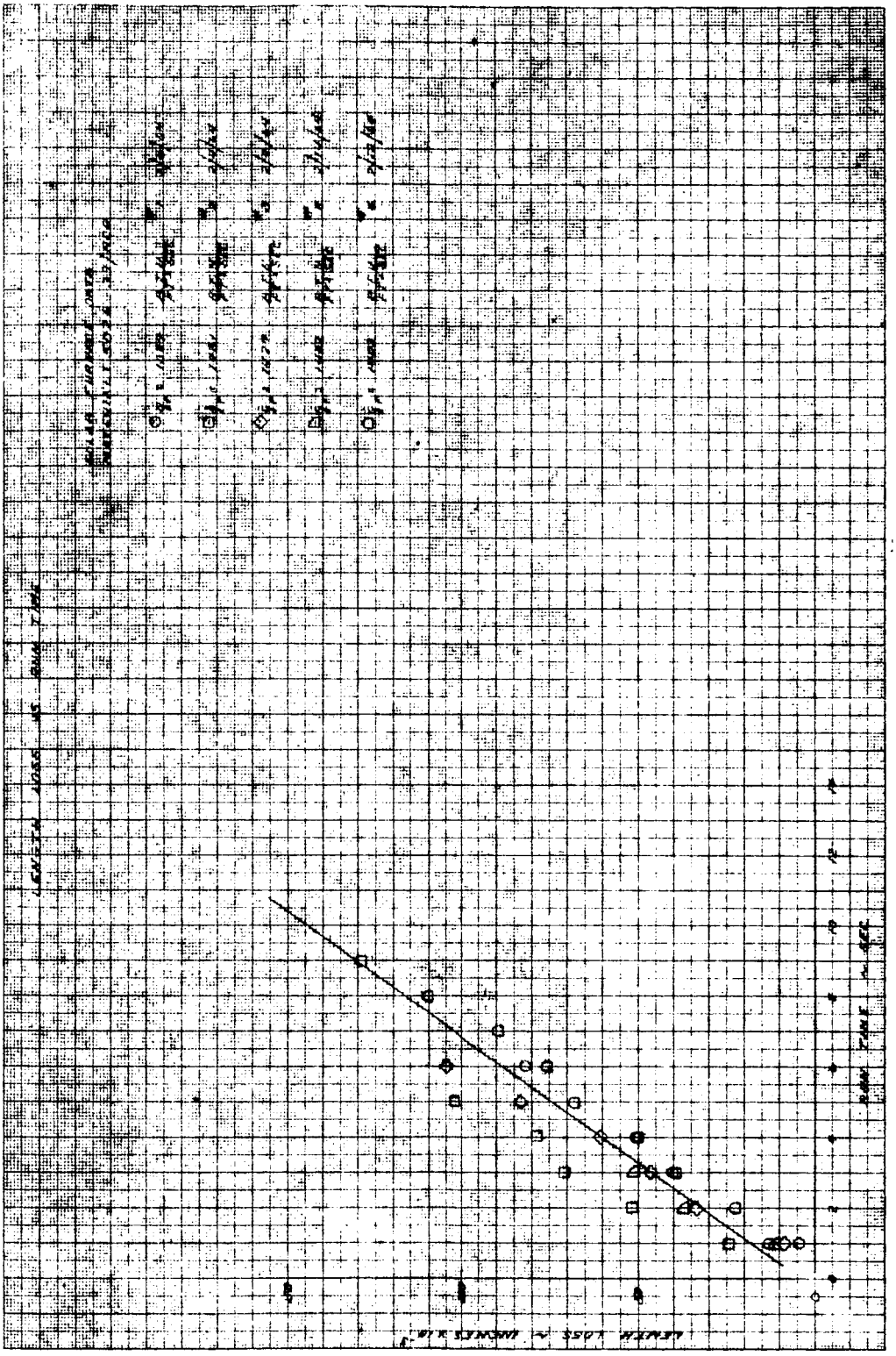

Figure 12 LENGTH LOSS VERSUS RUN TIME

[redacted]

= Absorbtivity of specimen = 0.95

$\dot{q}_i$ = Incident radiant heat flux $\frac{(Btu)}{ft^2\text{-sec}}$

ρ = Density of specimen $\frac{(lb)}{(ft^3)}$

$\dot{s}$ = Ablation rate $\frac{(ft)}{(sec)}$

The ablation rate ($\dot{s}$) variation with incident heat flux is presented in figure 13 and q^*_{cw} versus incident heat flux is presented in figure 14. Due to the additional data reported this month, there is considerably less variation in $\dot{s}$ and q^*_{cw} than was reported last month. Results continue to indicate q^*_{cw} data above the value of 12,000 Btu/lb selected for design use.

Analysis of Model 500 data from 5026-39/HC-T samples tested in air, N_2 and O_2 (AP1219) has begun. Using the value of wall enthalpy obtained from the Mollier chart of the particular working gas, a value of q^* was calculated for each sample using the actual test results. The results were plotted as a function of ΔH and a least squares fit to each set of data was calculated (figure 15). The results show the air data to fall between that of O_2 and N_2, as expected. The surface recession rates recorded were large, even for those samples tested in nitrogen. This indicates a significant shear effect.

An extension of char recession correlations now used strictly for convective heating are shown to be valid for combined fluxes in figure 16.

1.3 Test Planning and Analysis

Experimental data, obtained in the Avco 10-Megawatt Arc Facility, has shown that local accelerated erosion of Avcoat 5026-39/HC-G occurs due to heating perturbations. These perturbations are produced by the differential ablation between Avcoat and certain materials adjacent to Avcoat.

An example of the effects of differential ablation was demonstrated in turbulent pipe specimen AP1644-6 (Monthly Progress Report dated 9 January 1964, pp. 156). This specimen was 3 inches O.D., 1-1/2 inches I.D., 5 inches long and consisted of a fuzed quartz plug with circular fiberglass close-out member surrounded by Avcoat 5026-39/HC-G. This test is considered representative of the C-Band antennas and compression pads. The specimen was tested at a cold-wall heat flux of 715 Btu/ft^2-sec, gas enthalpy of 4540 Btu/lb and a shear of 8.5 psf for 20 seconds. Figure 17 shows the initial and post-test profiles of the specimen. These profiles were obtained from measurements of the internal surface of the pipe at 1/8-inch axial intervals. Analysis of these measurements show local heating increases of

[redacted]

24 percent downstream of the quartz plug at the end of the test, assuming steady ablation.

Other examples of local aggravation due to differential ablation were demonstrated in turbulent pipe specimens AP1643-1, AP1616-1, and AP1616-2. Data for specimen AP1643-1, similar to that shown in figure 17, is shown in figure 18. This specimen contained close-out members and a 0.200 inch gap, filled with RTV-560, plus a 0.15 inch circumferential forward-facing step. Analysis of measurements taken from the post-test profile of this specimen showed that local increases in heating in excess of 70 percent occurred downstream of the step. Specimens AP1616-1 and AP1616-2 contained interfaces of Avcoat 5026-39/HC-G with Avcoat 5026-39/M and also showed local increases in heating.

Tests of this nature indicate the requirement for defined heating perturbations at dissimilar materials, holes, steps, and protuberances. Further testing is planned to represent interface areas. Results of these tests may be expected to substantiate the trends indicated above.

OVERS splash data showing the thermal response of Avcoat 5026-39/M to heat fluxes up to 290 Btu/ft^2-sec have been compiled. These data were obtained from specimens of the plug-shroud design instrumented in depth with thermocouples located 0.10, 0.30, 0.50, 0.75 and 1.00 inches from the front surface of the specimen. Internal temperature response versus cold wall heat flux has been plotted for 60, 120, 180, 240, 600, and 780 seconds from the start of testing. Similar data will be compiled for Avcoat 5026-39/HC-G to insure verification of material performance. Typical curves showing the thermal response of Avcoat 5026-39/M at 120 and 180 seconds is shown in figures 19 and 20.

OVERS splash data are being analyzed to obtain values of q^* for high enthalpies and consequently, a value for the transpiration factor (η) due to char removal. These test data were reported in the Monthly Progress Report dated October, 1963 and were obtained on Avcoat 5026-39/HC-T. To determine the values of q^*, it is first necessary to correct length loss measurements for transient effects by evaluating the induction time. The induction times associated with enthalpy levels of 16,500 Btu/lb and 13,500 Btu/lb are approximately 3 seconds and 13 seconds, respectively.

2.0 Structural Studies

2.1 Intercompartmental Gap at $X_c = 81$

Analyses to determine the size of the meridional gaps which occur at $X_c = 81$ during HSE-3A reentry have been completed for times of 0, 200, 500 and 700 seconds. Reentry was assumed to be initiated from a space-flight

[redacted]

condition in which the sunlight shines on the $-Z_c$ axis with an incidence angle of 57.5 degrees. Initial reentry temperatures are listed in figure 21.

The models used in the analysis are shown schematically in figure 22 and represent the forward and crew compartment heat shields. The models are made up of a system of trapezoidal plates, and it is assumed that the thermal gradient and the reentry ablator thickness at their centers are constant over the particular plate. It was also assumed that the cross sections at X_c = 23.2 and 129.3 remain planar. The 1262 plate program was utilized to determine the extensional rigidity and thermal thrusts for each plate. The meridional distortion is then determined by summing the free meridional deflection of each plate along each meridian. The distorted shape of the forward and crew compartment interface cross section are plotted. Contact will occur at the high points, and there will be gaps at all other circumferential locations. The forward compartment is assumed to be free to rotate under the influence of the spring preload. The circumferential variation of the meridional gap is plotted in figures 23 to 26 for reentry times of 0, 200, 500 and 700 seconds.

The meridional gap at the initiation of reentry (t = 0) differs slightly from that which was reported in the November 1963 monthly progress report. The difference is due to updated Avcoat 5026-39/HC-G properties and new ablator thicknesses for new heating. Also ascent ablator thicknesses are not included in the present study.

2.2 Failure Criteria Analysis Effort

The failure criteria test program is oriented towards determining the crack width as a function of temperature and load, maximum load the edge bond stresses can develop, maximum load the composite heat shield can carry, and comparison of these values with vehicle conditions to determine margins of safety. To estimate the vehicle conditions, a simplified model of the crew compartment has been set up for analysis on the 1322 orthotropic shell of revolution program. The model considers the crew compartment to be rotationally symmetric with ablator thicknesses corresponding to the windward meridian under an isothermal cold soak temperature condition. Cutouts, intercompartment reactions and inner support reactions are neglected at present.

The uncracked heat shield is first analyzed to determine meridional moments, displacements, ablator strains, curvature and structure stresses as a function of distance along the meridian. The location of the peak ablator tensile strain is located and determined as a function of temperature. This will result in a prediction of the location and temperature of initial cracking. It will also give an indication as to whether bottoming of the heat shield on the stringers can occur. Having determined the location of the first

[redacted]

[redacted]

crack, the procedure is repeated with a reduced ablator section simulating the cracked regions and the same information determined. The procedure will be repeated as many times as is required to bring the ablator strain levels below ultimate tensile strain.

The end result of the study will indicate the maximum loads that must be transmitted across a cracked heat shield section, and these will be compared to the test program data.

3.0 Ground Test

3.1 Structural Tests

3.1.1 Back-to-Back Cold Soak Tests

A number of cold soak tests were completed this past month on back-to-back ablator specimens. Specimen APT-599 which consisted of a 1.97 inch thick Avcoat 5026-39/HC-G back-to-back ablators on 1/8 x 18 x 18 SS plate was tested in a cold chamber at a cooling rate which simulated the space flight temperature predictions. After 54 hours, the programmed temperature reached -260°F and was held there for 2 hours.

The first face grid separation occurred at a surface temperature of -174°F. Visual examination after test revealed that a crack extended across face "B" from edge to edge.

Four 18 x 18 inch back-to-back cold soak panels (1/2 inch S.S. sandwich substructure) were subjected to severe thermal shocks in order to produce cracks for fabrication of cracked tensile specimens. Two of the panels had 1.8 inch thick 5026-39/HC-G and two had 1.0 inch 5026-39/HC-G. The panels were placed in a chamber which was at a temperature of -260°F. After 15 minutes, the two 1.8 inch thick panels cracked but the 1.0 inch thick panels had not cracked after 45 minutes. The 1.0 inch thick panels were then hot soaked at 200°F and then placed in a chamber which was at -320°F. The panels cracked after 15 minutes at -320°F.

3.1.2 Bolt Plug Tests

Bolt plug sleeve specimen APT-595 was used to conduct tests on five reference design bolt plugs to check the general design feasibility. A second objective was to determine the acceptable installation torques and the useful plug life as a function of the number of installations. Table VI gives the torques required to install and remove the plugs. Plug 1 was installed in and removed five times from a fiberglass sleeve

[redacted]

[redacted]

in which the threads had been cut off center of the plug I. D. causing a variation in the torque during a revolution. This plug was then installed a sixth time and the assembly temperature was then reduced to -260° F; the plug was removed at this temperature (to determine relative tightness in cold environment) and the torque recorded.

Plugs 2, 3, 4, and 5 were installed in a new fiberglass sleeve which had been through inspection and, therefore, had the proper threads. These plugs were installed five times, with the exception of plug 2 which was installed ten times to determine if the torque levels off.

The locking inserts in these plugs were of poor quality, and generally the gasket height was not within the tolerance specified on the reference design drawing (0.000 to +0.010 above the plug O. D.). Some observations of the inserts are presented below:

Observations

Plug No.

1	The insert height, in some areas, was lower than the drawings specify.
2	The height of the insert was higher than specified towards the top of the gasket.
3	One side of the insert was higher than the other and the height was more than specified.
4	Insert height was within tolerance but was not centered in slot.
5	The insert height was lower than specified.

Future tests are planned on plugs which meet drawing and specification requirements to more closely determine the installation torques and plug life. It is expected that improved uniformity of plugs will reduce the spread of torque variation as noted in the test data presented in table VI.

The results shown in table VI are felt to demonstrate the suitability of the bolt plug design.

[redacted]

TABLE VI

APOLLO BOLT PLUG INSTALLATION
(Maximum Torques (in-lb))

Installation Sequence	Plug Number									
	1		2		3		4		5	
	Install	Remove	Install	Remove	Install	Remove	Install	Remove	Install	Remove
1	5.5	5.5	4.5	5.0	10.0	14.0	22.0	26.0	4.0	4.0
2	4.0	4.0	3.5	4.0	8.5	8.0	15.0	15.0	4.0	4.0
3	3.5	3.5	3.0	3.5	6.5	7.0	12.0	12.0	4.0	3.5
4	3.0	3.0	2.5	3.0	6.0	6.0	10.0	9.0	4.0	3.5
5	3.0	3.0	2.5	3.0	5.5	5.5	8.0	7.5	4.0	3.5
6		*6.25	3.0	2.5						
7			3.0	2.5						
8			3.0	2.5						
9			2.5	2.5						
10			3.0	2.5						

* Removed at -260° F

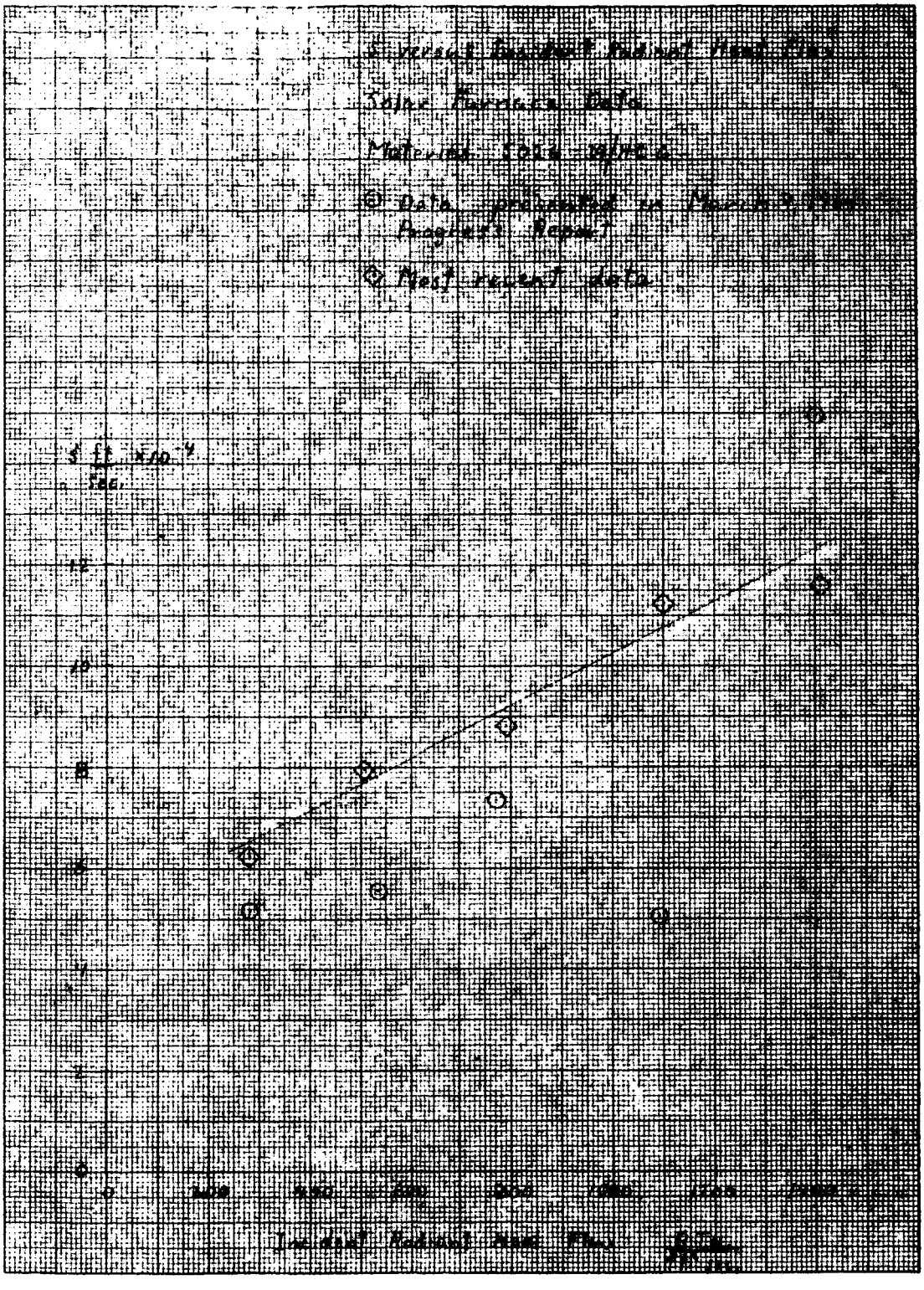

Figure 13 ϕ VERSUS INCIDENT RADIANT HEAT FLUX

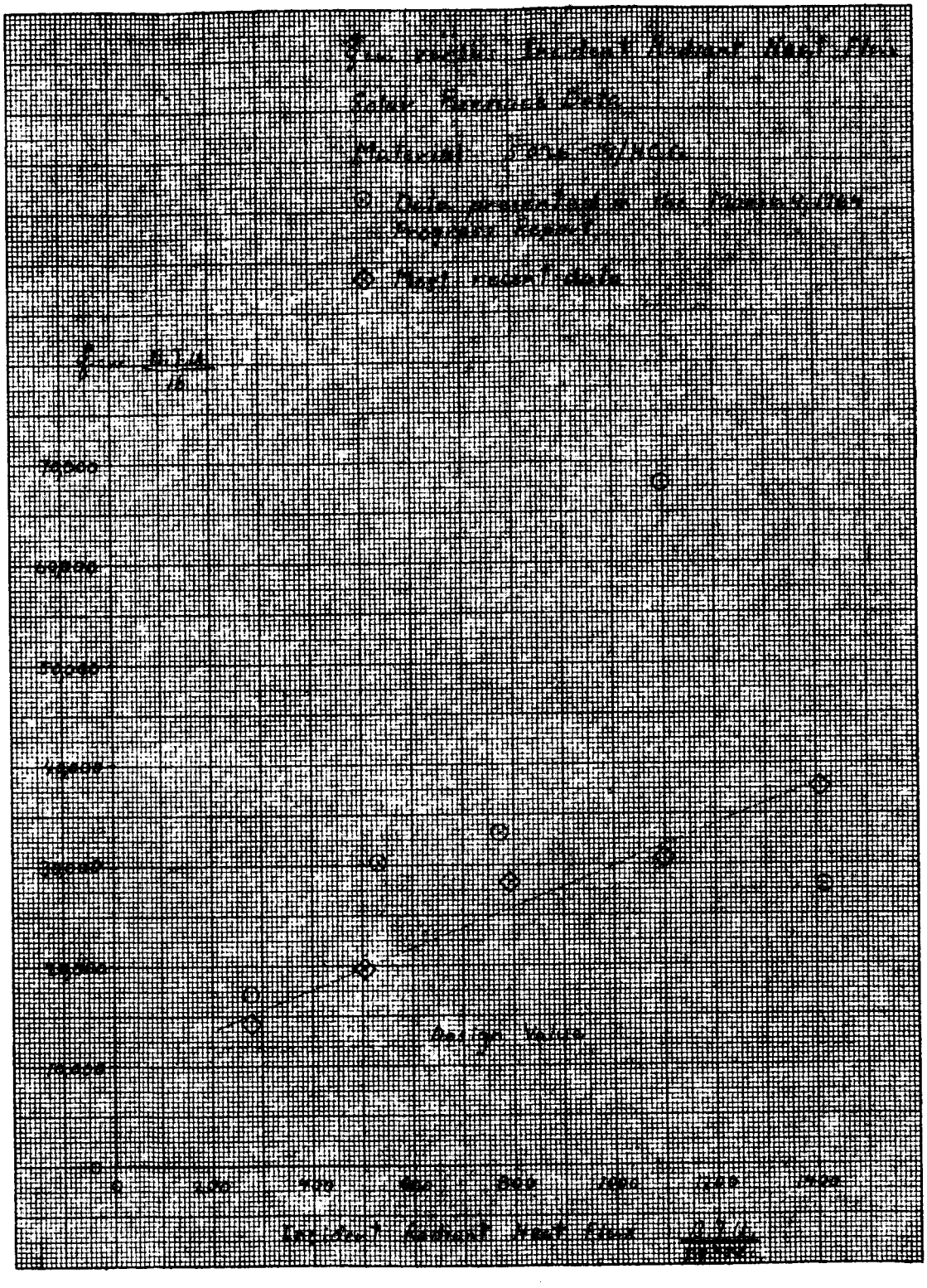

Figure 14 $\dot{q}_{cw}$ VERSUS INCIDENT RADIANT HEAT FLUX

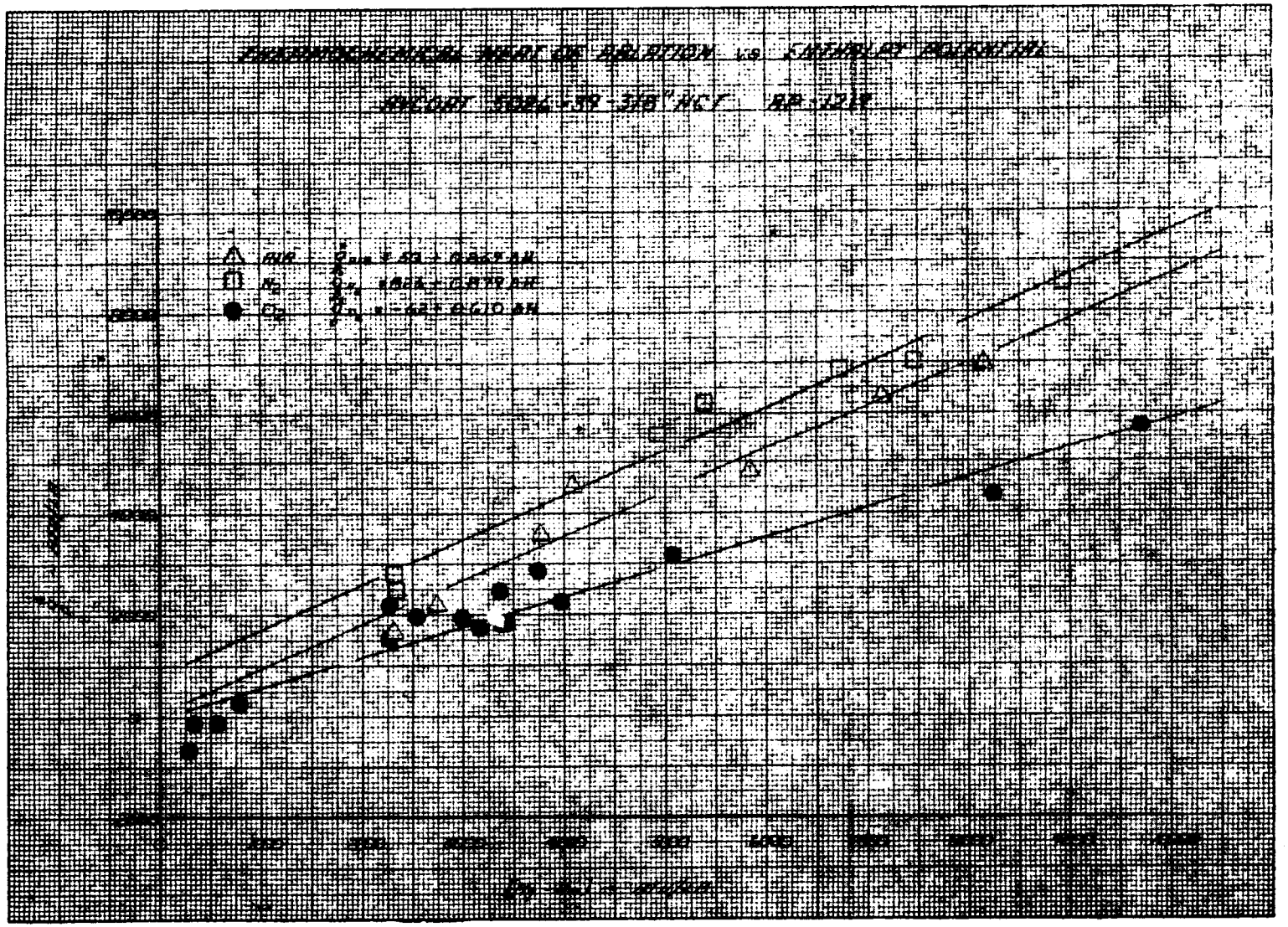

Figure 15 THERMOCHEMICAL HEAT OF ABLATION VERSUS ENTHALPY POTENTIAL, AVCOAT 5026-39-3/8-INCH HCT, AP-1219

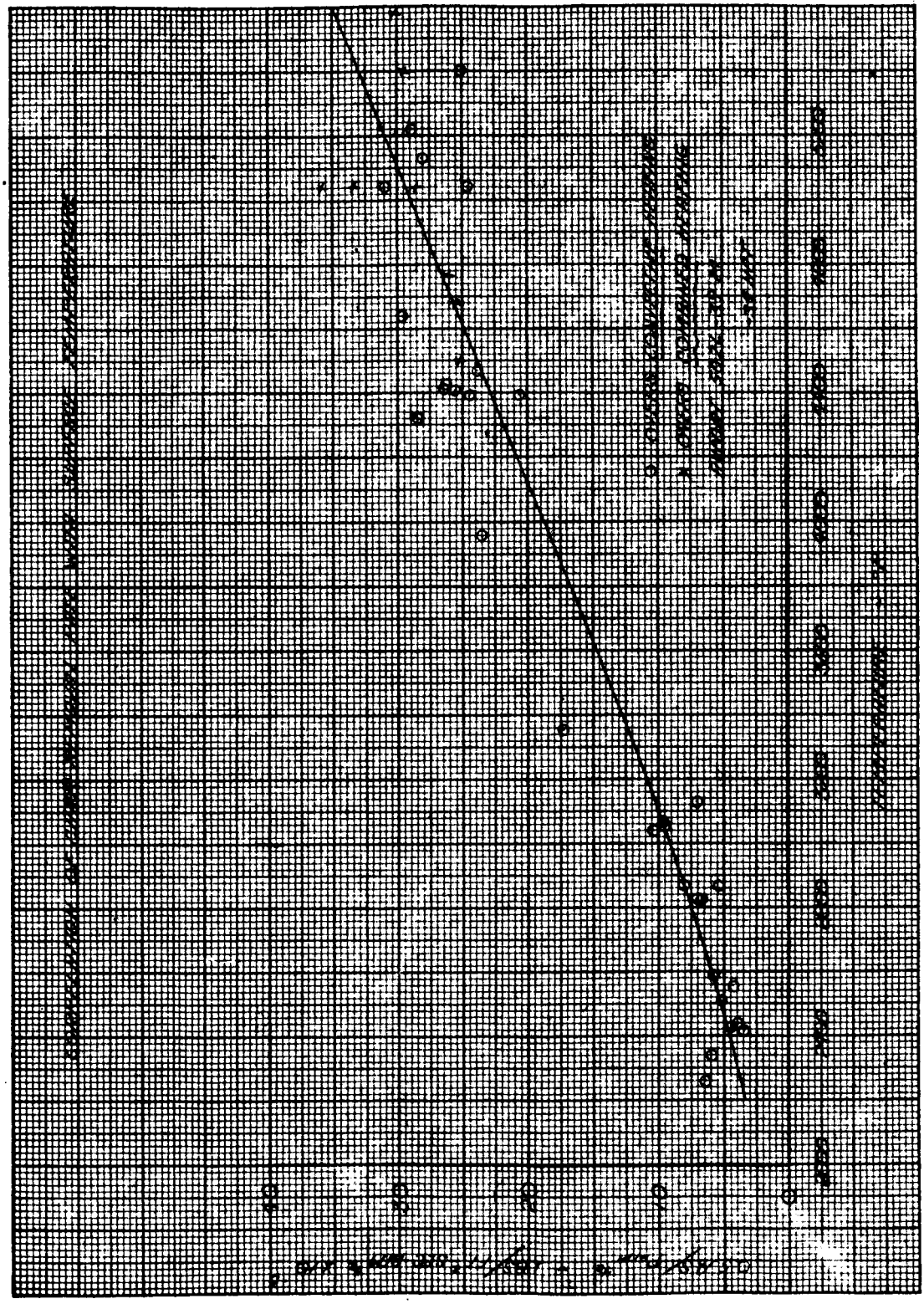

Figure 16 CORRELATION OF CHAR REMOVAL RATE WITH SURFACE TEMPERATURE

AP 1644-6

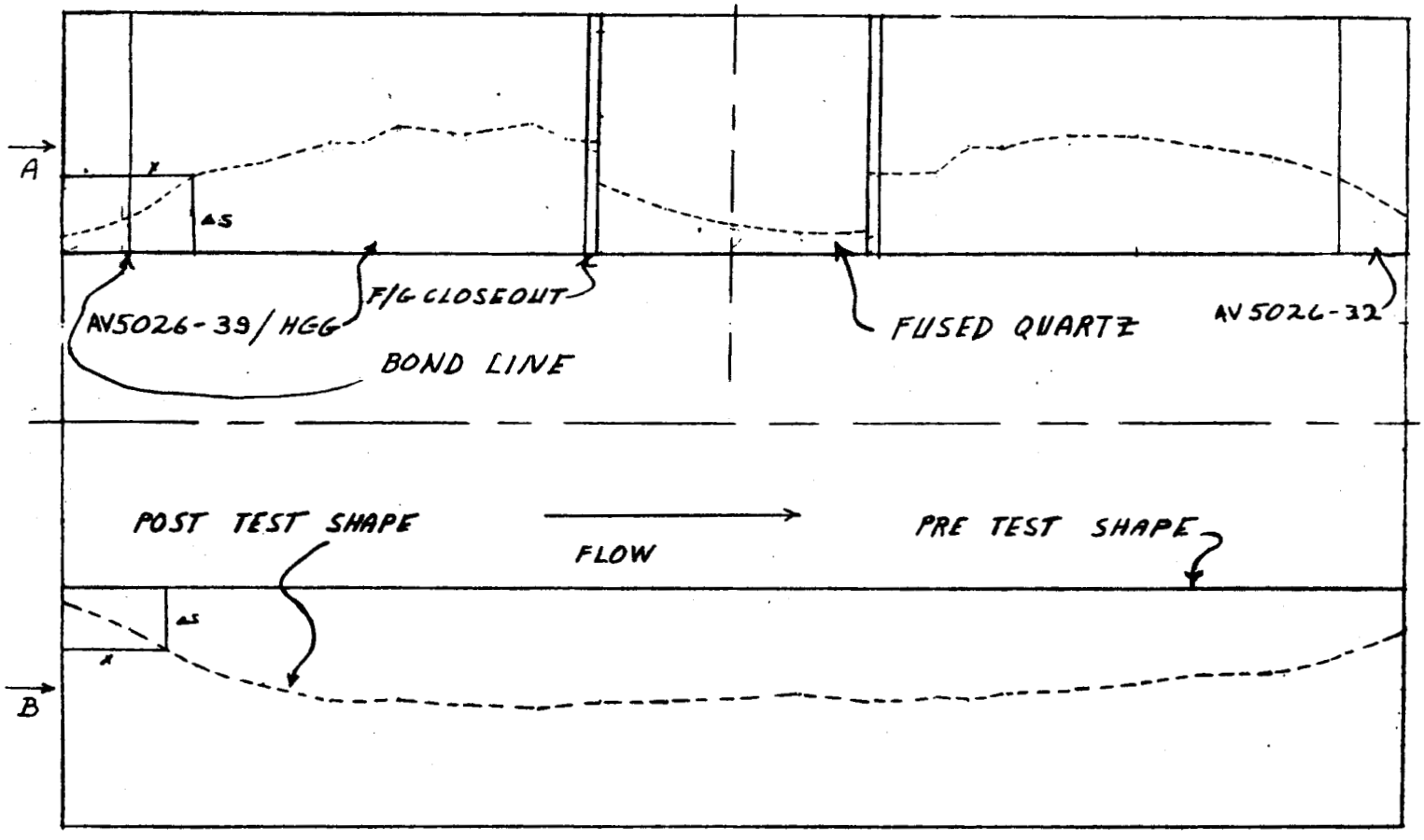

$H/RT_0 = 134$
$\dot{q} = 7.15$ BTU/FT²-SEC
$\tau = 0.46$ PSF
$\tau = 13.81$ SECONDS

Figure 17 C-BAND ANTENNA WINDOW

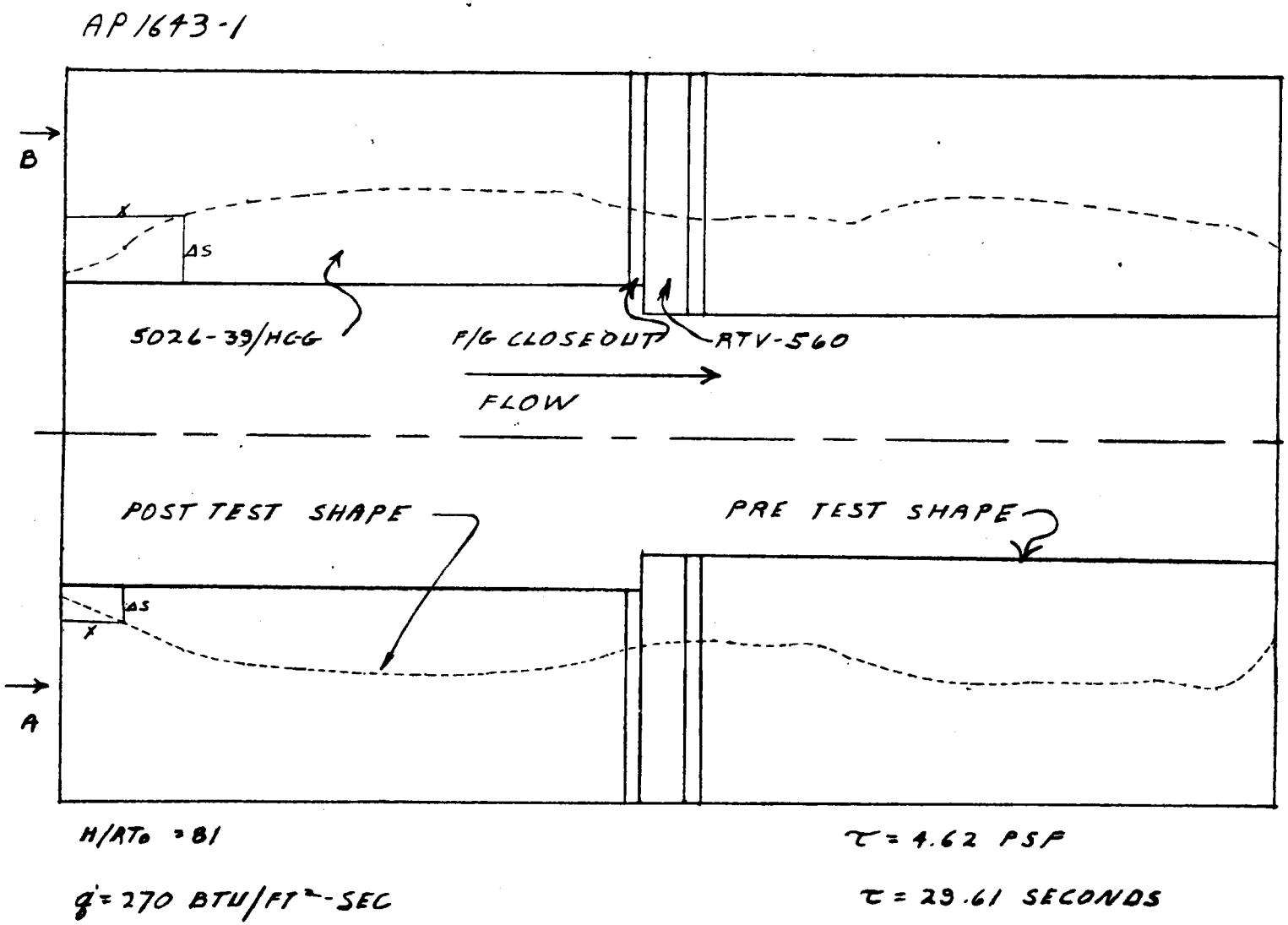

Figure 18 CIRCUMFERENTIAL GAP WITH FORWARD FACING STEP

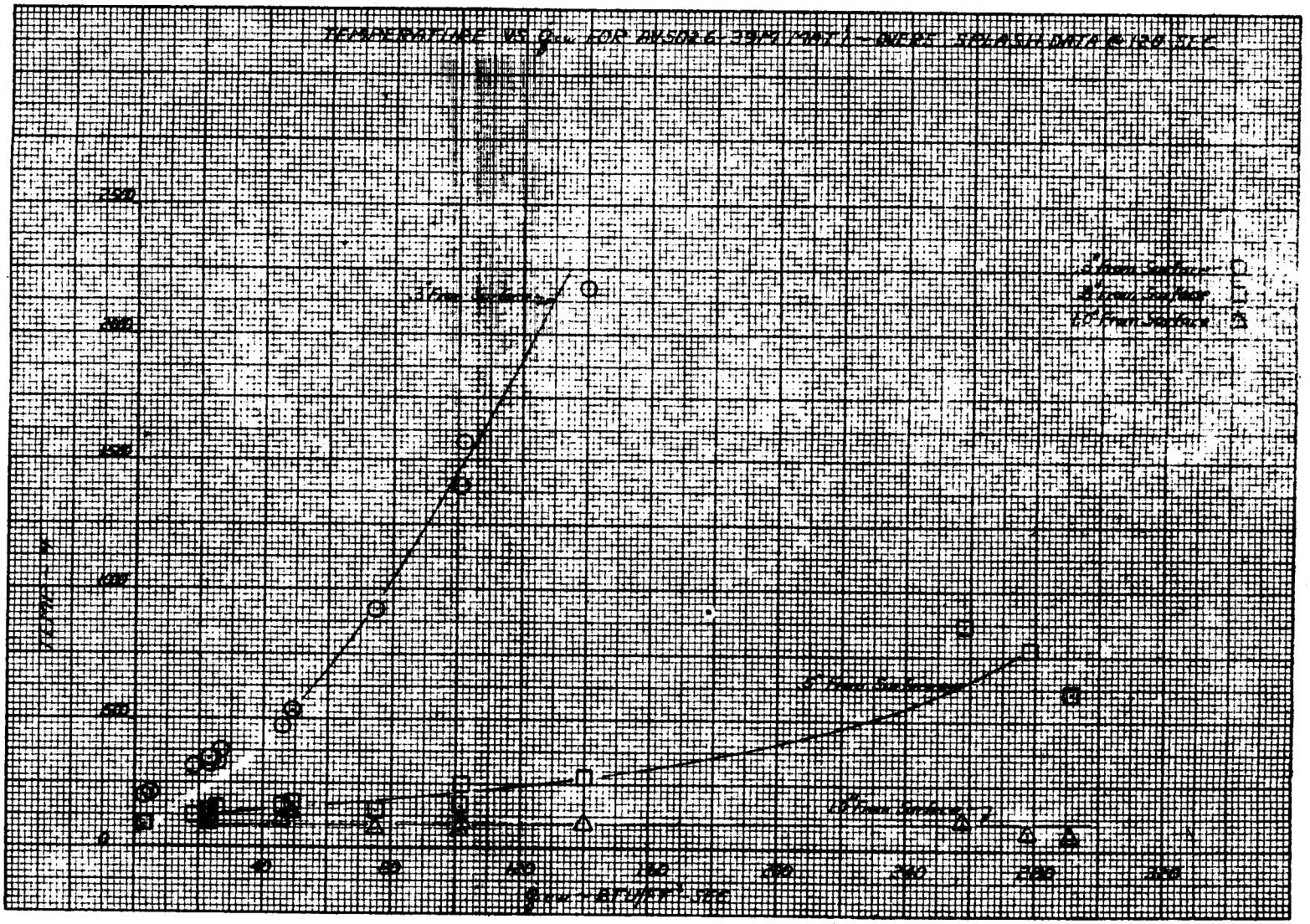

Figure 19 TEMPERATURE VERSUS $\dot{q}_{cw}$ FOR AVCOAT 5026-39M MATERIAL - OVERS SPLASH DATA AT 120 SEC.

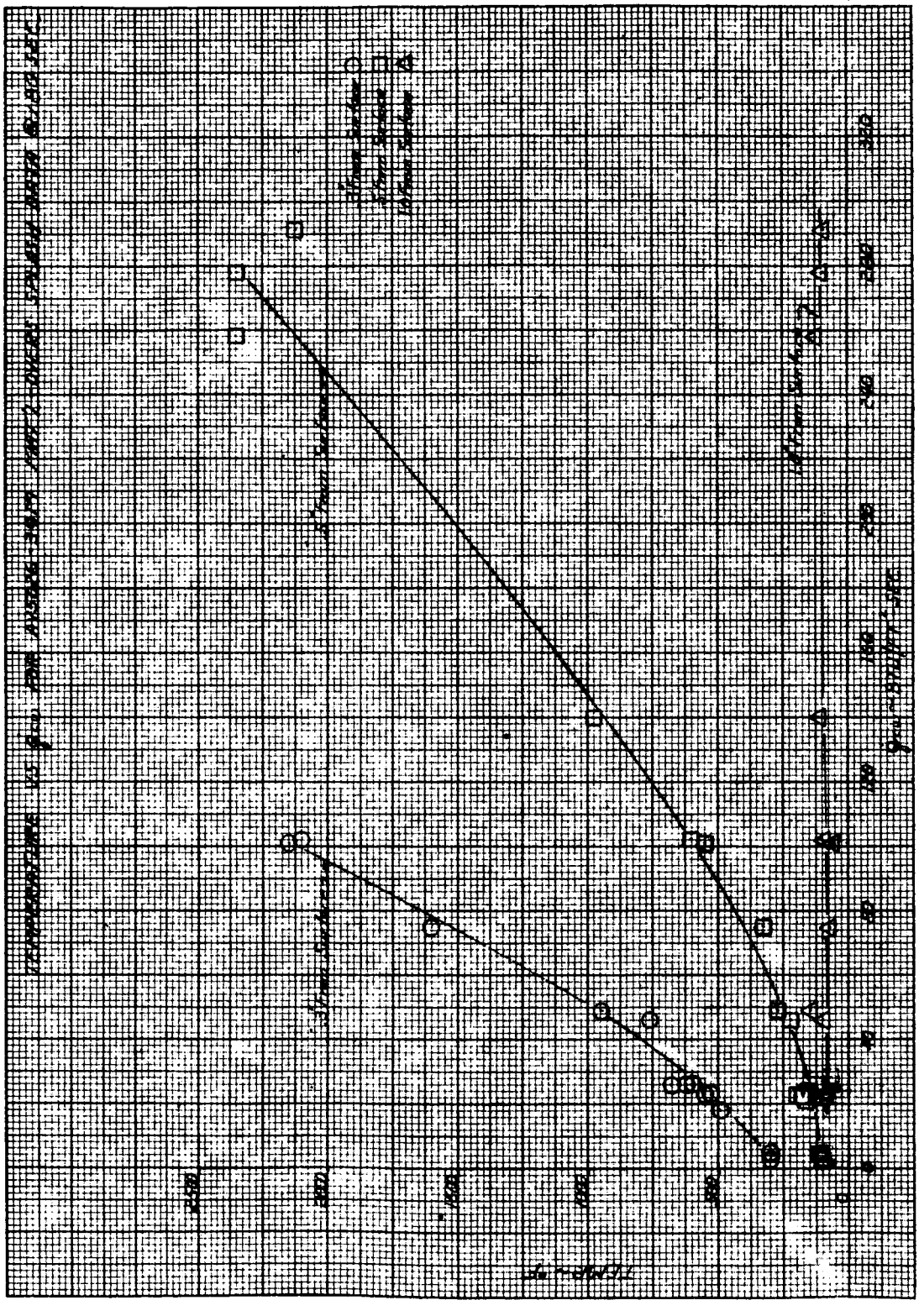

Figure 20 TEMPERATURE VERSUS q_{cw} FOR AVCOAT 5026-39M MATERIAL - OVERS SPLASH DATA AT 180 SEC

[redacted]

θ^* \ X_c	30	40	48	58	68	77	86	96	106	116	125
0	-258	-254	-250	-246	-242	-239	-235	-231	-227	-224	-219
22.5	-247	-243	-239	-235	-230	-226	-223	-219	-215	-211	-206
45.0	-212	-208	-203	-199	-194	-189	-185	-181	-176	-171	-166
67.5	-126	-123	-120	-116	-113	-110	-107	-103	-100	-97	-93
90.0	35	35	36	36	36	36	36	37	37	37	37
112.5	151	150	149	148	147	147	146	145	144	143	142
135.0	206	206	206	206	205	205	205	205	205	205	205
157.5	234	235	235	236	236	236	237	237	238	238	239
180.0	250	250	250	250	249	249	249	249	249	249	249

* $\theta = 0 = +Z_c$ AXIS

Figure 21 INITIAL REENTRY TEMPERATURE

[redacted]

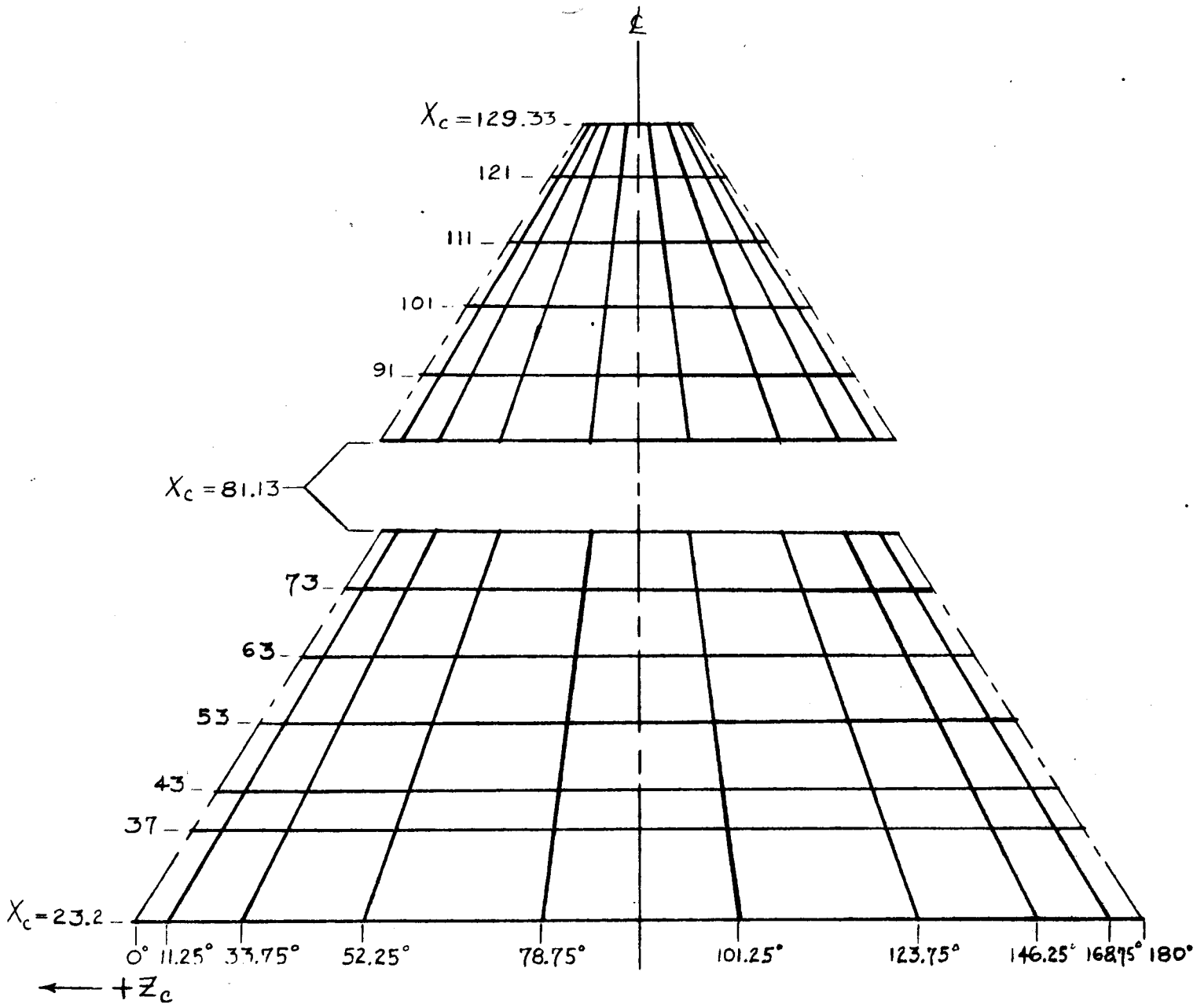

Figure 22 FORWARD AND CREW COMPARTMENT MODEL

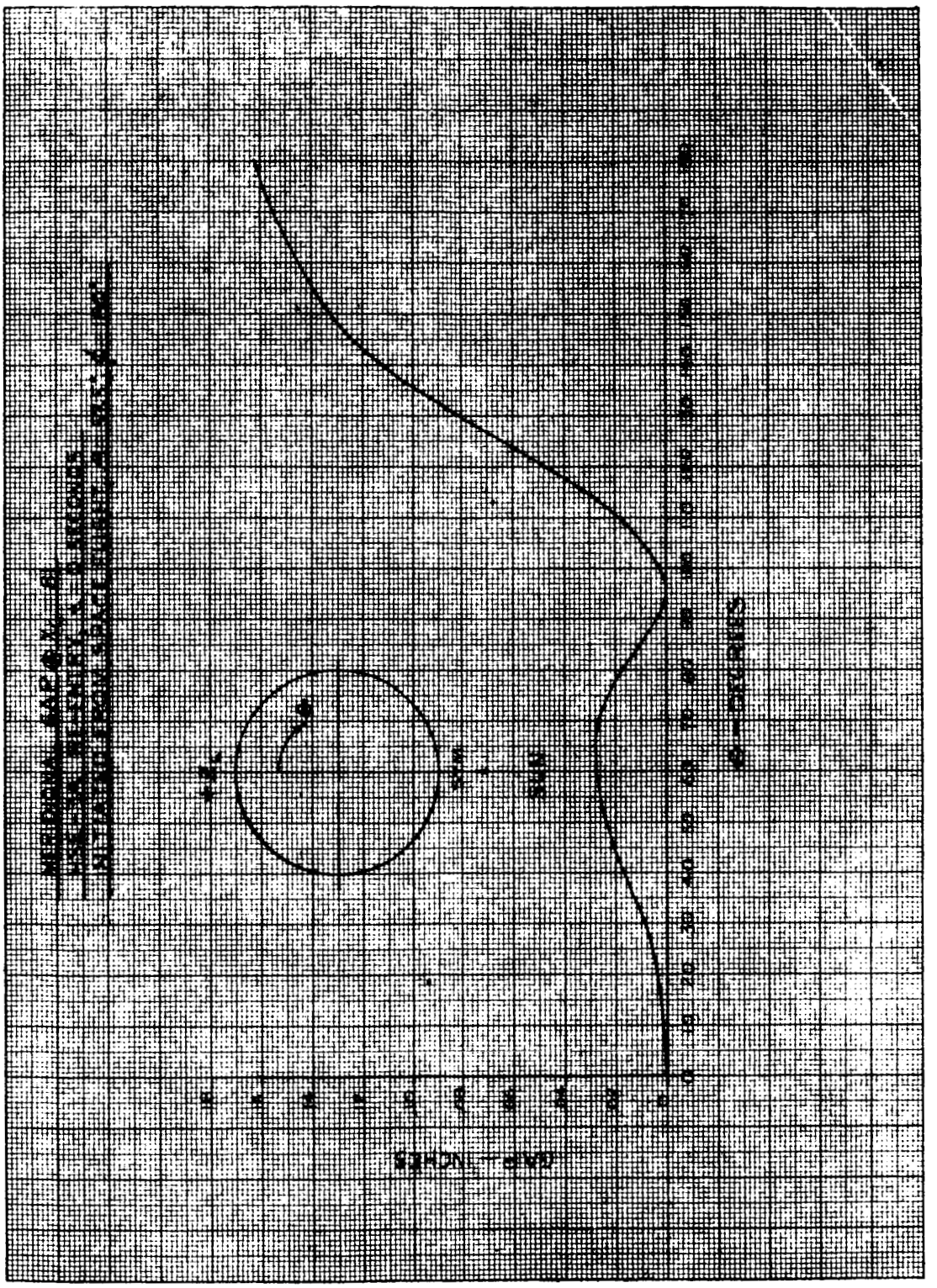

Figure 23 MERIDIONAL GAP AT x_c = 81, HSE-3A REENTRY, t = 0 SECONDS; INITIATED FROM SPACE FLIGHT, β = 57.5°, ϕ = 180°

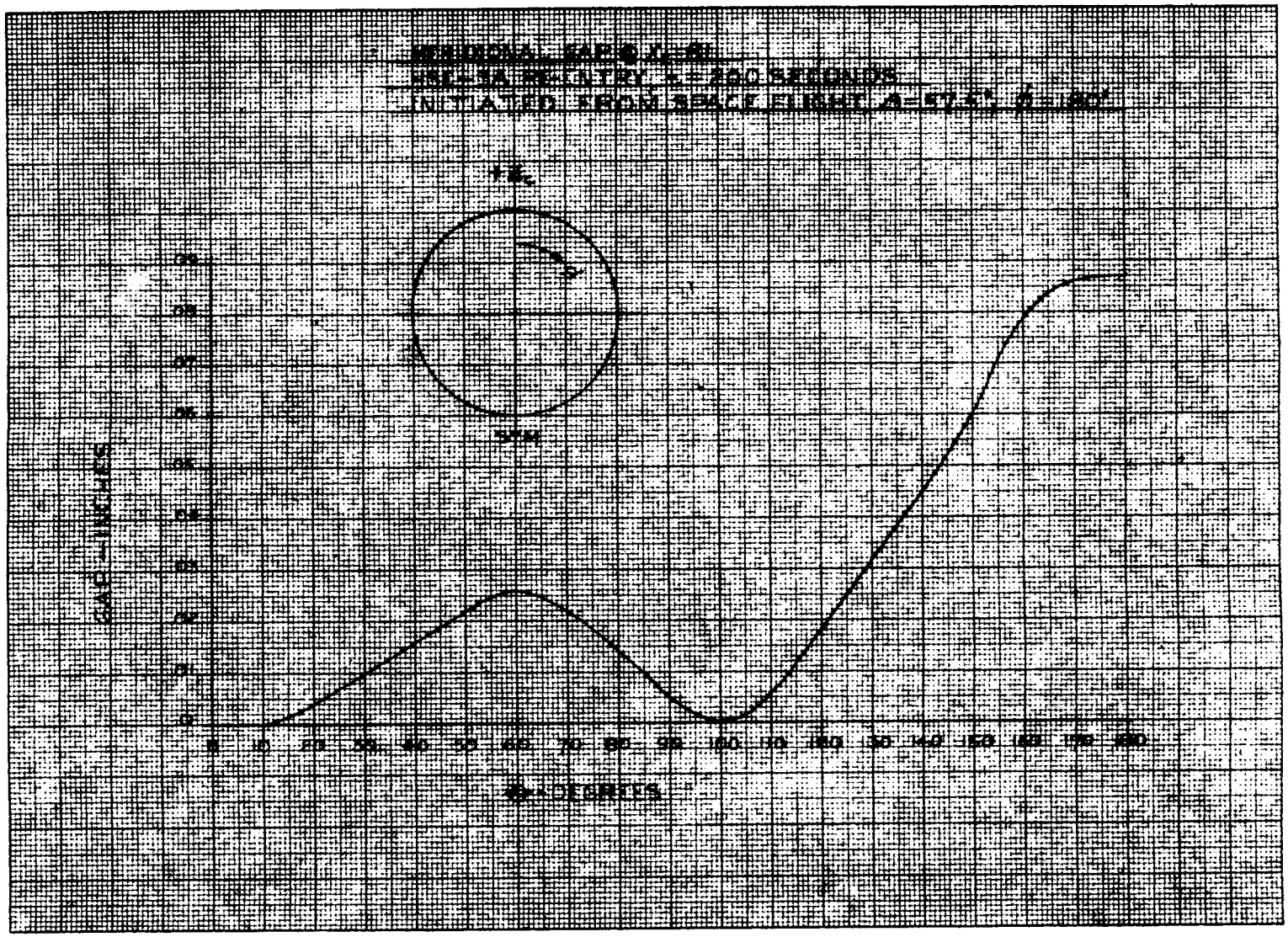

Figure 24 MERIDIONAL GAP AT x_c = 81, HSE-3A REENTRY, t = 200 SECONDS; INITIATED FROM SPACE FLIGHT, β = 57.5°, ϕ= 180°

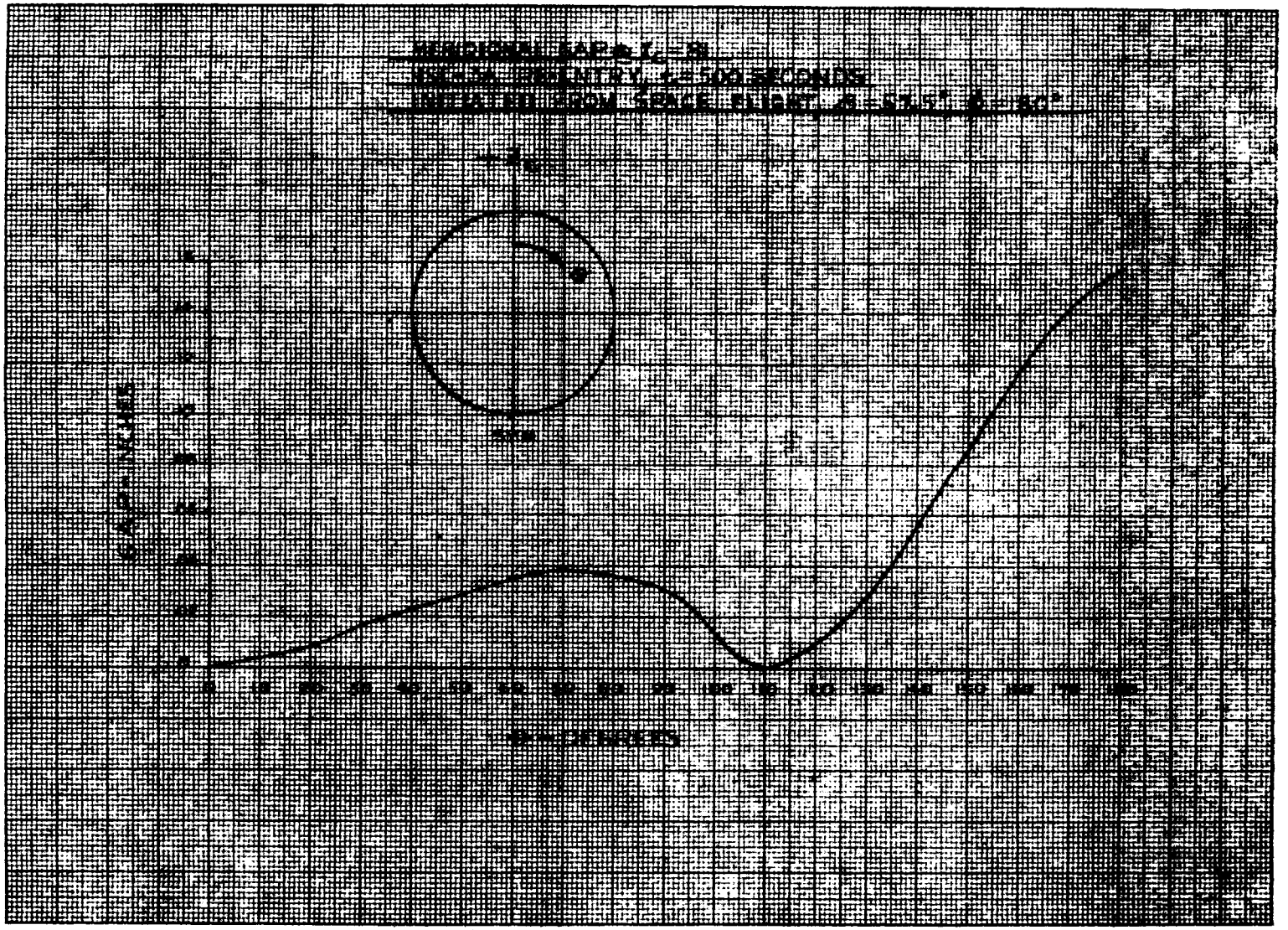

Figure 25 MERIDIONAL GAP AT $x_c = 81$, HSE-3A REENTRY, $t = 500$ SECONDS; INITIATED FROM SPACE FLIGHT, $\beta = 57.5°, \phi = 180°$

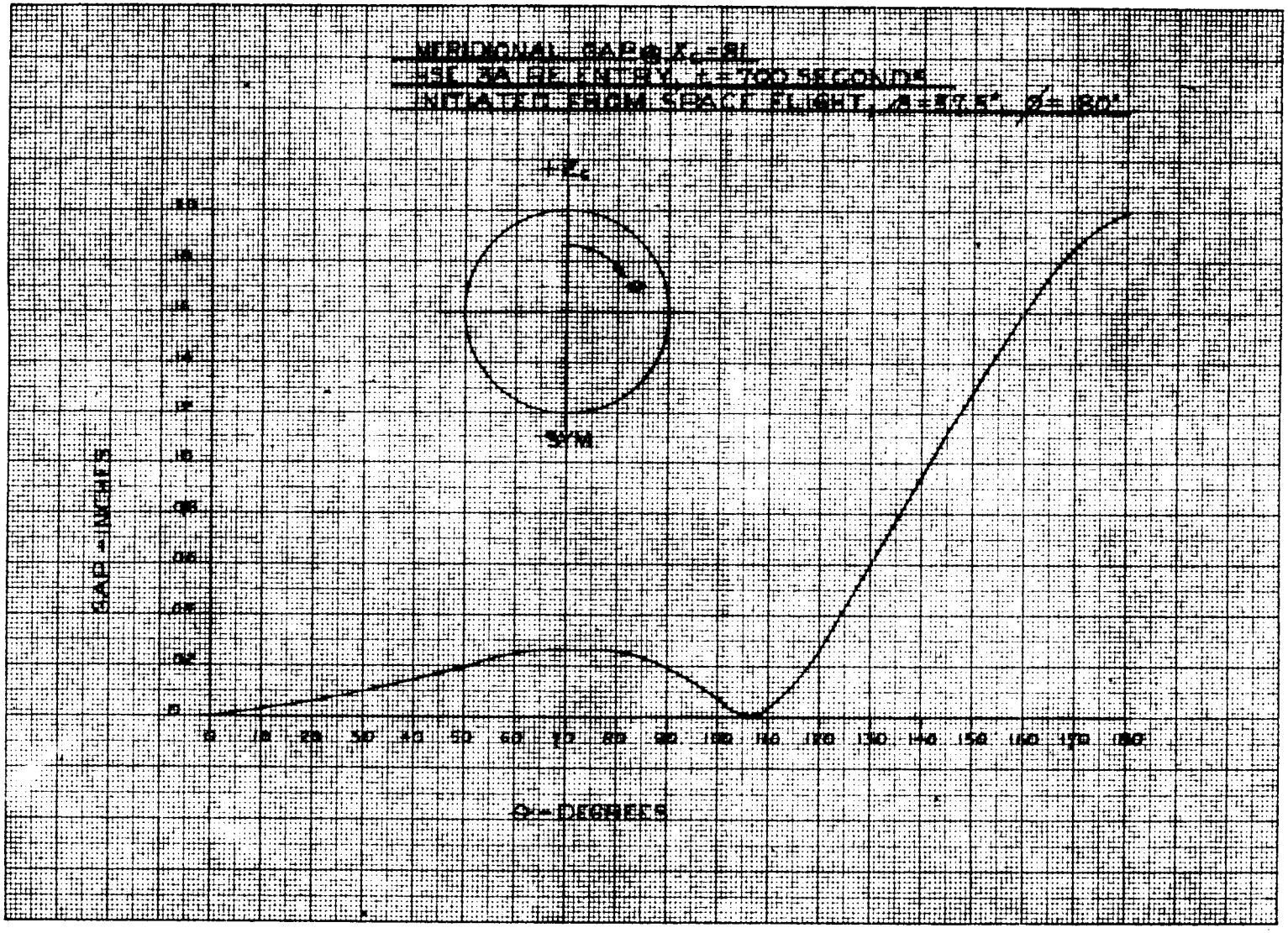

Figure 26 MERIDIONAL GAP AT x_c = 81, HSE-3A REENTRY, t = 700 SECONDS; INITIATED FROM SPACE FLIGHT, β = 57.5°, ϕ = 180°

[redacted]

3.1.3 Failure Criteria Beam Tests (Table VII)

Seven ablator failure criteria beam tests (APT-393, 394-1, 394-2, 395, 396, 397, 398) were completed. These beams consisted of 1.8 inch thick Avcoat 5026-39/HC-G ablator applied to a 5 x 22 x 1/2 inch (0.008 inch face skin) S.S. sandwich with the exception of APT-394-1 and 394-2 which were 2-11/32 inch wide rather than 5 inches.

These specimens were tested in a special loading fixture which applied a constant moment to the center eleven inches of the beam. Each beam was tested in the following manner: First, the specimen was raised to a zero stress temperature of +185°F and reference deflection dial gage readings were recorded with the upper loading beam resting on the specimen. Corrections were made to this dial gage reading at other temperatures to return to a reference deflection occurring with no weight on the beam. The specimen temperature was lowered to -260°F with loads at the reference deflection being recorded periodically. After an ablator crack was formed, each beam with the exception of APT-395 was subjected to additional loading at -260°F to cause failure. APT-395 was loaded to failure at -200°F.

The results of these tests are being analyzed at present for correlation with vehicle conditions.

3.1.4 Zero-Stress Beam Test

Beam specimen APT-321 was used for the purpose of taking deflection measurement during and following fabrication.

The specimen consisted of a 36 x 6 x 0.125 inch thick cold rolled steel plate to which was applied a 1.016 inch thickness of 5026-39/HC-G. This thickness includes the adhesive thickness.

The test setup included a separate 1/8 inch steel plate used as a reference so that the dial deflection gages could be reset if they were accidentally moved. To determine the initial curvature of the plates, readings were obtained for one side of the plate, and the plate was then rotated and readings taken of the second side. The plate curvature was then one-half the difference between these readings. The plate's initial curvature is shown in figure 27.

[redacted]

[redacted]

TABLE VII

FAILURE CRITERIA BEAM TESTS

Speciman Number (APT)	Test Temp. (°F)	Ablator Thickness (inches)	Thermal Moment (lb in/in)	Load at Failure (Pounds)	Applied Moment (lb in/in)
393	-260	1.8	964	1980	890
395	-200	1.8	770	2210	994
396	-260	1.8	964	1375	619
397	-260	1.8	964	1880	845
398	-260	1.8	964	2400	1080
394-1*	-260	1.8	964	650	607
394-2*	-260	1.8	964	675	624

* These beams were 2-13/32 inches wide.

[redacted]

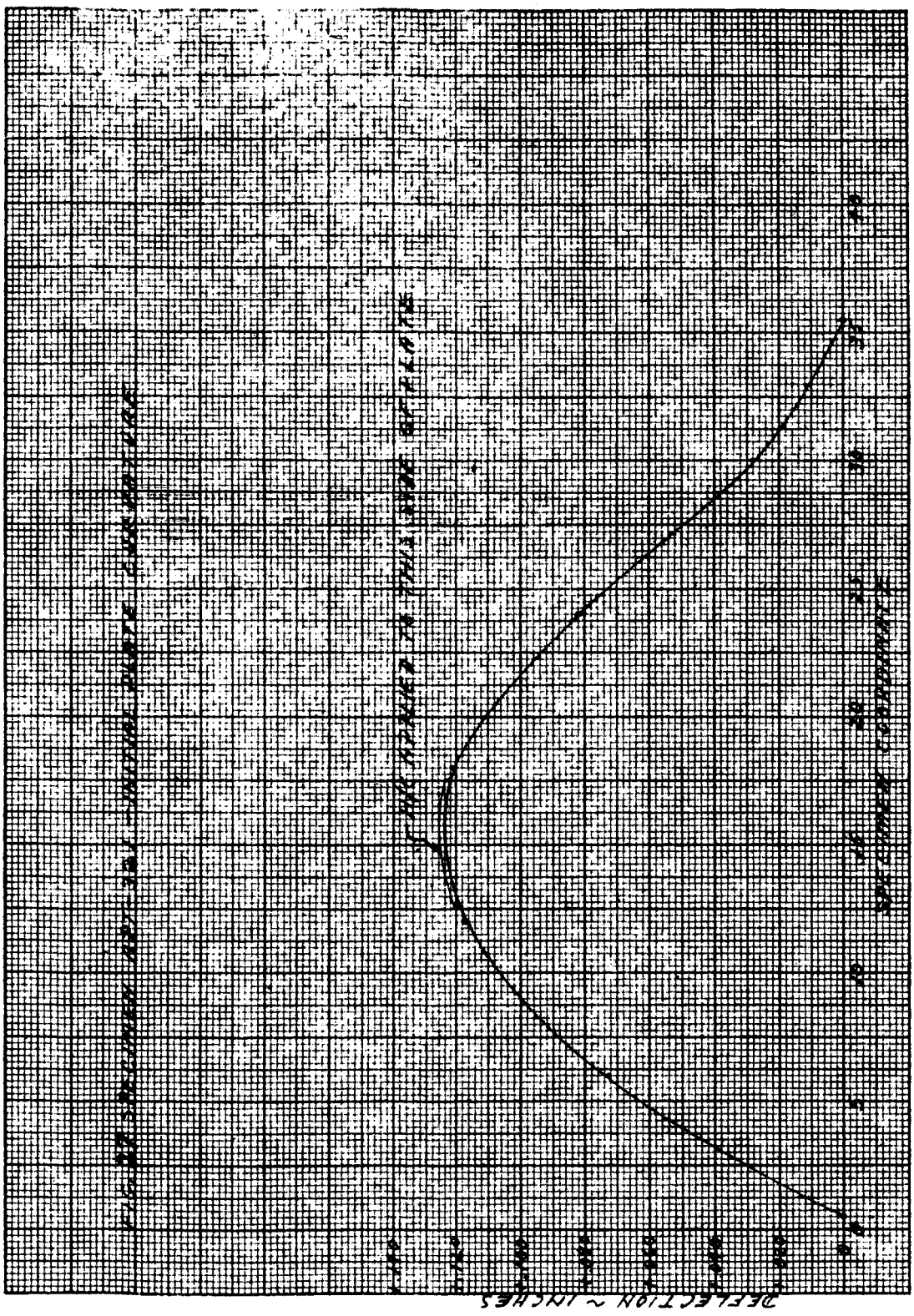

Figure 27 SPECIMEN APT-321, INITIAL PLATE CURVATURE

[redacted]

Subsequent deflection measurements were then taken:

a. After H/C application and cure

b. After filling with ablator by the gunned technique

c. During cure, postcure, and cool down to room temperature.

When the cure was complete a thermocouple was placed at one-half the ablator depth and a second thermocouple was taped to the steel plate.

The specimen was then cycled from R. T. to +250°F and back to room temperature. During cycle, deflection measurements were taken at 25°F increments, when the difference between thermocouples was within 5°F. The results of these measurements are shown in figure 28.

3.1.5 Beam Humidity Tests

Beam Specimens APT 267 and 268 were tested to determine the effect of a high humidity exposure on an ablator beam composite.

The specimens consisted of 6 x 36 x 0.765 inch of Avcoat 5026-39/HC-G applied to a 1/8 inch thick 15-7 Mo stainless steel plate. These are specimens for which deflections during manufacture and a subsequent thermal cycle were previously recorded. There was no moisture sealer on the specimens. Reference measurements were taken when the beams were at an ambient condition of 17 percent relative humidity. The specimens were then placed in a humidity chamber and exposed to a condition of 96 percent relative humidity for 3 days.

After this exposure, the beams were hermetically sealed in plastic bags until they reached the ambient temperature and measurements of the change in curvature were then recorded. Results of these tests are not yet available.

3.2 Thermal Tests

As the 10 mw pipe tests were recently completed, no analysis has been made of the data other than to note that the instrumented samples showed no significant temperature rise during the tests (1-2° Fahrenheit). The samples are being sectioned and will be photographed. Motion pictures

[redacted]

taken during the tests are being processed. The data analysis will be presented in the next progress report. Table VIII presents the description of the samples as well as the arc test conditions. On Run 4745 (AP1605-1), the outer fiberglass wrap was inadequate and the sample failed. The remaining two samples of the series were wrapped for proper sealing, were then tested and performed satisfactorily.

The two groups of specimens, AP1676-silicone rubber RTV-560 and AP1650-phenolic fiberglass, have been tested in the Model 500 arc. The results are presented on figures 29 and 30 and on the ablation property sheets where the nomenclature is:

Code Number

Material Designation

Number of samples

ρ = density

η = transpiration factor

$H_v + C_p \Delta T$ = effective heat of vaporization

q_l^* = regression line of q* data

p = stagnation and/or plenum pressure

H = gas enthalpy (referenced to absolute zero)

H/RT_o = dimensionless enthalpy

q^* = thermochemical heat of ablation

q_c^* = cold wall heat of ablation

q_c = cold wall heat flux measured with a flat-face, water calorimeter

H_w = air enthalpy at the surface of the specimen

V = ablative rate

$\dot{m}$ = gas flow rate

q_r = emitted radiation

[redacted]

T_T = True surface temperature

ϵ_λ = spectral emittance

ϵ_T = total emittance

The usual data reduction showed that the fiberglass data compared to the fiberglass closeout data previously reported (Nov. '63). The data for specimens AP1418 and AP1501 (found not to be significantly different) are plotted on figure 29. The regression line with the 95 percent tolerance band is also shown. The new data points are plotted on the same figure and agree with the closeout data.

The silicone rubber has a low level of q* which can be attributed to a high ablative rate. This material forms a thin, flaky char layer that can be rubbed off the surface. Because of this an estimate of 0.75 was used for the spectral emittance, ϵ_λ, at 0.65 micron to determine the true surface temperature from the brightness temperature. Even though there was a char layer on the surface of the specimen the total radiation and the surface temperature were not very high or changing with test enthalpy. The q* values obtained using this emittance assumption are presented on figure 30. The least squares regression line for these few data points is also given. The same data were reduced using a spectral emittance value of 0.95 at 0.65 micron. With this assumption the thermochemical heat of ablation results are only increased 1 percent, the true surface temperatures are reduced 100°F, and the total emittance values are increased on an average from 0.59 to 0.64. Until a measurement of the spectral emittance at 0.65 micron is made, the assumed value of 0.75 will be used. On figure 30 is the regression line for the 5026-39/HC-G. This silicone rubber material exhibits a lower q* than the 5026-39/HC-G material at the higher test enthalpies;

The heats of ablation are determined from the test runs as follows:

Cold Wall Heat of Ablation - q_c^*

$$q_c^* = \frac{q_c}{\rho V}$$

where, q_c is the heat flux measured with a water calorimeter, ρ is the density of the specimen tested, and V is the ablative rate of the specimen. (The product of ρV is the mass transfer rate).

[redacted]

ABLATION PROPERTY SHEET

Code No: AP1650

Material: Phenolic Fiberglass

No. of Samples: 5

ρ = 115 lb/ft^3

ϵ_λ = 0.95 at 0.65

P_s(Psig)	H(Btu/lb)	H/RT_o	q^*(Btu/lb)	q_c^*(Btu/lb)	q_c(Btu/ft^2-sec)	H_w(Btu/lb)	V(in/sec)	$\dot{m}$(lb/sec)	q_r(Btu/ft^2-sec)	T_T(°R)	ϵ_T
4.4	7191	212	3043	5163	1425	1766	0.0288	0.011	171	5387	0.43
5.3	4097	121	2000	4567	830	1369	0.0193	0.0165	167	4658	0.74
3.8	5376	159	3070	5807	985	1429	0.0177	0.0124	167	4790	0.67
6.4	5379	159	2929	5194	1175	1380	0.0234	0.0159	169	4683	0.74
2.0	8343	245	4767	7294	1275	1401	0.0184	0.0076	167	4729	0.70

ABLATION PROPERTY SHEET

Code No: AP1676

Material: Silicone Rubber RTV 560

No. of Samples: 5

ρ = 89.0 lb/ft^3

η_l = 0.37

ϵ_λ = 0.75

q_l^* = 363 + 0.37 H Btu/lb

$H_v + C_p \Delta T \approx$ 800 Btu/lb at 355 RT_O

P_s(Psig)	H(Btu/lb)	H/RT_O	q^*(Btu/lb)	q^*(Btu/lb)	q_c(Btu/ft^2-sec)	H_w(Btu/lb)	V(in/sec)	$\dot{m}$(lb/sec)	q_r(Btu/ft^2-sec)	T_T(°R)	ϵ_T
4.4	7191	212	3047	4204	1425	1225	0.0456	0.0119	89	4301	0.54
6.4	5379	159	2437	3684	1175	1205	0.0429	0.0159	94	4247	0.60
5.3	4097	121	1925	3331	830	1194	0.0336	0.0165	87	4216	0.58
2.0	8343	246	3450	4718	1275	1219	0.0364	0.0076	98	4285	0.61
3.8	5376	159	2184	3319	985	1180	0.0402	0.0124	87	4178	0.60

TABLE VIII

10 MEGAWATT ARC TURBULENT PIPE TEST SUMMARY

Run No.	Sample No.	Sample Description	Sample Instr.	Material Density (lbs/ft^3)	Gas Enthalpy H/RT_0	Test Time (seconds)	Heat Flux q_w (Btu/ft^2-sec)	Pipe Shear Stress (lbs/ft^2)	Gas Mass Flow (lbs/sec)	Plenum Pressure (atms)	Power to Air (mw)	Sonic Nozzle Diameter (inches)	Total Mass Loss of Sample (grms)	Avg. Sample Internal Dim. Prerun (inches)	Avg. Sample Internal Dim. Postrun (inches)	Remarks
		All Samples are 026-49 - 3/8 Honeycomb Canned														
4716	AP-1636-4	Plus Fiberglass Closeout Members Plus 0.200 inch RTV-560 Gasket Filled	B.F.T.C.	31.9	77	13.60	264	4.57	0.127	1.97	0.35	0.980	51.0	1.251	1.670	Good Run
4717	AP-1636-3	Plus F/G Closeout Members Plus 0.190 inch RTV-560 Gasket Filled	B.F.T.C.	31.5	78	19.65	260	4.44	0.122	1.89	0.34	0.980	48.1	1.249	1.630	Good Run
4718	AP-1636-5	Plus F/G Closeout Members Plus 0.180 inch RTV-560 Gasket Filled	B.F.T.C.	31.4	79	29.48	260	4.38	0.120	1.88	0.34	0.980	79.2	1.252	1.751	Good Run
4797	AP-1636-6	Plus F/G Closeout Members Plus 0.180 inch RTV-560 Gasket Filled	B.F.T.C.	31.8	228	11.64	750	3.90	0.080	5.74	0.85	0.825	51.4	1.252	1.734	Good Run
4798	AP-1636-7	Plus F/G Closeout Members Plus 0.180 inch RTV-560 Gasket Filled	B.F.T.C.	31.4	226	17.50	740	3.87	0.080	5.73	0.85	0.825	48.1	1.252	1.696	Good Run
4723	AP-1636-8	Plus F/G Closeout Members Plus 0.180 inch RTV-560 Gasket Filled	B.F.T.C.	30.8	152	12.65	560	5.13	0.115	2.83	0.51	0.891	59.5	1.252	1.729	Good Run
4807	AP-1636-9	Plus F/G Closeout Members Plus 0.180 inch RTV-560 Gasket Filled	B.F.T.C.	31.2	236	19.41	755	10.27	0.165	2.38	1.22	1.20	130.1	1.251	2.471	Good Run
4757	AP-1636-10	Plus F/G Closeout Members Plus 0.170 inch RTV-560 Gasket Filled	B.F.T.C.	30.5	66	36.9	239	3.76	0.125	2.23	0.30	0.891	68.9	1.252	1.766	Good Run
4758	AP-1636-11	Plus F/G Closeout Members Plus 0.200 inch K-1205 Gasket Filled	B.F.T.C.	30.6	49	22.4	227	3.90	0.129	2.21	0.29	0.891	50.7	1.254	1.643	Run Cut - Electrode Broke
4761	AP-1636-12	Plus F/G Closeout Members Plus 0.200 inch K-1205 Gasket Filled	B.F.T.C.	30.6	65	11.66	245	3.92	0.128	2.26	0.30	0.891	27.2	1.253	1.659	Run Cut - Electrode Broke
4801	AP-1636-13	Plus F/G Closeout Members Plus 0.180 inch K-1205 Gasket Filled	B.F.T.C.	29.7	68	29.61	227	3.42	0.121	2.20	0.30	0.891	69.9	1.251	1.827	Good Run T/C 2 in N.G.
4802	AP-1636-14	Plus F/G Closeout Members Plus 0.180 inch K-1205 Gasket Filled	B.F.T.C.	29.7	65	29.55	212	3.38	0.123	2.18	0.29	0.891	68.6	1.256	1.811	Good Run T/C 3 in N.G.
4735	AP-1643-2	Plus 0.200 inch RTV-560 Gasket and 0.015 inch Circumferential Step	None	30.8	88	25.56	276	4.32	0.119	1.95	0.37	0.980	79.9	1.249	1.764	All Joints in AP-1643 Series are 0.200 inch. Prerun sample I.D. at exit was 0.958 inch.
4753	AP-1643-3	Plus 0.180 inch RTV-560 Gasket and 0.015 inch Circumferential Step	B.F.T.C.	31.5	76	23.50	273	3.85	0.121	2.25	0.33	0.891	68.9	1.250	1.790	Run Cut-Electrode Broke. Prerun sample I.D. at exit was 0.955 inch.
4754	AP-1643-4	Plus 0.180 inch RTV-560 Gasket and 0.015 inch Circumferential Step	B.F.T.C.	30.5	65	29.43	250	3.99	0.112	2.29	0.30	0.891	81.4	1.250	1.767	Good Run. Prerun Sample I.D. at exit was 0.956 inch.
4733	AP-1643-5	Plus 0.200 inch Teflon Gasket (long-gap overfilled)	None	31.8	71	29.57	256	4.70	0.125	1.89	0.31	0.980	92.0	1.251	1.949	Good Run
4732	AP-1643-6	Plus 0.200 inch RTV-560 Gasket Filled and 0.07 inch Circumferential Step	None	31.9	67	29.61	231	4.43	0.128	1.89	0.32	0.980	84.3	1.252	1.838	Good Run
4739	AP-1644-5	Plus Fused Quartz Plug	None	----	153	19.50	550	5.98	0.109	2.24	0.60	0.980	81.7	1.249	1.903	Good Run
4810	AP-1605-2	Plus Longitudinal and Circumferential Gaps Filled with RTV-560 and Teflon	None	32.3	60	29.52	240	5.33	0.149	3.08	0.32	0.825	88.0	1.244	1.952	Good Run
4745	AP-1605-1	Plus Longitudinal and Circumferential Gaps Filled with RTV-560	None	32.3	56	8.40	189	4.77	0.140	2.54	0.30	0.825	35.9	0.385	1.460	Run Cut - Sample Failed Due Apparently to Open Porosity of the Fiberglass Wrap Around the Specimen
4813	AP-1605-3	Plus Longitudinal and Circumferential Gaps Filled with RTV-560	None	32.3	58	29.77	232	5.30	0.150	2.67	0.31	0.825	84.5	0.281	1.939	Good Run
4	AP-1644-1	Plus Adaptor to Fiberglass Step with Closeout and Gasket (Laminated F/C) (ECP/TT) 10 inch Turbulent Pipe	None	FC 113 3 Runs 30.3	262	12.28	1010	4	0.099	2.52	0.93	0.980	134.7	1.251	1.976	Run Cut - Electrode Broke Good Run

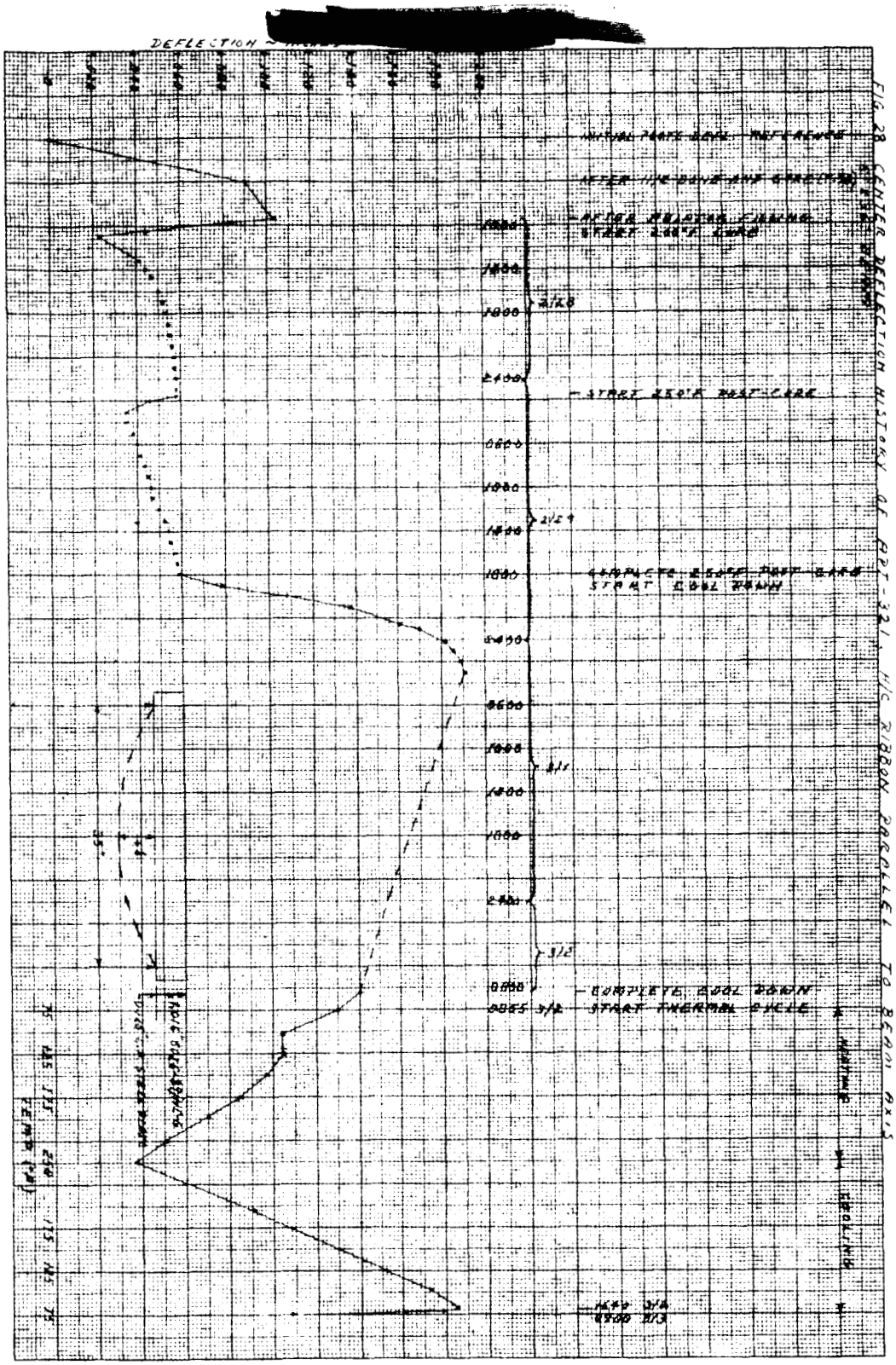

Figure 28 CENTER DEFLECTION HISTORY OF APT-321, HC RIBBON PARALLEL TO BEAM AXIS

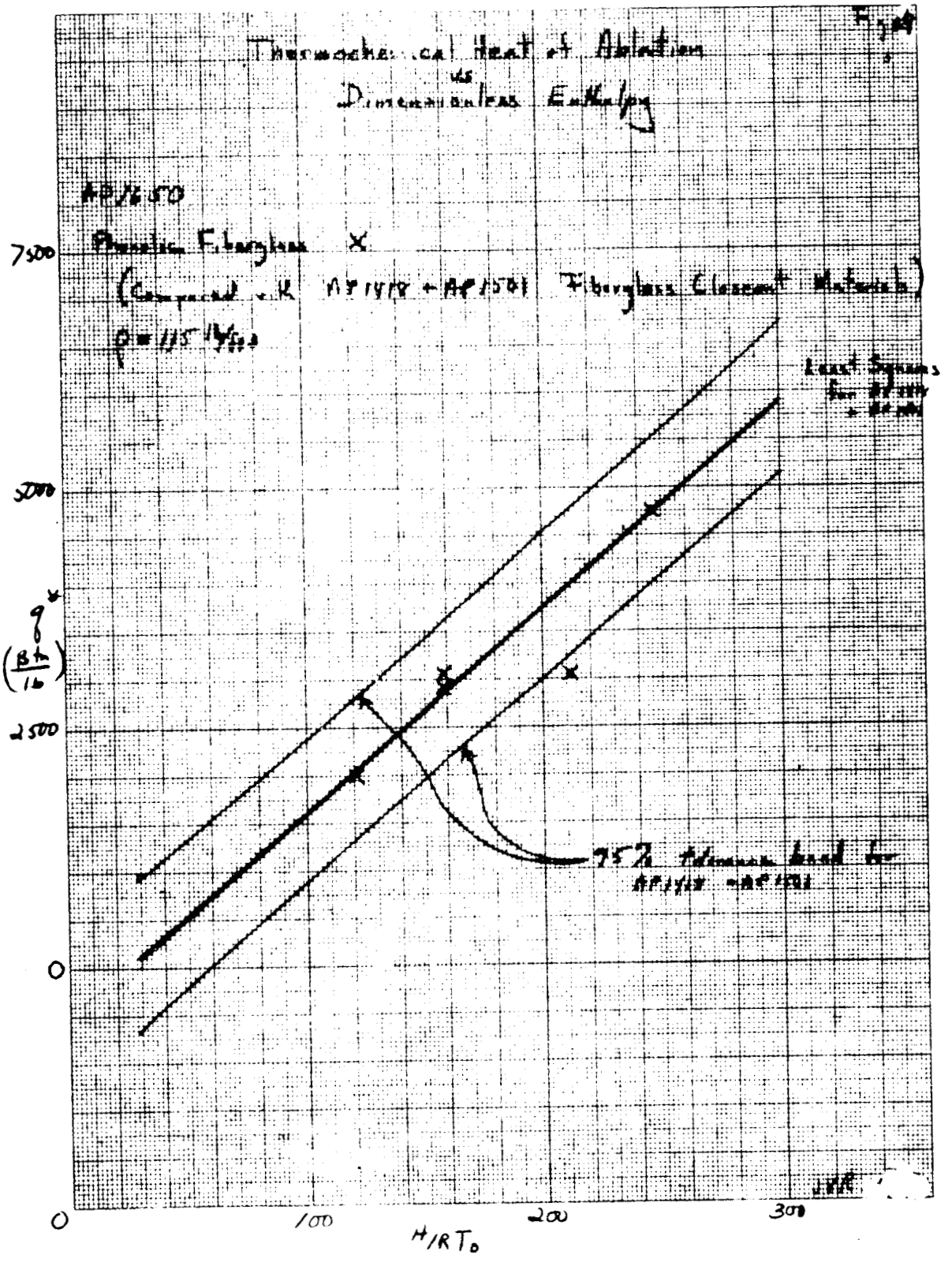

Figure 29 THERMOCHEMICAL HEAT OF ABLATION VERSUS DIMENSIONLESS ENTHALPY

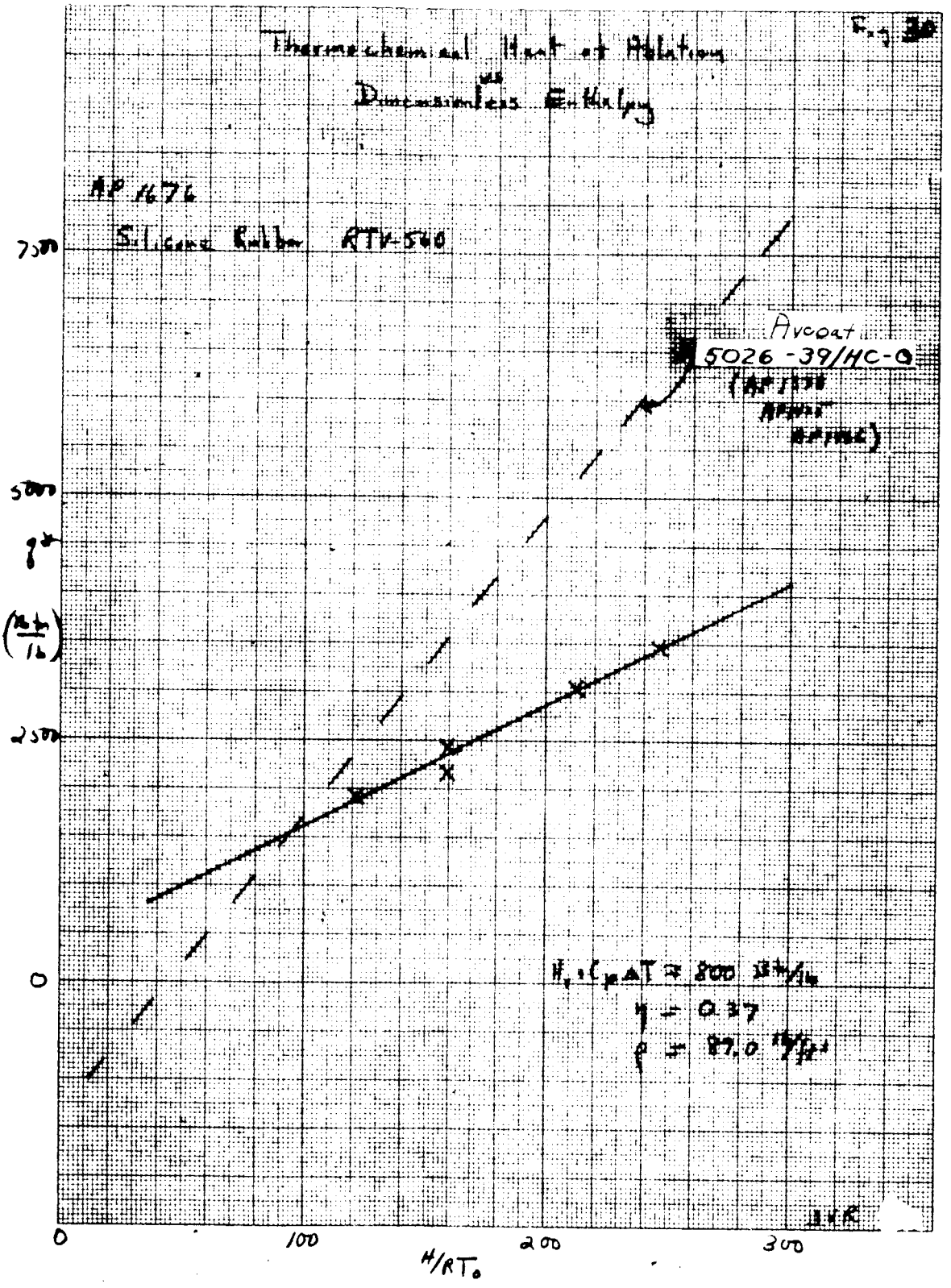

Figure 30 THERMOCHEMICAL HEAT OF ABLATION VERSUS DIMENSIONLESS ENTHALPY

Hot Wall Heat of Ablation - q_o^*

$$q_o^* = q_c^* \left(\frac{H - H_w}{H - H_{cw}} \right)_w$$

where, H is the air enthalpy referenced to absolute zero, H_w is the air enthalpy at the wall of the specimen determined from the surface temperature of the specimen, H_{cw} is the air enthalpy at the wall of the calorimeter determined in the same manner, and $w = \left(\frac{T_w}{720} \right)^{-0.04}$ is a correction applied because of the high wall temperatures.

Thermochemical Heat of Ablation - q^*

$$q^* = q_o^* - q_r^* = q_o^* - \frac{q_r}{\rho V}$$

where q_r is the emitted radiant flux from the surface of the specimen. Once the q^* values are obtained an attempt is made to apply a simplified analysis to these data. A least squares regression line is determined, and from this estimates of the transpiration factor, η, and the effective heat of vaporization including heats of reaction, $H_v + C_p \Delta T + Q_l$, are made. η is the slope of the line and $H_v + C_p \Delta T + Q_l$ is the intercept value at a particular enthalpy where the onset of ablation is believed to occur. Essentially what is being said is that the material is being brought up to the ablation temperature, melting or vaporizing, perhaps reacting chemically, and then the products of ablation are blocking the heat from reaching the surface causing a reduction in ablative rate. This blocking causes an increasing increase in the q^* values with increasing enthalpy. This can be shown on the figure 29, where η is the slope of the line and $H_v + C_p \Delta T$ is the intercept value for this material at $H = 29\ RT_o$.

Parallel splash tests were conducted in the OVERS facility on the remaining AP1308 5026-39/HC-T specimens in oxygen-nitrogen mixtures of zero and 10 percent oxygen at a nominal heating level of 500 Btu/ft^2-sec. The specimens employed in these tests consist of 3/4 inch O. D. plugs, 2 inches in length protected by a 2-1/2 inch O. D. shroud. A pretest photograph (figure 31) shows a typical specimen. The test conditions and ablation data are reported in table IX. Post-test photographs of the exposed surface and a half-section view of the exposed plugs are presented in figures 32-35. Surface temperature, total radiation, and emittance data are given for these specimens in table X, as well as for specimens of this series tested and partially reported in the February period.

Twelve additional tests were performed on instrumented specimens (AP1551-52). The specimens consist of 3/4 inch plugs protected by 4-1/4 inch O. D. shrouds in the AP1551 (5026-39/HC-G) set and by 3-1/2 inch O. D.

[redacted]

shrouds in the AP1552 (5026-39/M) set. Pretest photographs of typical specimens are given in figures 36 and 37. Each specimen was instrumented with five thermocouples: four imbedded in the material and one in a steel back plate (see figure 38). Ablation data from these tests is presented in table IX and plots of temperature versus time in figures 39-50.

The comparative performance of the AP1308 specimens subjected to a nominal heating of 500 Btu/ft^2-sec (see table IX) is similar to that reported for lower heating levels in the February 1964 Apollo Monthly Progress Report. Both the surface recession in the presence of pure nitrogen and the difference in surface recession between tests in pure nitrogen and ten percent oxygen are of the same order, indicating that both oxidation and non-oxidation surface ablation mechanisms are important.

Examination of table X reveals, that in general, the emissivity values recorded are lower than normally obtained. The emissivities were computed (as usual), using the Stefan equation and the tabulated values of total radiation and surface temperature obtained by data reduction of spectrometer measurements of spectral radiant intensity. The spectrometer was calibrated before any specimens were tested. The possibility exists, however, that the optical system became misaligned during the specimen runs. If this were true, negative errors would be introduced into the total radiation data and, consequently, the low values of computed emissivity explained. The system was checked and recalibrated before specimens 14 and 31 were tested. The emissivities recorded for these two tests are consistent with normally obtained values, apparently bearing out the hypothesis regarding misalignment. Reasonable values of emissivity were also determined for specimens 4, 6, and 9, the first three tested.

With the exception of specimen AP1552-4, the thermocouple output appeared representative of material performance. Large discontinuities were observed in the temperature response recorded for this specimen by the first three thermocouples, indicating thermocouple malfunction. Consequently, temperature data for these thermocouple positions are given only until the times at which the discontinuities arose.

[redacted]

TABLE IX

OVERS ABLATION DATA

Specimen	Specific Gravity	Shroud O. D. (inches)	Test Time* (seconds)	Impact Pressure (mm-Hg)	Mass flow of Jet (lb/sec x 10^3)	Percent O_2	Cold Wall Heat Flux (Btu/ft-sec)	Enthalpy (Btu/lb x 10^{-3})	Length Loss (inches)	Char Depth (inches)	Weight Loss (grams)
AP1308-30	0.544	2-1/2	60	18.4	3.2	0	487	18.9	0.114	0.22	0.98
AP1308-29	0.513	2-1/2	120	18.4	3.2	0	487	18.9	0.249	0.29	1.44
AP1308-31	0.525	2-1/2	45	22.3	3.2	10	525	18.9	0.173	0.14	1.00
AP1308-14	0.589	2-1/2	75	22.3	3.2	10	525	18.9	0.244	0.19	1.70
AP1551-1	0.485	4-1/4	400/200	8.2	2.2	0.23	270	18.6	0.863	0.36	4.40
AP1551-2	0.488	4-1/4	600/200	4.6	1.2	0.23	95	17.1	0.540	0.35	2.97
AP1551-3	0.491	4-1/4	500/200	5.8	1.7	0.23	130	10.9	0.764	0.30	3.58
AP1551-4	0.499	4-1/4	800/70	4.7	1.3	0.23	81	10.1	0.685	0.29	3.32
AP1551-5	0.481	4-1/4	1500/200	1.0	0.8	0.23	27	9.7	0.272	All	2.57
AP1551-6	0.485	4-1/4	1200/200	1.5	0.9	0.23	41	10.9	0.452	0.66	2.77
AP1551-7	0.497	4-1/4	1700/200	0.7	0.4	0.23	7	9.3	0.071	0.37	1.59
AP1551-8	0.484	4-1/4	400/200	7.1	2.0	0.23	260	19.6	0.819	All	5.48
AP1552-1	0.540	3-1/2	400/200	8.2	2.2	0.23	270	18.1	0.650	0.34	3.59
AP1552-2	0.548	3-1/2	500/200	5.6	1.7	0.23	130	10.6	0.585	0.34	2.22
AP1552-3	0.546	3-1/2	800/200	4.7	1.3	0.23	81	10.4	0.504	0.47	2.85
AP1552-4	0.560	3-1/2	1500/200	1.0	0.8	0.23	30	9.8	0.309	0.46	2.36

*The first value refers to the heating period and the second to the thermal soak.

[redacted]

TABLE X

OVERS TEMPERATURE DATA

Specimen	Test Time (seconds)	Percent O_2	Cold Wall Heat Flux (Btu/ft^2 sec)	Enthalpy (Btu/lb x 10^{-3})	Surface Temperature (°K)	Total Hemispherical Radiant Emittance (watts/cm^2)	Total Emissivity
AP1308-4	300	40	97	4.15	1850 ± 50	52 ± 5	0.77 ± 0.08
AP1308-6	600	40	97	4.15	1800 ± 50	45 ± 5	0.75 ± 0.08
AP1308-28	300	10	43	10.3	1600 ± 50	22 ± 2	0.58 ± 0.06
AP1308-20	600	10	43	10.3	1550 ± 50	21 ± 2	0.63 ± 0.06
AP1308-10	300	40	46	10.3	1600 ± 50	25 ± 3	0.67 ± 0.07
AP1308-9	600	40	46	10.3	1600 ± 50	26 ± 3	0.71 ± 0.07
AP1308-16	120	0	238	10.6	2200 ± 75	91 ± 9	0.69 ± 0.07
AP1308-15	200	0	238	10.6	2200 ± 75	91 ± 9	0.69 ± 0.07
AP1308-17	90	10	230	10.9	2200 ± 75	84 ± 8	0.64 ± 0.06
AP1308-18	150	10	230	10.9	2200 ± 75	96 ± 10	0.73 ± 0.07
AP1308-22	90	40	270	10.6	2200 ± 75	88 ± 9	0.66 ± 0.07
AP1308-26	60	10	470	15.0	2600 ± 75	157 ± 16	0.60 ± 0.06
AP1308-25	100	10	470	15.0	2550 ± 75	157 ± 16	0.65 ± 0.07
AP1308-30	60	0	487	18.9	2450 ± 50	107 ± 11	0.52 ± 0.05
AP1308-29	120	0	487	18.9	2450 ± 50	122 ± 12	0.60 ± 0.06
AP1308-31	45	10	525	18.9	2650 ± 75	205 ± 21	0.73 ± 0.07
AP1308-14	75	10	525	18.9	2800 ± 25	253 ± 25	0.73 ± 0.07

[redacted]

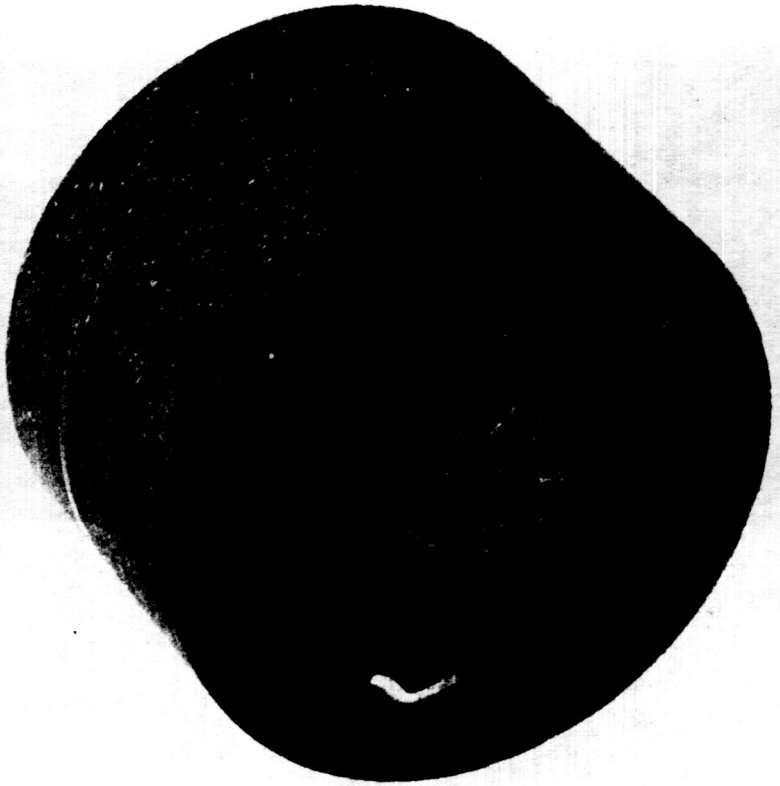

Typical Specimen

AP1308

Plug 5026-39-3/8 HC
Shroud 2 1/2-in. dia.

Figure 31 TYPICAL SPECIMEN, AP1308
9807C

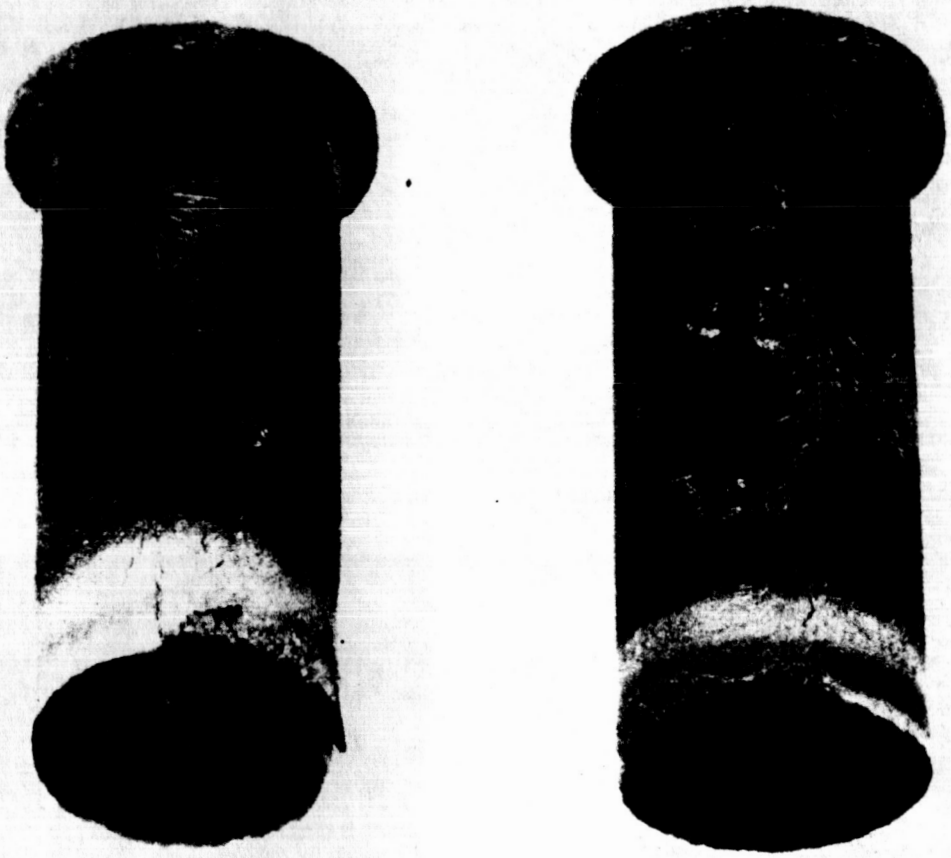

AP1308-29 AP1308-30

5026-39-3/8 HCT

Figure 32 THREE-QUARTER VIEW OF THE FRONT SURFACE, AP1308-29, 30
10914A

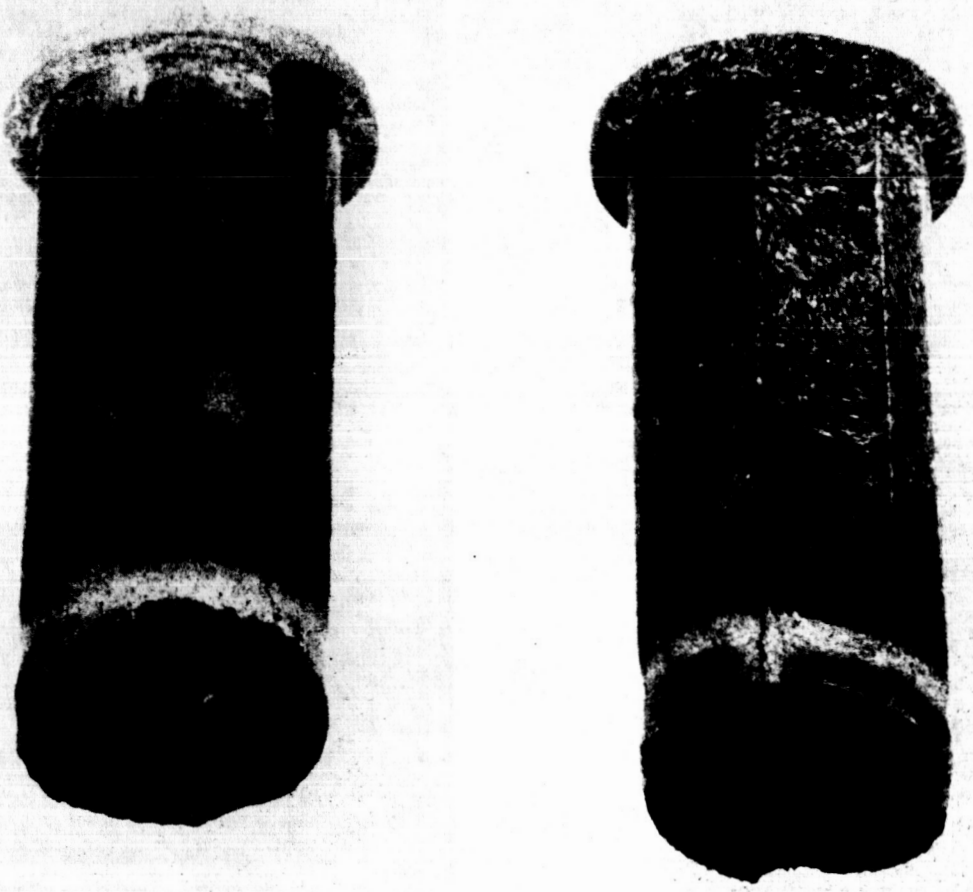

5026-39-3/8 HCT

Figure 33 THREE-QUARTER VIEW OF THE FRONT SURFACE, AP1308-14, 31
10914A

5026-39-3/8 HCT

AP1308-29

AP1308-30

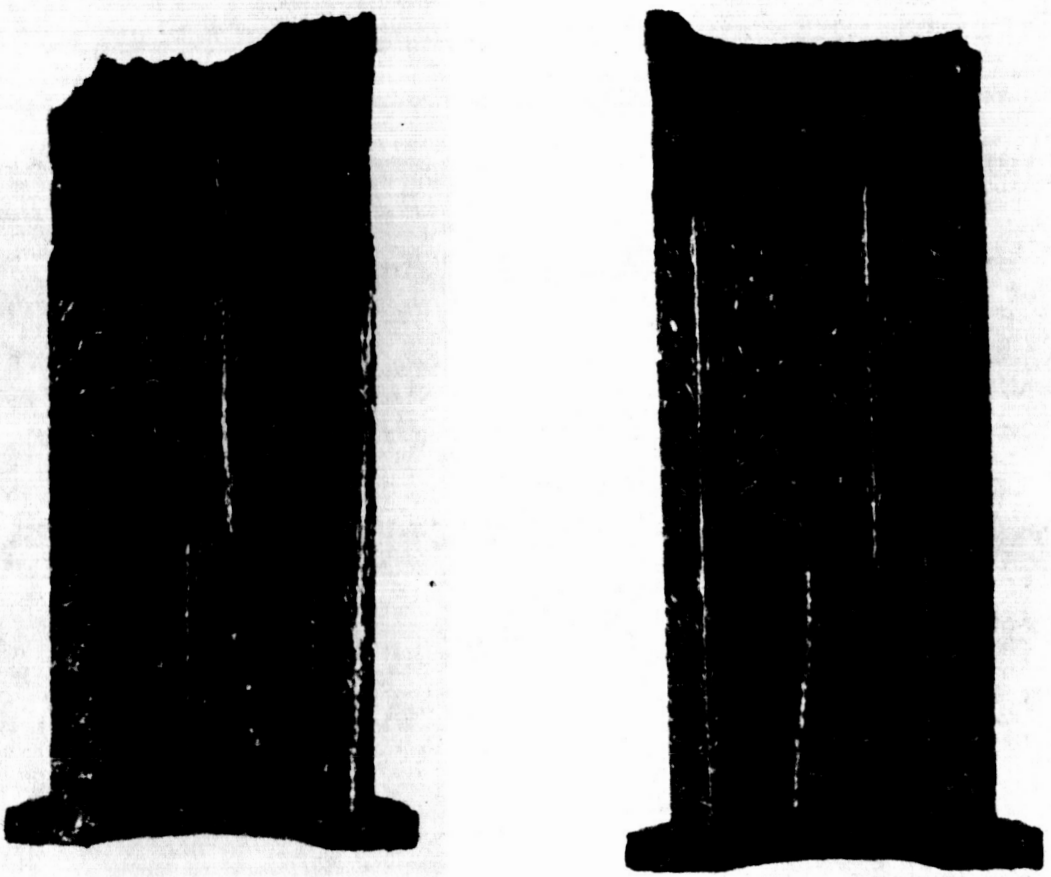

Figure 34 HALF-SECTION, AP1308-29, 30
10914D

[redacted]

5026-39-3/8 HCT

AP1308-14 AP1308-31

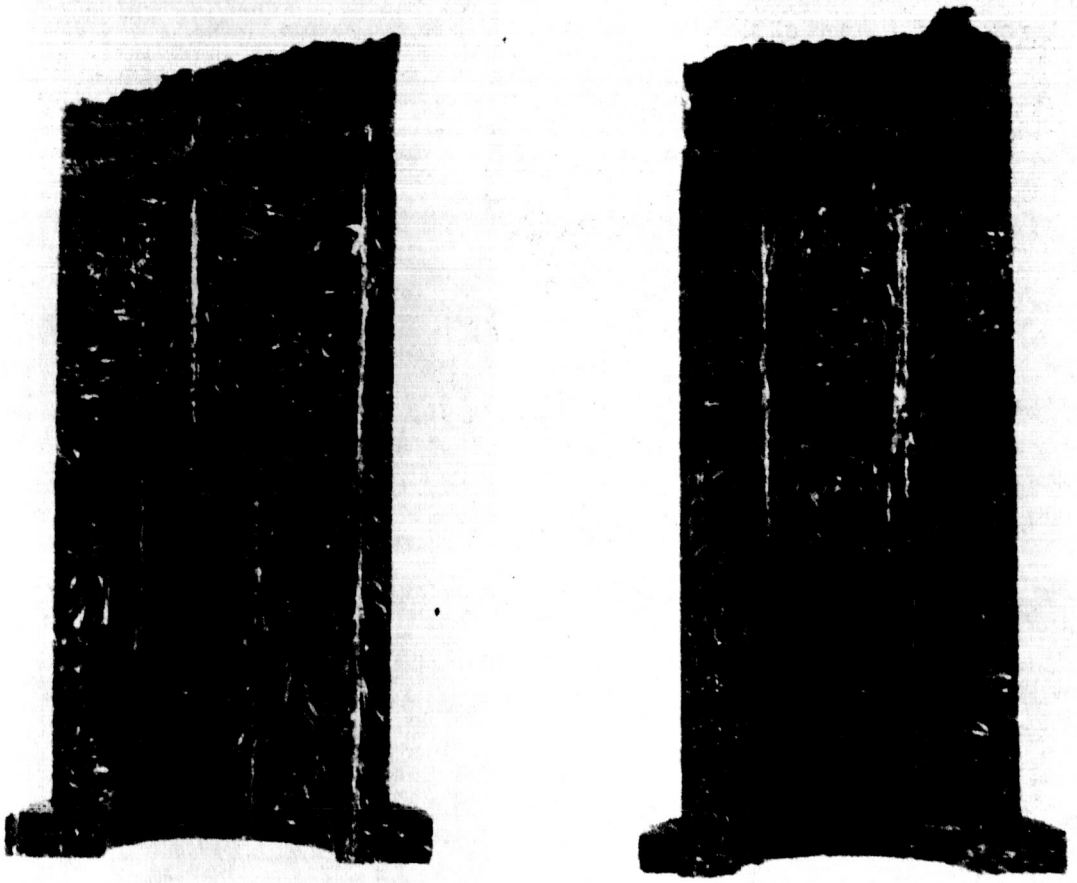

Figure 35 HALF-SECTION, AP1308-14, 31
10914C

[redacted]

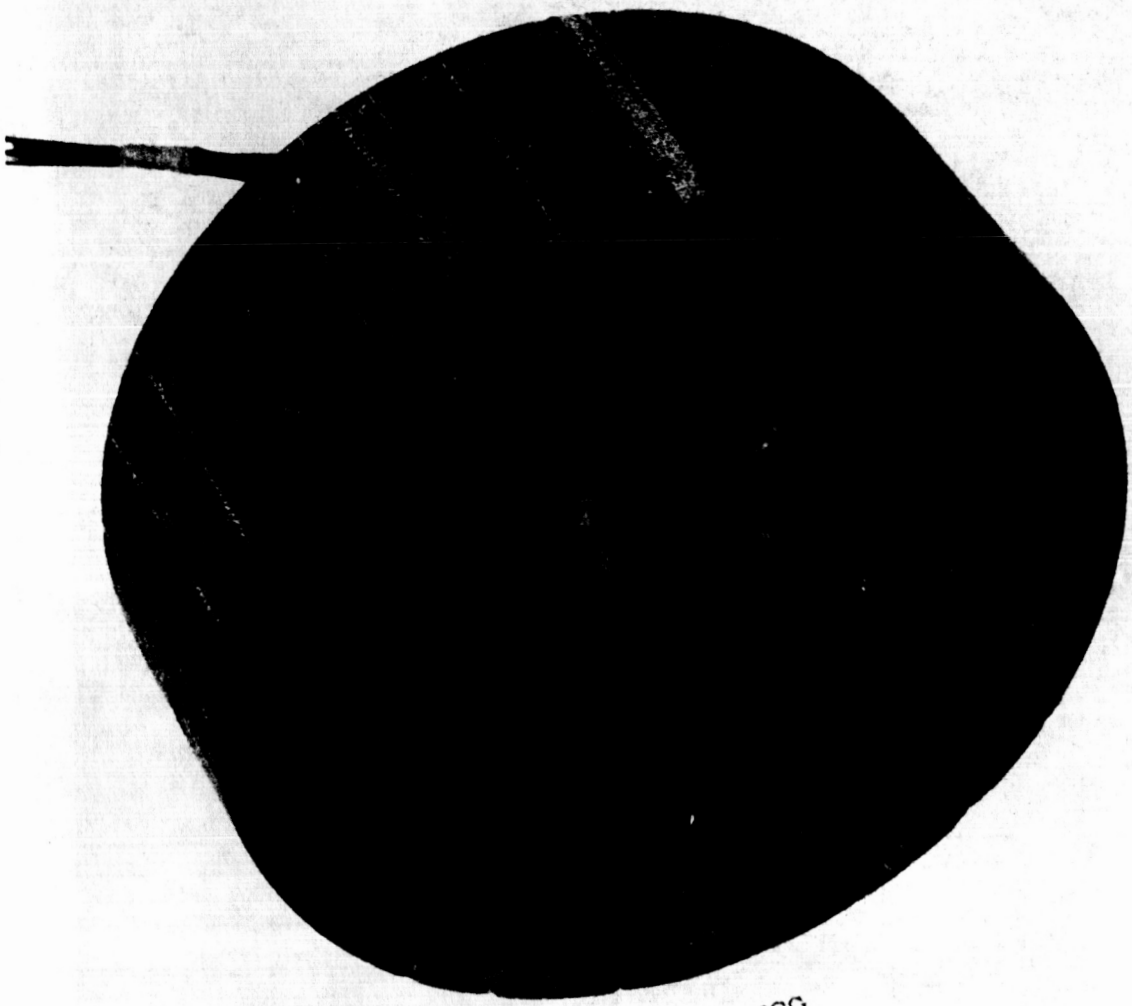

X5026-39-3/8 HCG

AP1551-1
(typ. of -2 thur -8)

Figure 36 TYPICAL SPECIMEN, AP1551
10412C

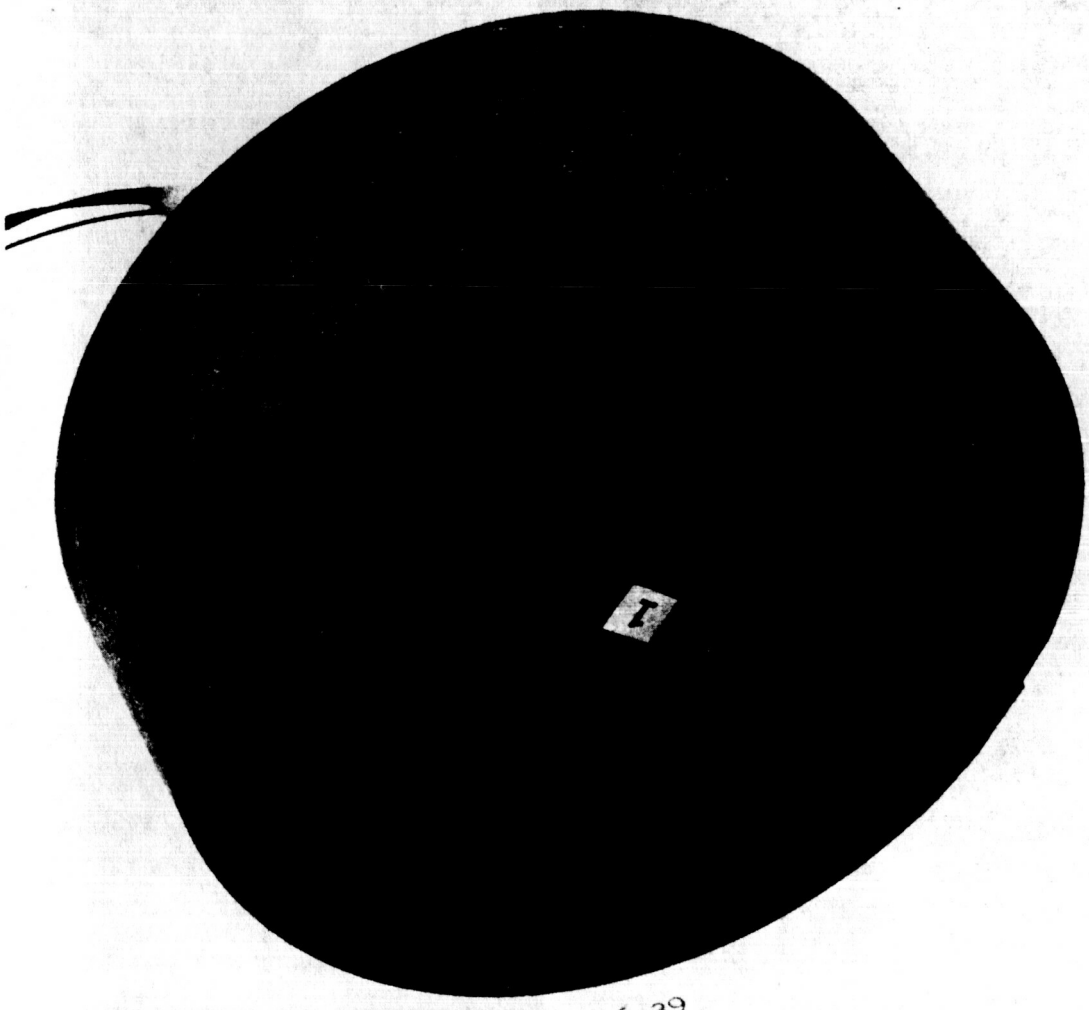

X5026-39

AP1552-1
(typ. of -2 thru -4)

Figure 37 TYPICAL SPECIMEN, AP1552
10412D

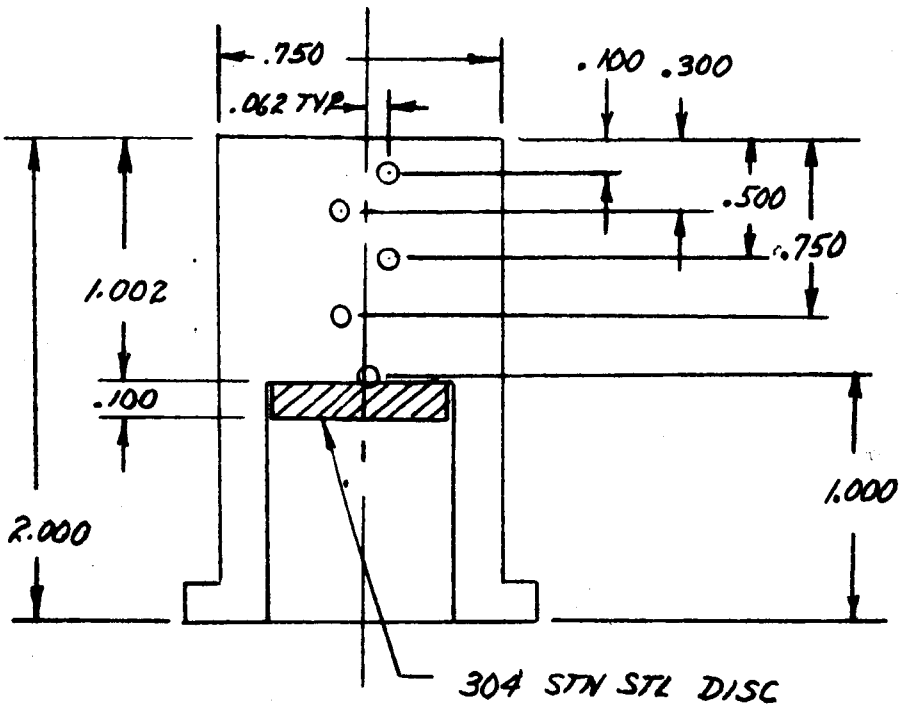

Figure 38 CROSS-SECTIONAL VIEW OF INSTRUMENTED PLUG, SHOWING THERMOCOUPLE LOCATIONS

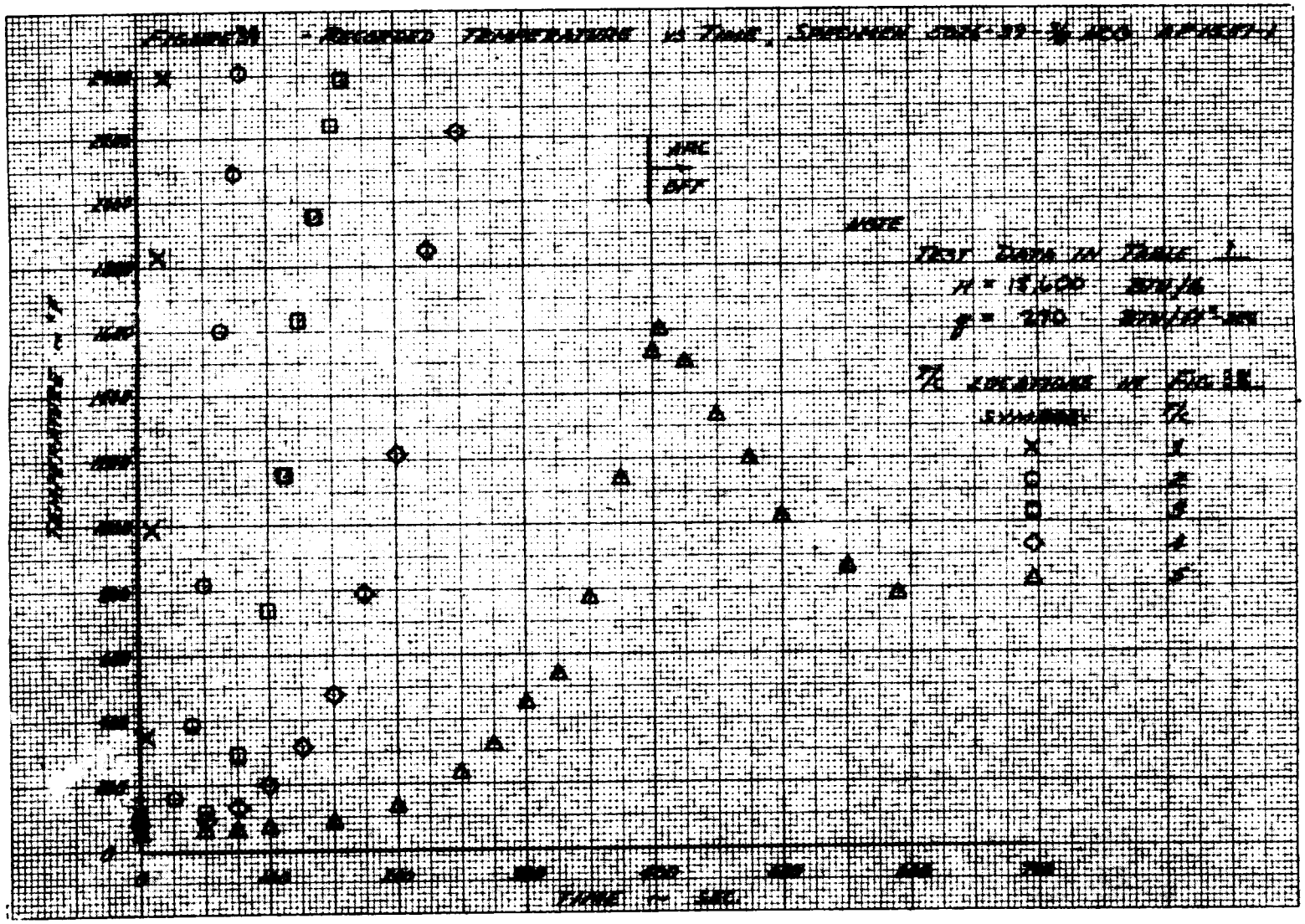

Figure 39 RECORDED TEMPERATURE VERSUS TIME, SPECIMEN
5026-39-3/8 INCH HCG, AP1551-1

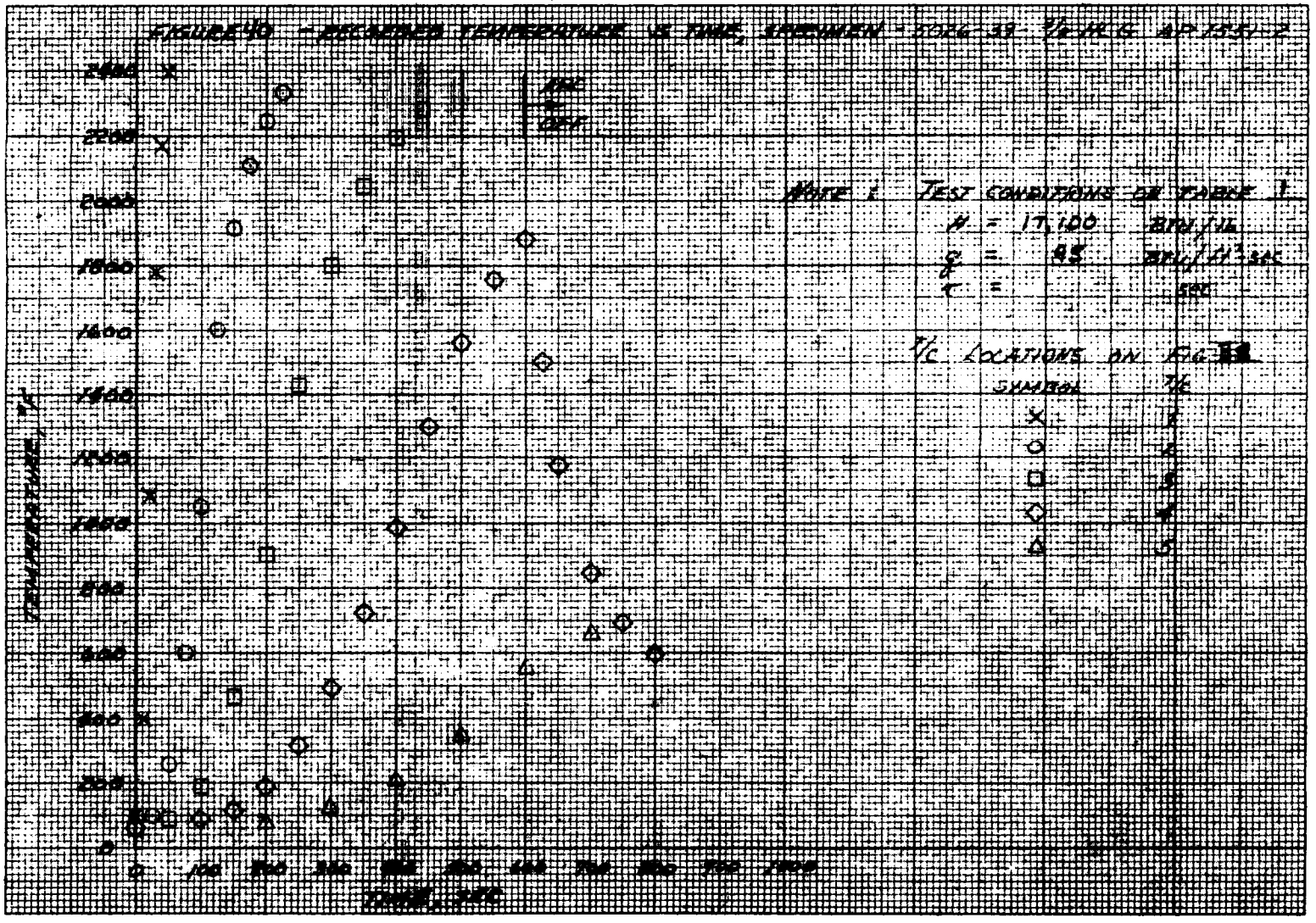

Figure 40 RECORDED TEMPERATURE VERSUS TIME, SPECIMEN
5026-39-3/8 INCH HCG, AP1551-2

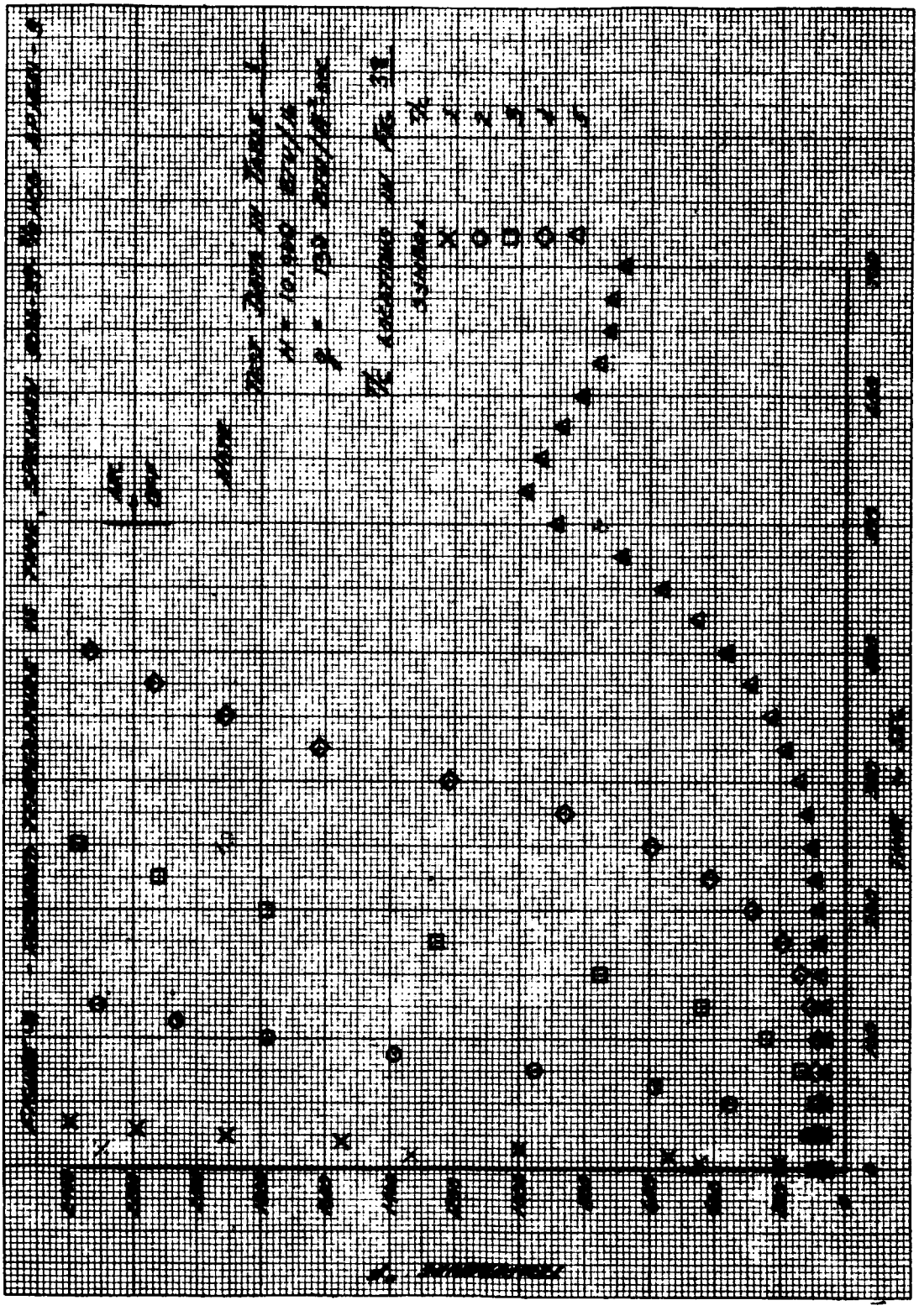

Figure 41 RECORDED TEMPERATURE VERSUS TIME, SPECIMEN 5026-39-3/8 INCH HCG, AP1551-3

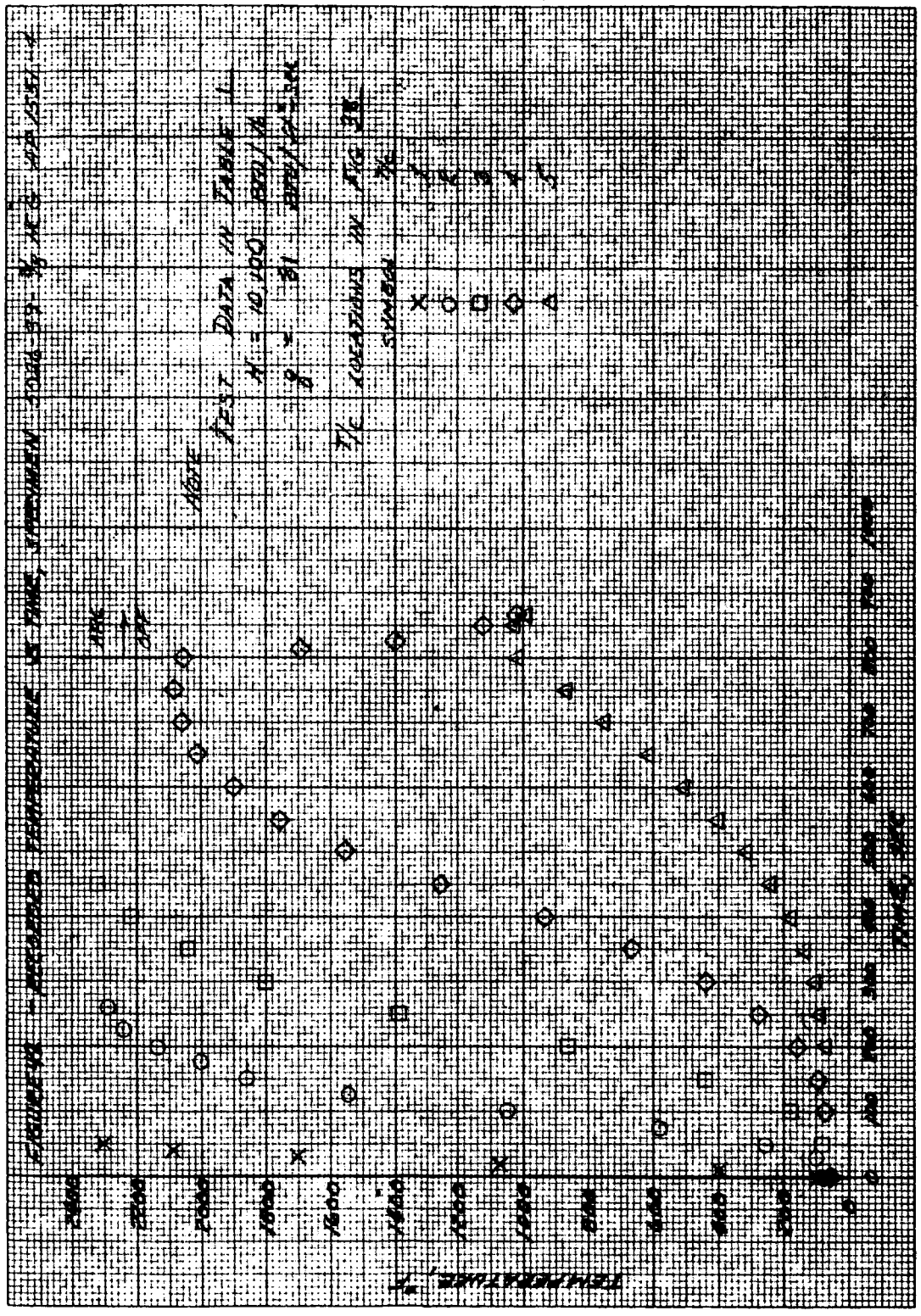

Figure 42 RECORDED TEMPERATURE VERSUS TIME, SPECIMEN 5026-39-3/8 INCH HCG, AP1551-4

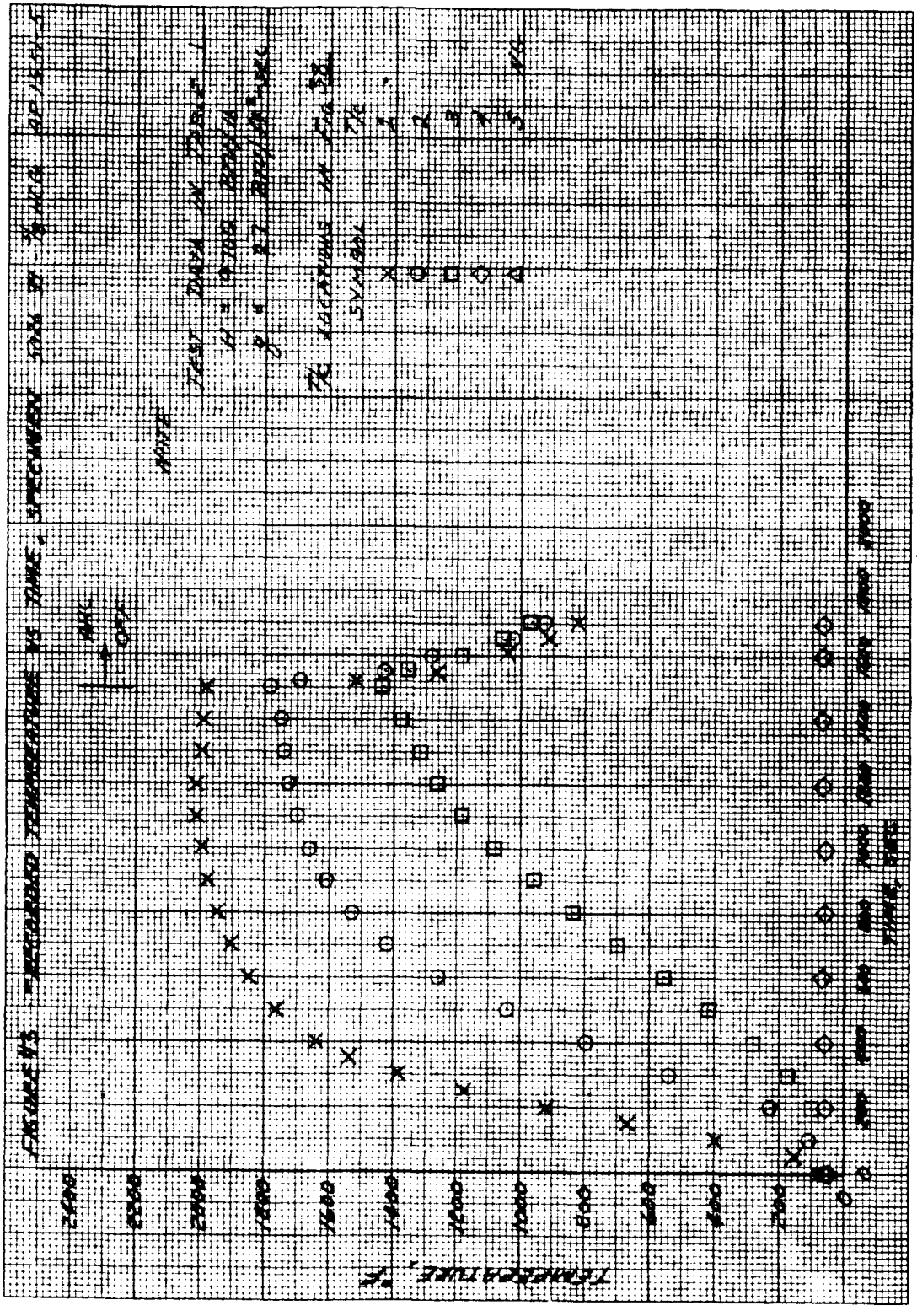

Figure 43 RECORDED TEMPERATURE VERSUS TIME, SPECIMEN 5026-39-3/8 INCH HCG, AP1551-5

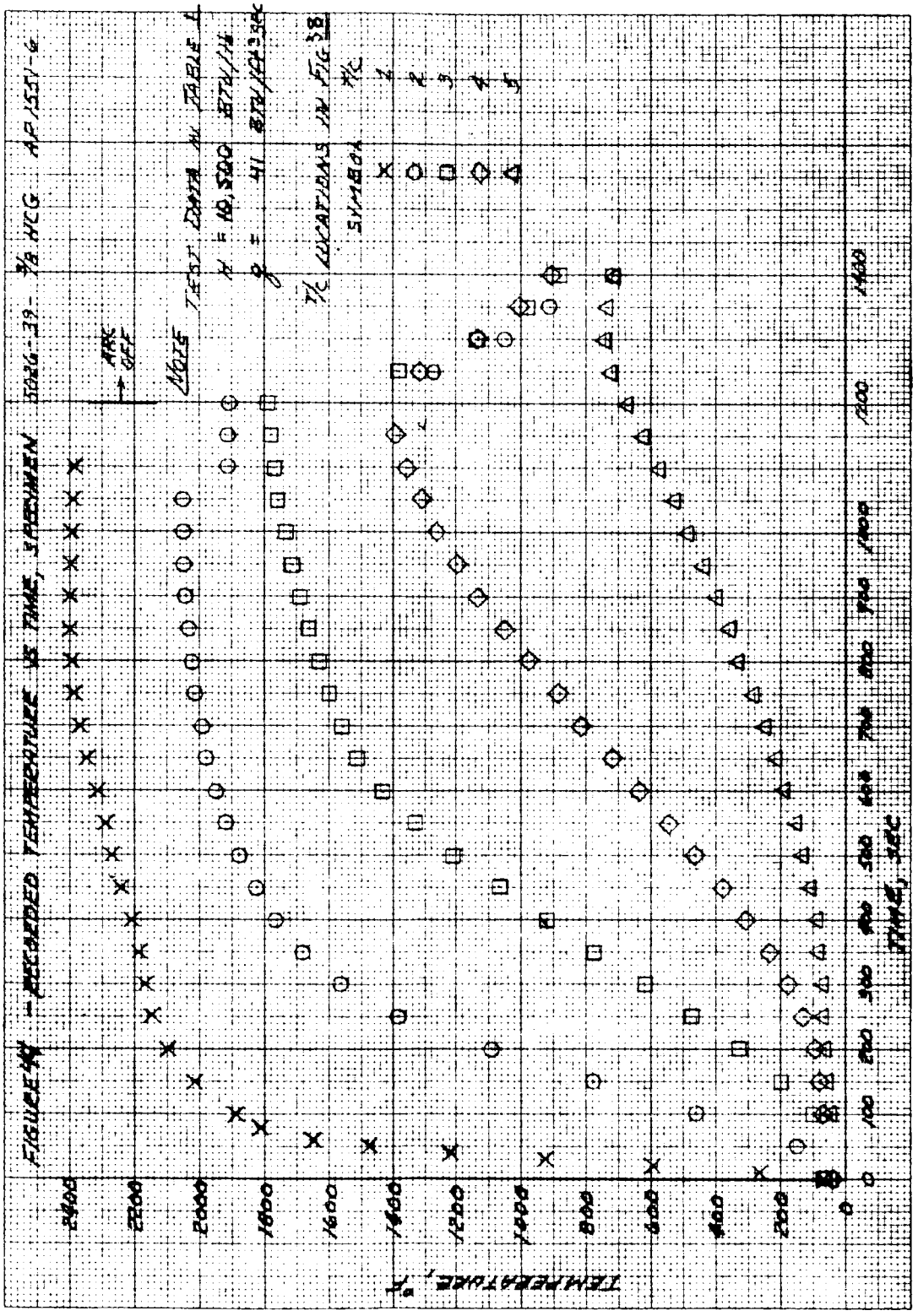

Figure 44 RECORDED TEMPERATURE VERSUS TIME, SPECIMEN 5026-39-3/8 INCH HCG, AP1551-6

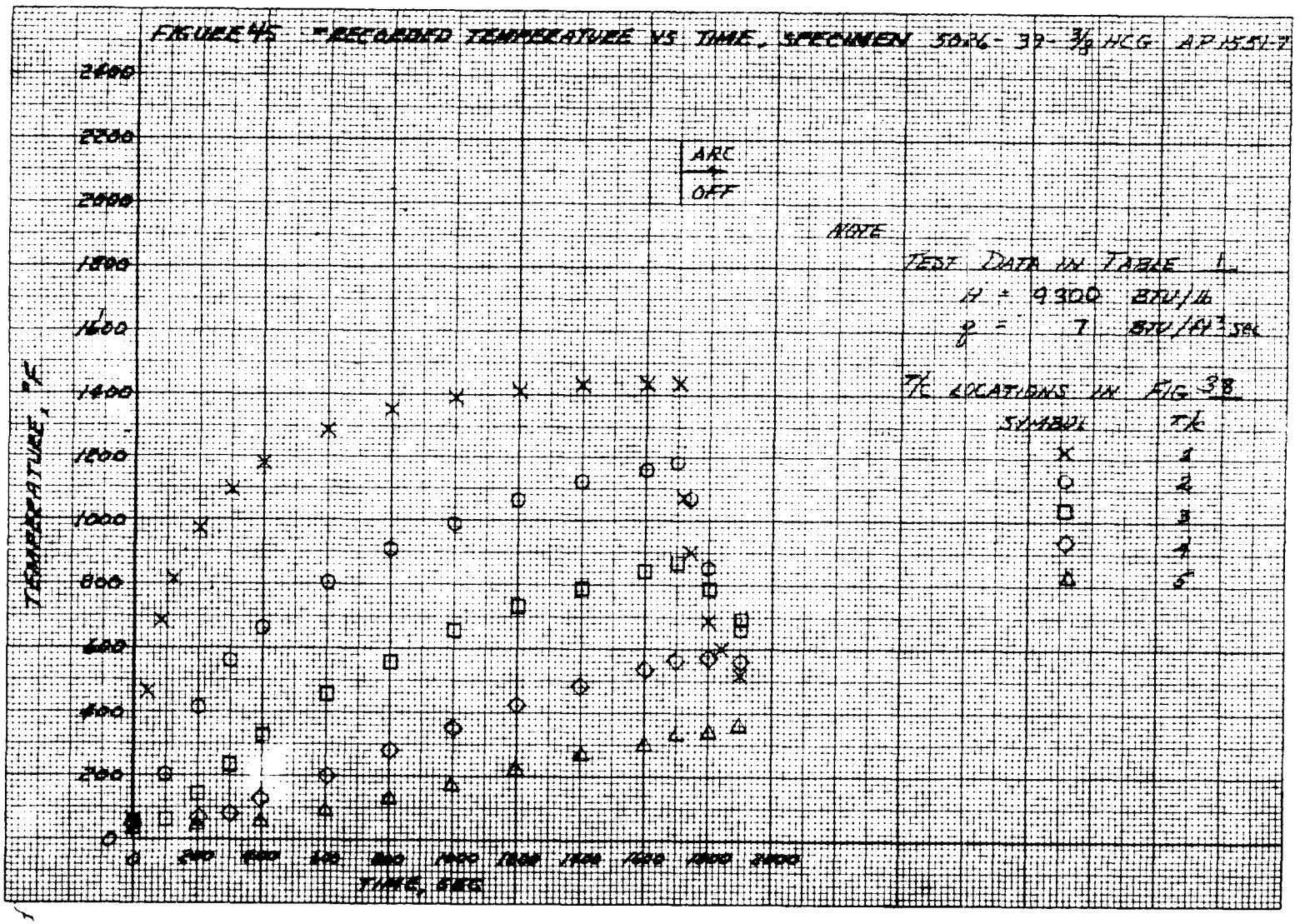

Figure 45 RECORDED TEMPERATURE VERSUS TIME, SPECIMEN
5026-39-3/8 INCH HCG, AP1551-7

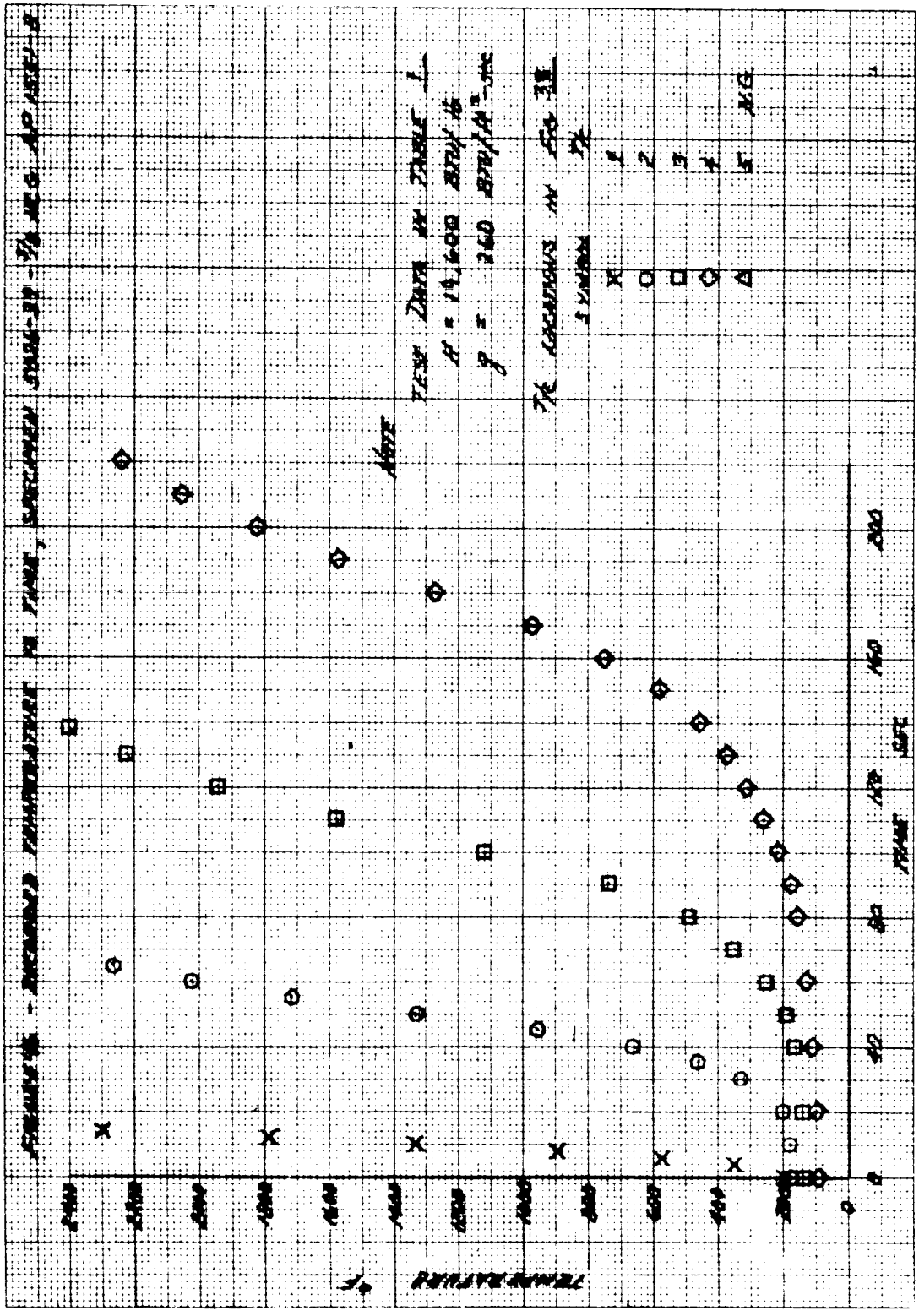

Figure 46 RECORDED TEMPERATURE VERSUS TIME, SPECIMEN 5026-39-3/8 INCH HCG, AP1551-8

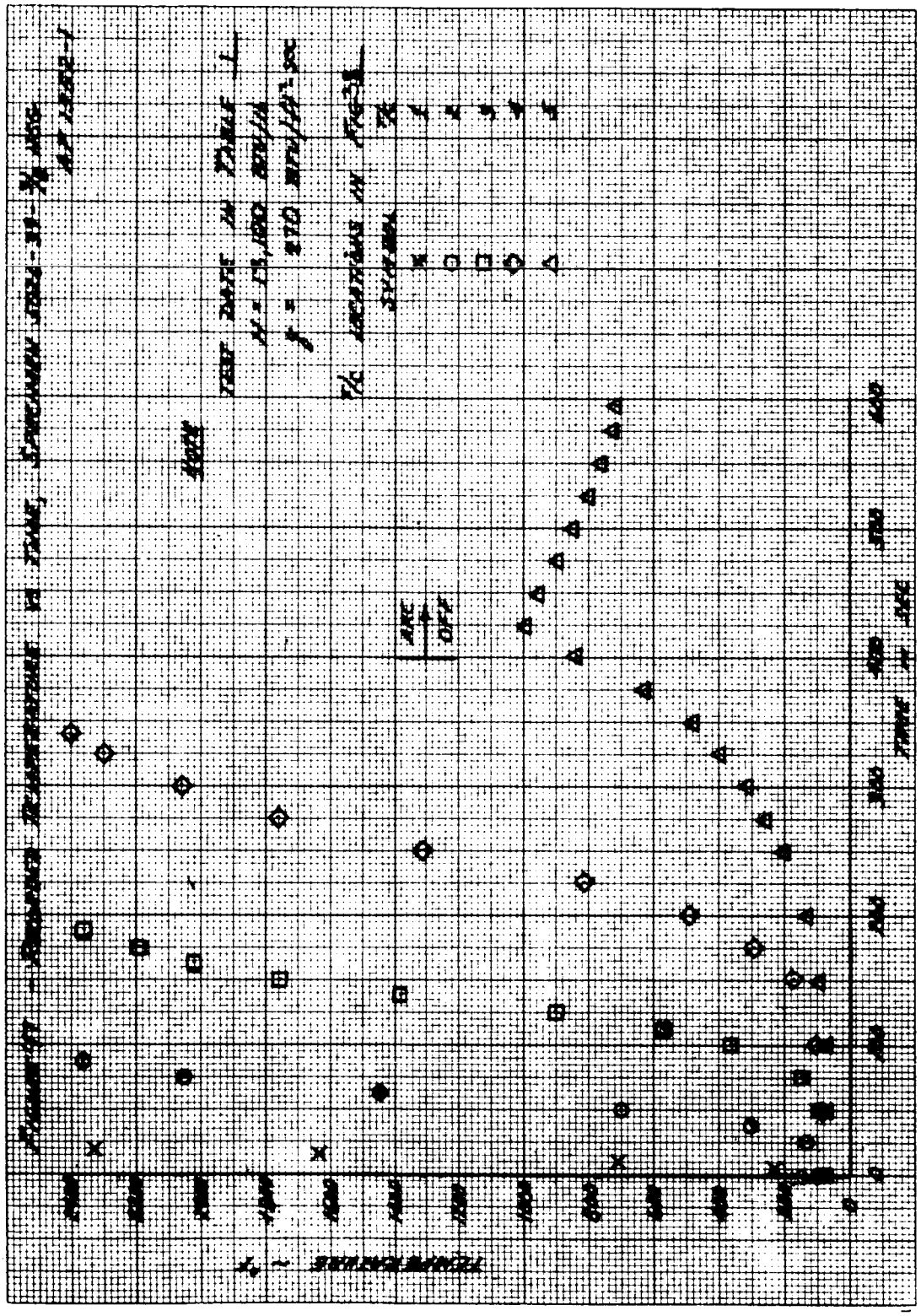

Figure 47 RECORDED TEMPERATURE VERSUS TIME, SPECIMEN 5026-39-3/8 INCH HCG, AP 1552-1

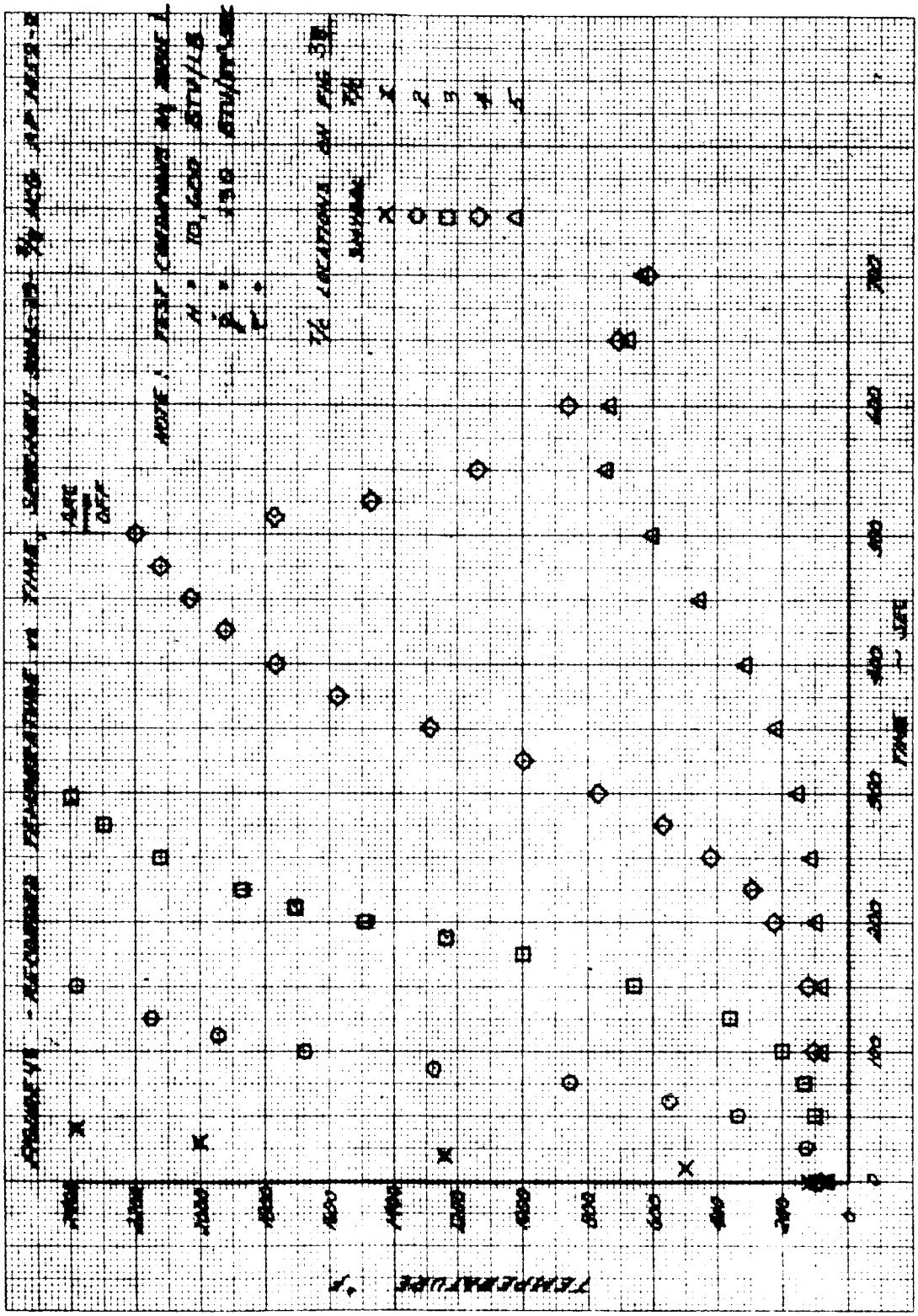

Figure 48 RECORDED TEMPERATURE VERSUS TIME, SPECIMEN 5026-39-3/8 INCH HCG, AP1552-2

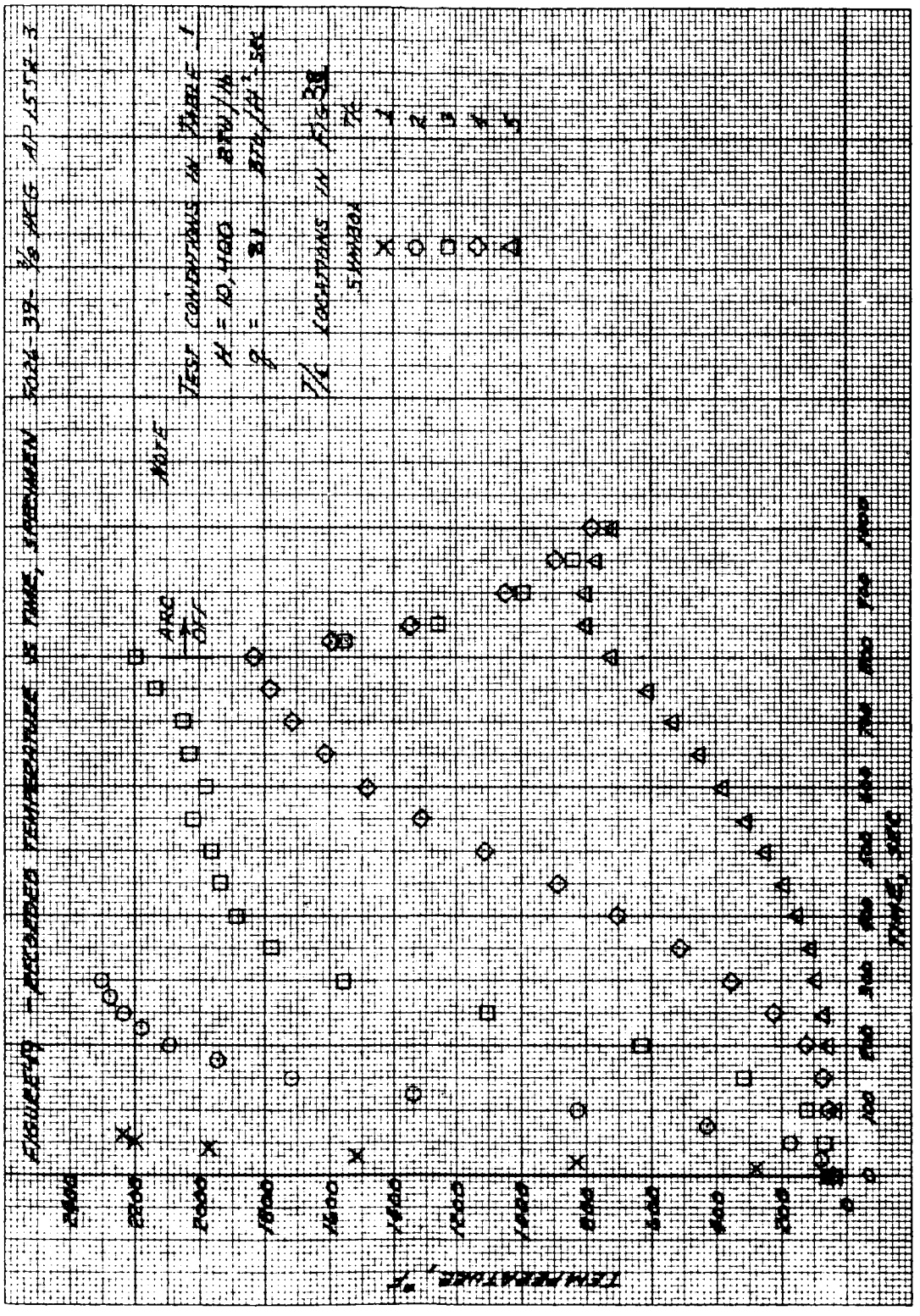

Figure 49 RECORDED TEMPERATURE VERSUS TIME, SPECIMEN 5026-39-3/8 INCH HCG, AP1552-3

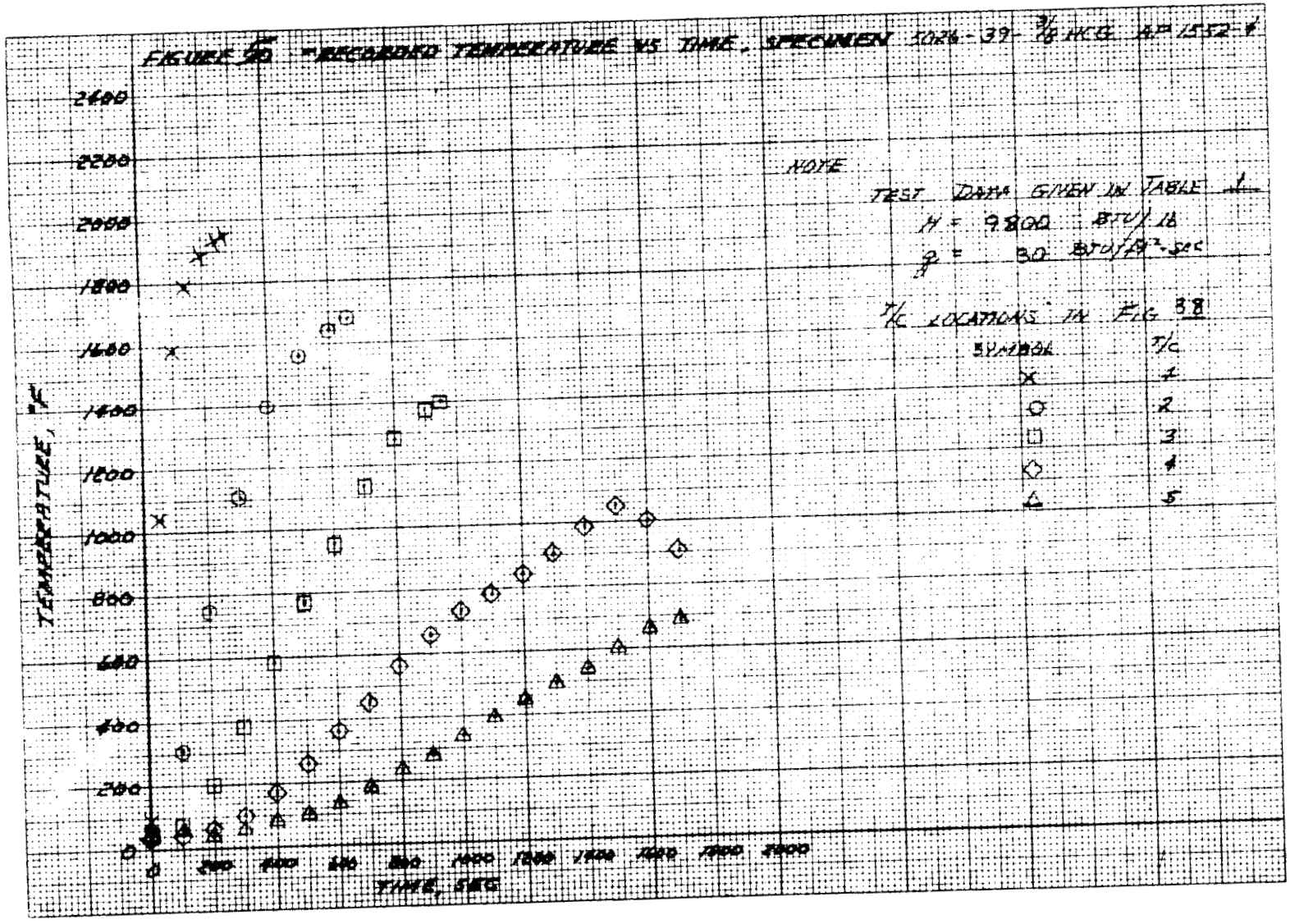

Figure 50 RECORDED TEMPERATURE VERSUS TIME, SPECIMEN
5026-39-3/8 INCH HCG, AP1552-4

[redacted]

DISTRIBUTION

Addressee	No. of Copies
NAA/S&ID (+ 1 reproducible)	25
John Carden (Florida)	1
R. H. Hugghins (Avco Rep. at NAA)	1
B. Mathews (NAA Resident Rep.)	1
Apollo Central Files (+ 1 reproducible)	5
Central Files (1 reproducible)	
Research Library	5
R. J. Albert	1
P. T. Andrews	1
E. B. Belason	1
R. L. Bentley	1
Y. G. Biry	1
R. Bussey (Lawrence)	1
C. A. Caputo	1
C. Cohen	1
J. A. Collins	1
F. DeGiacomo	1
R. E. Demming	1
F. W. Diederich	1
A. H. Diming	1
J. Dowd	1
M. G. Friedman	1
G. C. Kipps	1
K. Goodman	1
M. Guidi	1
A. Hall	1
L. A. Hammond	1
A. J. Hanawalt	1
H. Hoercher	1
E. Hogan	1
C. L. Huffine	1
M. E. Ihnat	1
J. J. Johnson	1
E. L. Kaminsky	1
E. D. Kenna	1
R. S. Knower	1
J. Kossar	1
J. A. Kyger	1
A. T. Lavigne	

[redacted]

[redacted]

DISTRIBUTION (Concl'd)

Addressee	No. of Copies
R. N. Lurie	1
E. S. McNellie	1
T. W. Mix	1
D. Moodie	1
D. A. Mosher	1
R. J. Mykytyn	1
A. Nahabedian	1
J. J. O'Dea	1
E. Offenhartz	1
A. Ogman	1
D. Pennington	1
J. Phaneuf	1
J. E. Richards	1
R. Roberts	1
A. A. Rothstein	1
C. W. Spencer	1
D. E. Stafford	1
R. Timmins	1
R. B. Wagner	1
A. S. Woodhull	1
W. Winterling	1
W. Zeh	1

[redacted]